AD-753 415

EVALUATION OF BALLISTIC DAMAGE RESISTANCE AND FAILURE MECHANISMS OF COMPOSITE MATERIALS

Elliot F. Olster, et al

Avco Corporation

Prepared for:

Air Force Materials Laboratory

April 1972

AFML-TR-72-79

EVALUATION OF BALLISTIC DAMAGE RESISTANCE AND FAILURE MECHANISMS OF COMPOSITE MATERIALS

Elliot F. Olster

Howard A. Woodbury

Avco Corporation

Technical Report AFML-TR-72-79
AVSD-0311-72-CR

This document has been approved for public release and sale; its distribution is unlimited.

AIR FORCE MATERIALS LABORATORY
AIR FORCE SYSTEMS COMMAND
Wright-Patterson Air Force Base, Ohio 45433

NOTICE

When Government drawings, specifications, or other data are used for any purpose other than in connection with a definitely related Government procurement operation, the United States Government thereby incurs no responsibility nor any obligation whatsoever; and the fact that the government may have formulated, furnished, or in any way supplied the said drawings, specifications, or other data, is not to be regarded by implication or otherwise as in any manner licensing the holder or any other person or corporation, or conveying any rights or permission to manufacture, use, or sell any patented invention that may in any way be related thereto.

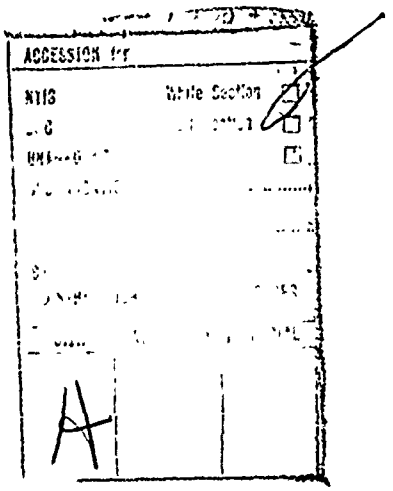

Copies of this report should not be returned unless return is required by security considerations, contractual obligations, or notice on a specific document.

Unclassified

Security Classification

DOCUMENT CONTROL DATA - R & D

(Security classification of title, body of abstract and indexing annotation must be entered when the overall report is classified)

1 ORIGINATING ACTIVITY (Corporate author) Avco Corporation Lowell, Massachusetts 01851	2a. REPORT SECURITY CLASSIFICATION Unclassified 2b. GROUP

3 REPORT TITLE

Evaluation of Ballistic Damage Resistance and Failure Mechanisms of Composite Materials

4 DESCRIPTIVE NOTES (Type of report and inclusive dates)

Final 1 June 1970 to 1 January 1972

5 AUTHOR(S) (First name, middle initial, last name)

Elliot F. Olster
Howard A. Woodbury

6 REPORT DATE April 1972	7a. TOTAL NO. OF PAGES 129	7b. NO OF REFS 24
8a CONTRACT OR GRANT NO F33615-70-C-1570 b. PROJECT NO 7360 c. Task No. 763006 d.	9a. ORIGINATOR'S REPORT NUMBER(S) AVSD-0311-72-CR 9b. OTHER REPORT NO(S) (Any other numbers that may be assigned this report) AFML-TR-72-79	

10 DISTRIBUTION STATEMENT

This document has been approved for public release and sale; its distribution is unlimited.

11 SUPPLEMENTARY NOTES	12. SPONSORING MILITARY ACTIVITY Air Force Materials Laboratory Air Force Systems Command Wright-Patterson AFB, Ohio 45433

13. ABSTRACT

The tolerance to ballistic impact of graphite/epoxy and boron/epoxy composites has been investigated. The effects of preimpact loads, of ply layups, and of projectile velocity have been determined for 30 caliber armor piercing projectiles striking the plate at a 0° obliquity. A limited number of tests were performed on glass/epoxy laminates and on type 6061-T6 aluminum panels. Several tests were conducted using 50 caliber armor piercing projectiles.

High speed photography was used to determine the overall ballistic response, as an additional check on projectile velocity, and to determine when crack initiation occurred.

The fracture toughness of each type of laminate was determined and both the residual strength (the nominal stress to which a panel which did not fail during perforation can be loaded) and the threshold strength (the lowest preimpact stress which results in failure upon impact) are shown to correlate directly with the toughness.

Details of illustrations in this document may be better studied on microfiche

DD FORM 1 NOV 1473

Unclassified

Security Classification

Unclassified

Security Classification

14 KEY WORDS	LINK A		LINK B		LINK C	
	ROLE	WT	ROLE	WT	ROLE	WT
Ballistic Damage						
Composite Materials						
Fracture Mechanics						
Retained Strength						

Unclassified

Security Classification

AFML-TR-72-79

EVALUATION OF BALLISTIC DAMAGE RESISTANCE AND FAILURE MECHANISMS OF COMPOSITE MATERIALS

AVSD-0311-72-CR

Elliot F. Olster

Howard A. Woodbury

FOREWORD

This document was prepared by the Avco Corporation, Lowell, Mass., as a final report describing research carried out for the Air Force under Contract F33615-70-C-1570. The project was initiated under Project 7360: Chemical, Physical, and Thermodynamic Properties of Aircraft, Missile, and Spacecraft Materials; Task 763006: Impact Damage and Weapons Effects on Aerospace Materials. The work was adminstered under the direction of Mr. Gordon H. Griffith of the Air Force Materials Laboratory, Air Force Systems Command, Wright-Patterson Air Force Base, Ohio.

This report describes research conducted from June 1970 to January 1972 and was submitted by the authors in April 1972.

The authors are grateful to Mr. O. L. Bowie and Mr. C. E. Freese both of the U. S. Army Materials and Mechanics Research Center, Watertown, Massachusetts for computing the stress intensity factors associated with cracks emanating from holes in the orthotropic materials studied.

This technical report has been reviewed and is approved.

BEN A. LOVING, Major USAF
Chief, Exploratory Studies Branch
Materials Physics Division
Air Force Materials Laboratory

ABSTRACT

The tolerance to ballistic impact of graphite/epoxy and boron/epoxy composites has been investigated. The effects of pre-load, of ply layups, and of projectile velocity have been determined for 30 caliber armor piercing projectiles striking the plate at a 0^{o} obliquity. A limited number of tests were performed on glass/epoxy laminates and on type 6061-T6 aluminum panels. Several tests were conducted using 50 caliber armor piercing projectiles.

High speed photography was used to determine the overall ballistic response, as an additional check on projectile velocity, and to determine when crack initiation occurred.

The fracture toughness of each type of laminate was determined and both the residual strength (the nominal stress to which a panel which did not fail during perforation can be loaded) and the threshold strength (the lowest preimpact stress which results in failure upon impact) are shown to correlate directly with the toughness.

TABLE OF CONTENTS

LIST OF FIGURES

FIGURES (Continued)

FIGURES (Continued)

LIST OF TABLES

SYMBOLS AND NOMENCLATURE

a	crack length, or plate length
A_{ij}	generalized modal displacement
$\dot{A}_{ij}$	the derivative with respect to time of A_{ij}
AP	armor piercing
b	plate width
B/E	boron epoxy
DLF	dynamic load factor
E	isotropic modulus
Eij	modulus of an orthotropic material
E_{45}	modulus at 45° to the principal axis of orthotropy
fps	feet per second
Fij	stress distribution function
F_T	total force
F_H	horizontal force
g	radial distance
G/E	glass epoxy
Gr/E	graphite epoxy
Gij	shear modulus
h	plate thickness
HV, LV	high velocity, low velocity
K	stress intensity factor
K_c	notch toughness
K'	stress intensity at initiation of failure
KIPS	1000 pounds
KSI	1000 pounds per square inch
m	density of plate having a thickness equal to h
MHz	10^6 cycles per second

CONTINUED

NDT	non-destructive tests
PSI	pounds per square inch
P	normal force, load, or internal pressure
r, θ	polar coordinates
R	radius of a hole
s	an orthotropic constant
t	time
t_d	duration of impulse
UTS	ultimate tensile strength
V	shear force
V_L	longitudinal sonic velocity
V_{ij}	Poisson's ratio
Y	boundary modification term
β	unit conversion constant
ρ	mass density
ν	Poisson's ratio
μ	10^{-6}
ω	radians per second
σ	nominal extensional stress
σ_{ij}	stress in the vicinity of a crack
σ_{zz}	in-plane stress in a flexurally loaded plate
σ_{hoop}	hoop tensile stress

CONTINUED

$\sum$	summation sign
K	total kinetic energy
U	total strain energy
W_e	total external work
∂, d	partial and total differentiation signs

Subscripts

ij	coordinate system indicators, they take values of 1 or 2
n	nominal
ST	static

1.0 INTRODUCTION

The systems approach to aircraft design using redundant structures to minimize the probability of overall failure is only as reliable as the estimates of the potential for failure of each structural element. Fibrous composites have only recently been incorporated into structural elements for flight vehicles and it is important to characterize these materials as accurately as possible. One area in which much work still remains is that of the effects of ballistic impact and penetration on the load carrying capability of a structural composite.

Some preliminary data obtained several years ago on boron/epoxy laminates showed the following:

1. On a (0 ± 45) sym. laminate (Reference 1) drilled holes, varying in diameter from 0.067 in. to 1.000 in., caused a 30% reduction in the net section failure stress. Identical reductions were found as a result of holes formed by a .30-06 ball shot at a velocity of 2579 fps.

2. On a $(0_3/90)$ sym. laminate (Reference 1) drilled holes, varying in a diameter from 0.125 in. to 0.750 in., caused a 35% reduction in the net section failure stress.

3. On a $(0_2/\pm45/90)$ sym. laminate (Reference 2) drilled holes, varying in diameter from 0.257 in. to 0.504 in., caused a 45% reduction in the net section strength.

From this data it appeared that the strength reduction depended primarily upon the layup and, for at least the one laminate studied ballistically, that the strength reduction was the same regardless of whether the hole was formed by conventional drilling or by ballistic perforation.

Although these preliminary studies did not indicate any detrimental ballistic effect over and above that caused by a drilled hole, it is possible, under certain conditions, to obtain dynamic strength reductions. One such condition would be if the composite panels were preloaded during impact and subsequently perforated by a hard, strong projectile traveling at ordnance velocities.

If the panel is carrying load prior to impact, i.e. a prestress, several cumulative effects occur. First, the impulse delivered to the plate results in a flexural response which generates additional in-plane stresses. Second, perforation by a cone shaped projectile, striking the plate at normal incidence, will result in an in-plane compression wave and a transverse shear wave radiating from the hole at the sonic velocity. The in-plane compression arises from the wedging action of the projectile and causes a hoop tension stress at the periphery of the hole (Reference 5). Thirdly, the sudden introduction of a hole in a preloaded panel could result in a dynamic amplification greater than that associated with the static stress field near a hole in a loaded plate (Reference 6). These combination of effects may be significant and hence the strength reductions, especially of preloaded panels, might be more severe than those reported in the preliminary tests. These cumulative effects on a preloaded panel could manifest themselves in either of two ways; either by causing failure of

the panel during impact at preload levels much lower than that reported for the earlier tests, or by causing more damage during impact such that the retained strength of the panel under subsequent loading would be reduced over that for the static drilled holes or from ballistically introduced holes on unstressed panels.

Advanced composites are seeing increased use on military aircraft. These materials do not possess the capability for yielding as do the conventional structural metals and therefore holes, even those used for joining, result in a decrease in the net section failure stress. Because of the postulated dynamic effects it was assumed even greater strength reductions could result from ballistic perforation of preloaded panels; hence this study was undertaken. Its goals were to determine, from ballistic perforation tests on advanced structural composites, the tensile threshold strength (i.e., that prestress level which will result in immediate failure upon penetration of the projectile) and the residual strength (i.e., that final stress level to which a material can be loaded after it has been perforated by a bullet). The ratio of the threshold to residual strength is indicative of the effects of panel prestress on the ballistic performance of those materials.

This program is but one of several aimed at defining the tolerance of advanced composites to ballistic damage. It considers the effect of projectile velocity and preload level on the behavior of thin boron/epoxy and graphite/epoxy panels having three different ply layups. Complimentary studies are being conducted at Grumman, McDonnell Douglas, and Northrop (References 7, 8, and 9) where the effects of the angle of impact (obliquity), of compression loadings, and of full depth honeycomb cores faced with metals as well as composites are being evaluated.

2.0 SUMMARY

The effects of panel prestress, of projectile velocity, fiber, and ply orientation on the behavior of ballistically perforated boron/epoxy and graphite/epoxy composites was determined and compared to identical tests performed on 6061-T6 aluminum and on glass/epoxy composites.

A total of 36 graphite/epoxy and 28 boron/epoxy panels, 22 in. long by 8 in. wide, were manufactured containing reinforcement in either the $0/\pm45^{\circ}$, the $0/\pm45/90^{\circ}$, or the $0/\pm60^{\circ}$ directions. Several of these panels were machined into standard coupon test specimens and used for material characterization studies which included the determination of the tensile strengths at various orientations, the four orthotropic elastic constants, and the fracture toughness.

Most of the remaining panels were preloaded in uniaxial tension to stress levels ranging from 30 to 70% of their ultimate strength (UTS) and then perforated by a 30 caliber armor piercing (AP) projectile. Projectile velocities of either 2750 feet per second (fps), muzzle velocity or a lower velocity of 1200 fps, in an attempt to approach the maximum energy transfer condition, were employed for these series of tests. In addition a limited number of preloaded panels were impacted by 50 caliber AP projectiles at velocities of 3,000 fps. All tests were performed using stable projectiles (non-tumbling) fired at 0° obliquity to the panel.

In all cases the projectiles perforated the panels leaving a relatively clean hole with slightly more damage observed on the exit side of the panel. For the 30 caliber AP test series the "residual strength" of the panels that did not fail during impact was found to be independent of both initial preload and projectile velocity. However the results indicated that the "residual strength" of the panels was a function of the type of filamentary reinforcement and ply orientation. The $0/45/90^{\circ}$ boron/epoxy laminate had the highest absolute residual strength (75 ksi) which is 187% of that obtained with the aluminum alloy. The residual strength as a percentage of the ultimate tensile strength varied from 52 to 65% for the boron/epoxy (depending upon the layup) and from 61 to 73% for the graphite/epoxy (depending upon the layup).

In terms of absolute values the boron/epoxy laminates have the highest "residual strengths" ranging from 41 to 75 ksi depending upon fiber orientation. These strengths compare favorably with data obtained on 6061-T6 aluminum panels which showed no detectable loss in strength after ballistic impact resulting in a "residual strength" of approximately 40 psi. On a specific strength basis both composite materials appear to be about equivalent but exhibit even greater advantages over the 6061 aluminum. For the preloaded panels that failed during impact it was observed that the "threshold strength" (i.e. the prestress level which resulted in catastrophic failure of the panel upon impact) was independent of projectile velocity but dependent upon the filamentary reinforcement and ply orientation. In general the "threshold strength" was approximately 90% of the "residual strength."

From the limited number of tests performed with 50 caliber projectiles it appeared that the residual strength for 50 caliber projectile impact is slightly lower than for the 30 caliber projectiles.

Crack propagation velocities obtained from the high speed photographs taken during the tests showed that the crack velocities were higher in the graphite epoxy laminates than in the boron epoxy composites. These photos also showed that crack initiation did not begin until the projectile had reached its full diameter. This data was used to form a consistent approach for the analytical prediction of the threshold strength.

In all cases linear fracture mechanics, using the notch toughness found in the characterization studies, could be used to accurately predict the residual strength. The threshold strength was also linearly dependent on the notch toughness and by using a modified crack length, it too, could be predicted.

3.0 TECHNICAL APPROACH

3.1 Overview

The purpose of this program was to experimentally evaluate the ballistic response of two advanced composites and to determine the criteria for predicting failure based upon consistent mathematical models.

The approach was broken down into two phases, one experimental and one analytical and is most easily described by the chart in Figure 1. The experimental phase included static and ballistic tests on several materials. Preliminary tests were conducted using 6061-T6 aluminum alloy and using a 0/45 layup of a glass/epoxy composite, in specific S901 glass/5206 resin. The primary evaluation was conducted on three different layups of fiber reinforced composites; namely, 0/45, 0/45/90, and 0/60 layups of Thornel 50-S/5206 graphite/epoxy and RIGIDITE 5505/4 boron/epoxy composite.

The quasi static testing consisted of: (1) straight sided coupon tests at various angles to the laminate axis and, (2) single edge notch toughness tests. This data provided not only an assessment of the material uniformity but allowed the computation of the elastic constants, the tensile strengths and the fracture toughness of each composite.

The bulk of the ballistic testing was performed with large (6 in. x 6 in. gage section) specimens preloaded in uniaxial tension and shot at their mid point. Most of the experiments were performed using the 0/45 layup but the 0/45/90 and 0/60 layups were also used in order to assess the importance of ply orientation, relative moduli, and relative strengths on the behavior during ballistic penetration. Most of the tests were performed using 30 caliber AP projectile; several panels however, were perforated with 50 caliber AP projectiles.

Since projectile velocity has been found to have an effect on the ballistic behavior of various materials (Reference 18) the 30 caliber tests were performed using full and approximately one-half muzzle velocity. The actual projectile velocities used were 2750 and 1200 feet per second (fps). The lower velocities (1200 fps) were obtained by using a reduced powder charge. The 50 caliber projectiles were all shot at approximately 3000 fps. All rounds were individually hand loaded using the correct charge as determined from a series of chronographic tests performed at the Avco ballistic test facility. Chronographic tests were also periodically performed during the program to ensure that the projectile velocities were within $\pm$ 10% of the desired velocity. Projectile velocities monitored during each test confirmed the accuracy of the loads and velocities all test rounds fell well within the previously set limits.

The analytical investigations consisted of a plate dynamic analysis and a fracture mechanics study. The dynamic analysis investigated the magnitude of the dynamic bending stresses due to the impulsive loading during penetration. The second and more fruitful study relied upon relating the residual and threshold strengths to the fracture toughness of the laminates.

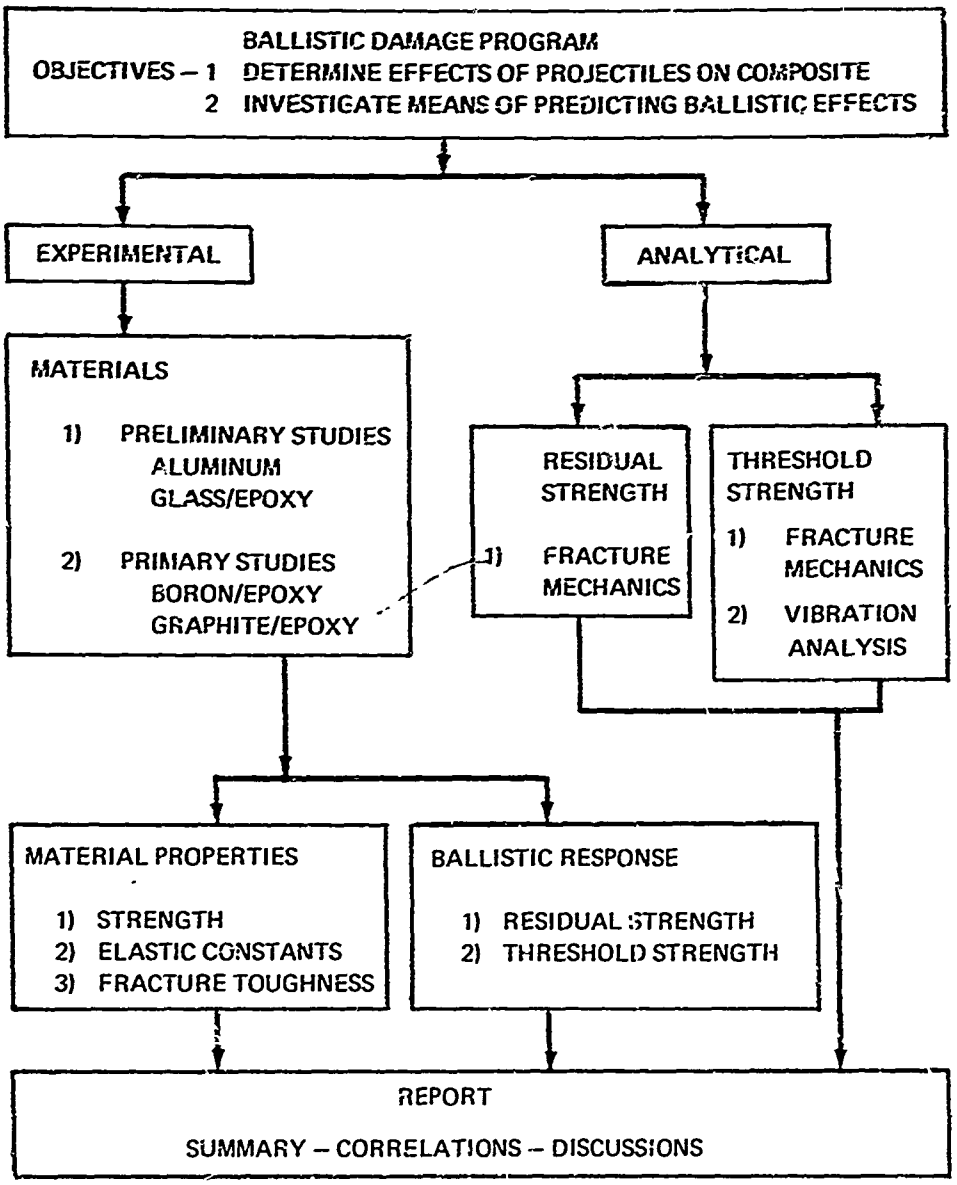

Figure 1 FLOW CHART

3.2 Experimental Investigation

3.2.1 Materials

The materials used in this program are described in Table 1. The composites all have the same basic resin system and relative thickness, hence the major variations are in types of fiber and ply orientation. Table 2 shows the useage of each panel in this program.

3.2.2 Quasi Static Material Characterization

3.2.2.1 Non-Destructive Testing

Prior to mechanical testing, 22 graphite/epoxy, 8 boron/epoxy, and 8 glass/epoxy panels all having the 0/45 layup were subjected to a variety of non-destructive tests. The panels were 8 in. x 20 in. as shown in Figure 2 and were examined only in the 8 in. x 8 in. gage section. The tests include: radiography, ultrasonic velocity and ultrasonic "C" scan flaw detection. The radiographic and ultrasonic "C" scan tests were used for observing flaw content and material variability. The data has been reported using a graded system (key in Table 3 explains the grading) which shows the relative assessment from panel to panel. The ultrasonic velocity readings were taken at the center point of the 8 in. x 8 in. area. The panels were then weighed, dimensioned, and a bulk density calculated. Ultrasonic velocity and gravimetric density were used to calculate ultrasonic elastic modulus in the thickness direction.

Radiographic results show the material density to be fairly uniform for most of the panels tested. Of the graphite epoxy panels examined specimens 1117-61A and 61B had the lowest average density. These panels also had the largest local density variations. As can be seen in the radiograph of 1117-61A (Figure 3a) there are low density regions in the 0°, $+45^{\circ}$, and -45° directions. These correspond to lack of graphite fiber which in turn is attributed to poor tow spacing. For comparison the radiograph of a uniform quality panel (Specimen 1117-82A) is given in Figure 3b.

All of the C scan tests were conducted at a frequency of 1.0 megahertz (MH_Z) using a standard through transmission immersed technique. High, intermediate and low sensitivity data was obtained. Light areas indicate regions of poor sound transmission. The dark rectangle marked on the recordings is the 8 in. x 8 in. area of interest. Marking on the low sensitivity C scan is interpreted as being severe porosity or delamination. Marking on the intermediate sensitivity C scan is interpreted as heavy porosity, very bad surface condition or delamination. Marking on the high sensitivity C scan is interpreted as either light porosity or a bad surface condition. No marking at all on the high sensitivity C scan is indicative of flaw free material. C scan recordings from panels 1117-61A and 1117-82A are given in Figures 4a and 4b. Panel 1117-82A is flaw free whereas 1117-61A has a significant amount of variability. These same conclusions were reached by examining the X-ray data (Figures 3a and 3b); the nature of the variability is different however. A qualitative assessment of the other panels examined is given in Table 3.

TABLE 1

MATERIALS

I. Preliminary Studies

A. Aluminum Alloys

Type 6061-T6

Thickness 0.064 inches

Orientation - Longitudinal axis coincided with rolling direction

B. Glass/Epoxy

Type S901 Glass/5206 Epoxy

Layups	1.	(0, +45, -45, +45, -45, 0) sym	12 Ply
	2.	(0, +45, -45, 0) sym	8 Ply

II. Primary Studies

A. Graphite/Epoxy

Type Thornel 50 S/5206*

Layups	1.	(0, +45, -45, 0) sym	8 Ply
	2.	(0, 0, +45, -45, 90) sym	10 Ply
	3.	(0, 0, +60, -60, +60, -60, +60, -60, 0, 0)	10 Ply

B. Boron/Epoxy

Type RIGIDITE 5505/4**

Layups	1.	(0, +45, -45, +45, -45, 0) sym	12 Ply
	2.	(0, 0, +45, -45, 0, 90) sym	12 Ply
	3.	(0, +60, -60, +60, -60, 0) sym	12 Ply

*Union Carbide's Graphite Filament.
**Avco Corporation's Boron Epoxy Prepreg.

TABLE 2

DESCRIPTION AND DISPOSITION OF TEST PANELS

Specimen Designation	Material Type & Remarks	NDT Tests	Static Characterization (Coupon & Fracture)	Ballistic Characterization			Remarks
				30 Cal 2750 fps	30 Cal 1200 fps	50 Cal 3000 fps	
AL 1	Aluminum, 6061-T6						Drilled Hole - Stress Distribution Studies
AL 2	(.064" Thick)						Drilled Hole - Stress Distribution Studies
AL 3				x			
AL 4				x			
AL 5				x			
AL 6				x			
1117-62A	Glass/Epoxy 8 Ply						Drilled Hole - Stress Distribution Studies
62B	(0/45)						Drilled Hole - Stress Distribution Studies
63A				x			
63B							Drilled Hole - Stress Distribution Studies
64							Drilled Hole - Stress Distribution Studies
1117-120A	Glass/Epoxy 12 Ply	x				x	
120B	(0/45)	x				x	
121A		x		x			
121B		x				x	
122A		x		x			
122B		x		x			
123A			x				
123B		x		x			
136A		x		x			
1117-61A	Graphite/Epoxy	x	x				
61B	8 Ply (0/45)	x		x			
66A		x		x			
66B		x		x			
67A		x		x			
67B		x		x			
72A		x			x		
72B		x			x		

TABLE 2 CONTINUED

Specimen Designation	Material Type & Remarks	NDT Tests	Static Characterization (Coupon & Fracture)	Ballistic Characterization			Remarks
				30 Cal 2750 fps	30 Cal 1200 fps	50 Cal 3000 fps	
1117-73A	Graphite/Epoxy	x			x		
73B	8 Ply (0/45)	x		x			
75A		x			x		
75B		x			x		
76A		x			x		
76B		x		x			
77A		x			x		
77B		x			x		
78A		x		x			
78B		x		x			
82A		x	x				
82B		x			x		
83A		x		x			
83B		x			x		
1109-78	Graphite/Epoxy					x	
85A	(10 Ply (0/45/90)			x			
85B				x			
86A				x			
86B				x			
87A			x				
87B				x			
1109-77	Graphite/Epoxy					x	
82A	10 Ply (0/60)		x				
82B				x			
83A				x			
83B				x			
84A				x			
84B				x			

TABLE 2 CONTINUED

Specimen Designation	Material Type & Remarks	NDT Tests	Static Characterization (Coupon & Fracture)	Ballistic Characterization 30 Cal 2750 fps	30 Cal 1200 fps	50 Cal 3000 fps	Remarks
1117-94A	Boron/Epoxy	x		x			
94B	12 Ply (0/45)	x			x		
95A		x			x		
95B		x			x		
96A		x		x			
96B		x		x			
97A		x	x				
97B		x		x			
141A					x		
141B						x	
142A					x		
142B					x		
143A					x		
143B					x		
144A					x		
144B					x		
1109-69A	Boron/Epoxy			x			
69B	12 Ply (0/45/90)			x			
70A						x	
70B				x			
71A				x			
71B				x			
75			x				
1109-72A	Boron/Epoxy					x	
72B	12 Ply (0/60)			x			
73A				x			
73B				x			
74A				x			
74B				x			
76			x				

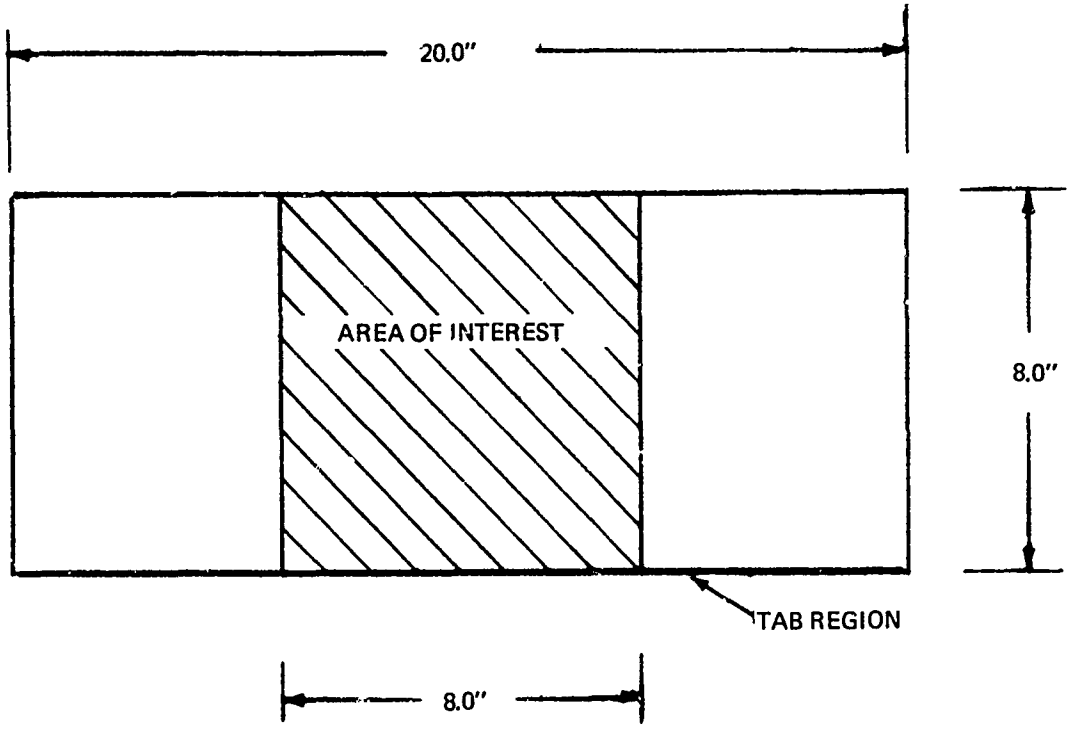

Figure 2 PANELS USED FOR BALLISTIC DAMAGE STUDIES CROSS HATCHED REGION IS THE GAGE SECTION AND HENCE IS THE "AREA OF INTEREST".

TABLE 3

SUMMARY OF NDT DATA

Panel	Xray	Ultrasonic "C" Scan	Ultrasonic Velocity in/sec $\times 10^{-6}$	Average Panel Density g/cm^3	Ultrasonic Modulus $E = k V_L^2$ 10^6 psi
0/45 Graphite					
1117-61A	Poor	Poor	0.079	1.374	0.70
61B	Poor	Poor	0.092	1.400	0.95
1117-66A	Fair	Excellent	0.096	1.403	1.03
B	Fair	Excellent	0.092	1.446	0.99
1117-67A	Good	Poor	0.088	1.500	0.94
67B	Good	Good	0.089	1.486	0.95
1117-72A	Good	Good	0.094	1.503	1.06
72B	Excellent	Excellent	0.092	1.529	1.04
1117-73A	Fair	Excellent	0.091	1.467	0.98
73B	Good	Excellent	0.092	1.468	1.01
1117-75A	Fair	Good	0.089	1.478	0.94
75B	Good	Excellent	0.092	1.468	0.99
1117-76A	Fair	Fair	0.089	1.498	0.96
B	Fair	Good	0.089	1.519	0.97
1117-77A	Fair	Excellent	0.093	1.487	1.04
77B	Excellent	Excellent	0.092	1.516	1.03
1117-78A	Fair	Good	0.088	1.486	0.92
78B	Good	Good	0.091	1.480	0.99
1117-82A	Good	Fair	0.092	1.476	0.99
82B	Good	Excellent	0.091	1.484	0.99
1117-83A	Excellent	Excellent	0.092	1.481	1.02
83B	Excellent	Excellent	0.092	1.478	1.00
Average			.0907	1.4740	0.977

"NDT Grading"

XRAY

Excellent: No low density lines present. Uniform density throughout.

Good: 1 or 2 low density lines present. Background density generally uniform.

Fair: 3 - 6 low density lines present. Background density sometimes has slight variations.

Poor: Numerous low density lines (too many to count) present for three directions. Pronounced density variations noted.

ULTRASONIC "C" SCAN

Excellent: No marking for all sensitivity levels.

Good: Light marking noted for high sensitivity level only.

Fair: Light markings plus some heavier markings for the high sensitivity level only.

Poor: Light plus heaving markings for the high sensitivity level, and also markings observed for intermediate and lowest sensitivity levels.

TABLE 3 CONTINUED

Panel	Xray	Ultrasonic "C" Scan	Ultrasonic Velocity in/sec x10^{-6}	Average Panel Density g/cm^3	Ultrasonic Modulus $E = k V_L^2$ 10^6 psi	"NDT Grading"
0/45 Boron						
1117-94A	Fair	Poor	0.159	1.950	3.98	
94B	Fair	Fair	0.155	1.950	3.78	
1117-95A	Fair	Poor	0.148	1.931	3.41	
B	Good	Poor	0.149	1.931	3.46	
1117-96A	Fair	Excellent	0.149	1.927	3.45	
96B	Good	Excellent	0.152	1.927	3.59	
1117-97A	Good	Excellent	0.143	1.962	3.24	
97B	Good	Excellent	0.159	1.962	4.00	
Average			0.15	1.9	3.00	
0/45 Glass						
1117-120A	Fair	Fair	0.157	2.17	4.39	
B	Fair	Fair	0.154	2.17	4.15	
1117-121A	Fair	Poor	0.157	2.16	4.41	
B	Good	Fair	0.165	2.16	4.74	
1117-122A	Good	Good	0.144	2.12	3.73	
B	Good	Excellent	0.157	2.12	4.21	
1117-123A	Good	Good	0.156	2.28	4.26	
B	Good	Fair	0.156	2.28	4.47	
Average			0.15	2.1	4.2	

Figure 3a RADIOGRAPH OF CENTRAL REGION OF PANEL 1117 61A (GRAPHITE/EPOXY)

THE DENSITY VARIATIONS IN THE 0^{o} AND $\pm 45^{o}$ DIRECTIONS INDICATE LACK OF FIBER

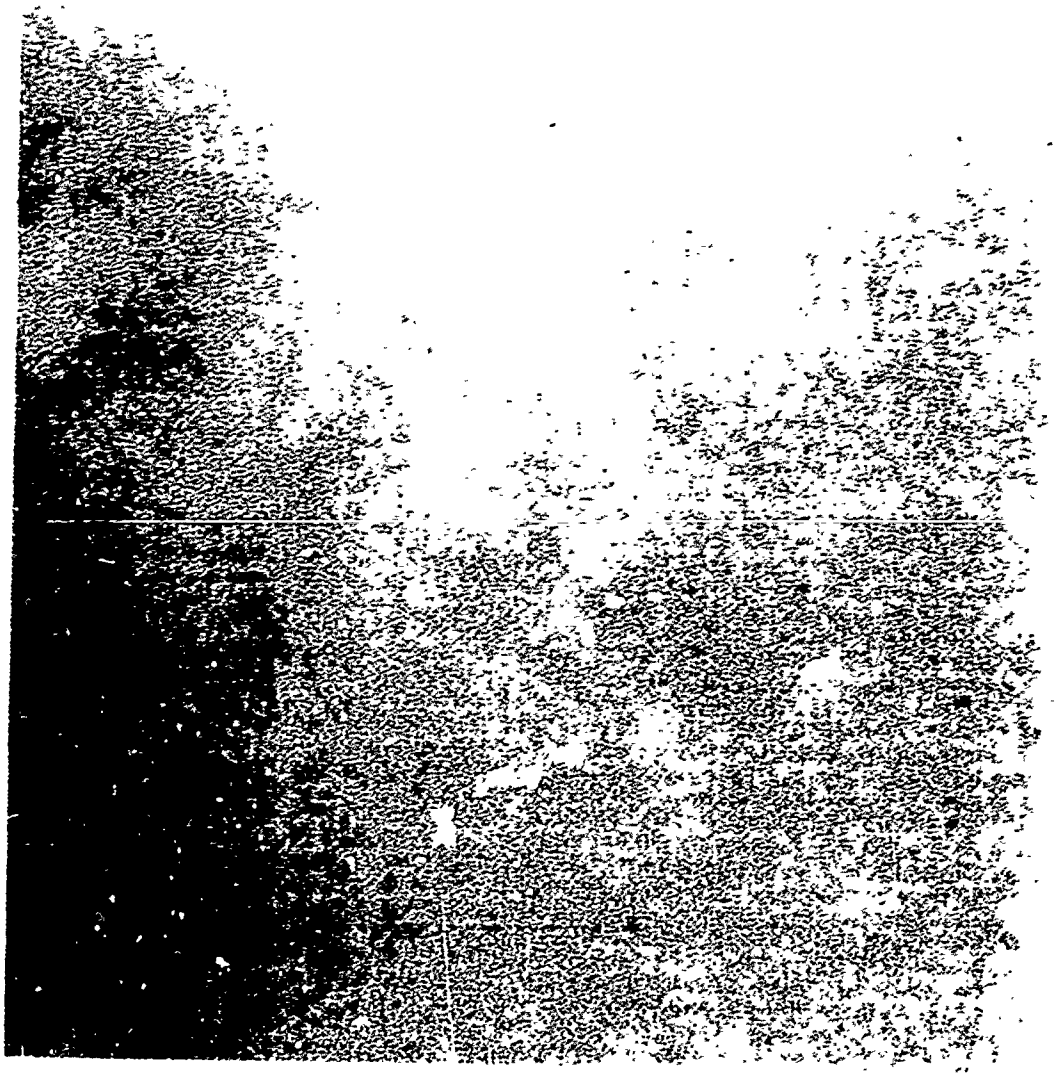

Figure 3b RADIOGRAPH OF CENTRAL REGION IN PANEL 1117-82A (GRAPHITE/EPOXY)

NOTE THE UNIFORMITY AS COMPARED TO FIGURE 3a.

Figure 4a C-SCAN OF SPECIMEN 1117-61A (GRAPHITE/EPOXY)

THE LIGHT REGIONS INDICATE MATERIAL IMPERFECTIONS.
(REDUCED PHOTO)

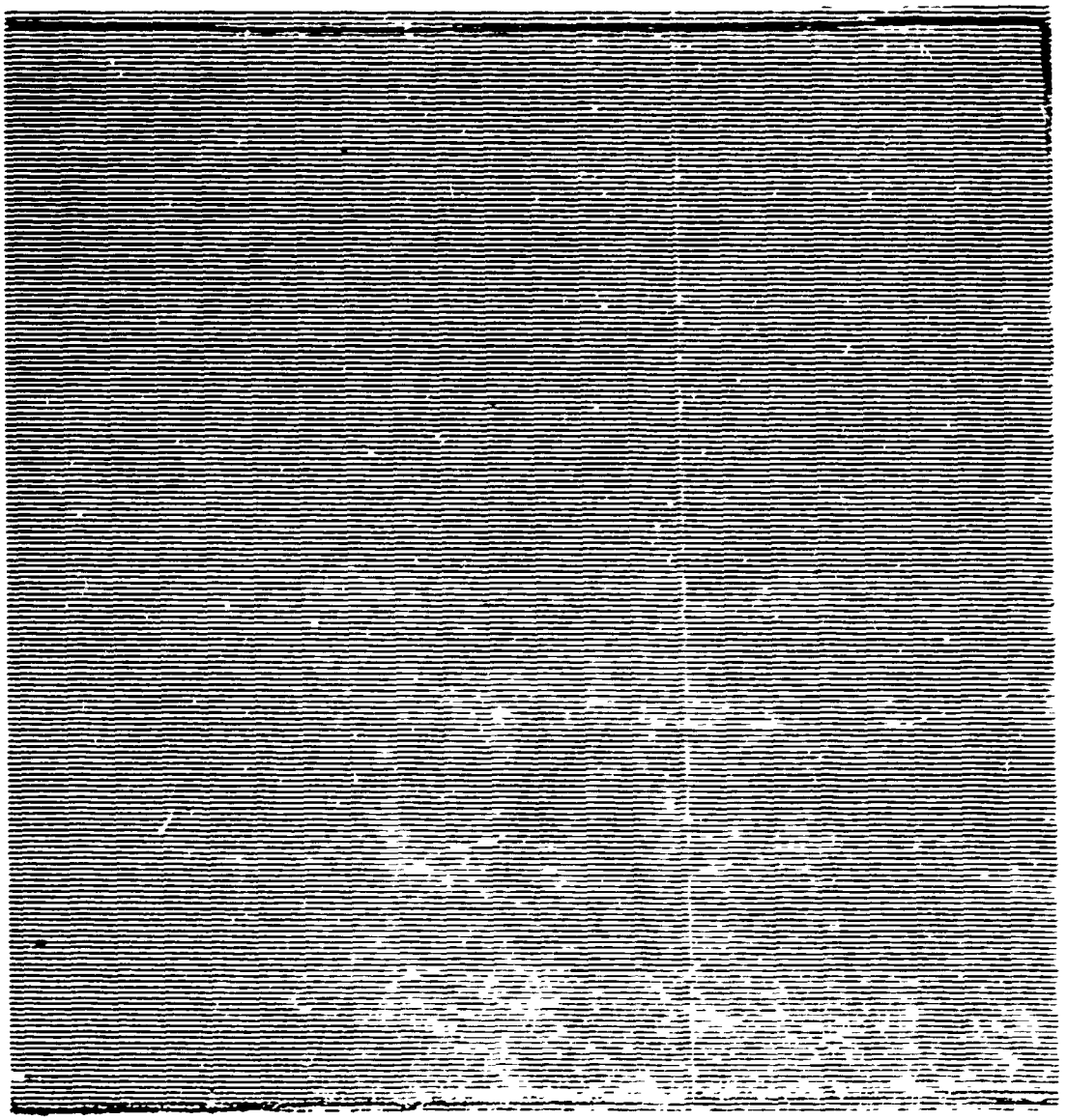

Figure 4b C-SCAN OF SPECIMEN 1117-82A (GRAPHITE/EPOXY)

NOTE THE MATERIAL UNIFORMITY. (REDUCED PHOTO)

All velocity measurements were conducted at a frequency of 1.0 MHz. The ultrasonic velocity, V_L, was measured through the thickness of the panel at the center of the 8 in. x 8 in. area. Ultrasonic velocity is related to the elastic sonic modulus for a nondispersive media through the equation:

$$E = \beta \rho (V_L)^2 \qquad (1)$$

β = Constant to adjust units

V_L = Longitudinal wave velocity (in/sec x 10^{-6})

ρ = Density (g/cm^3)

E = Young's modulus (10^6 psi)

Solving equation (1) for E leads to the NDT determined ultrasonic modulus which is presented in Table 3.

3.2.2.2 Coupon Tests

Coupon tests were performed on the composites only; the aluminum alloy is sufficiently well characterized. The tests were conducted at room temperature on $\frac{1}{2}$ in. wide straight sided specimens. The purpose of these tests were: (1) to establish the elastic constants which were required for the fracture toughness analysis, (2) to establish the material uniformity and correlations with NDT data, and (3) to establish a lower bound on the tensile strength. The data is summarized in Table 4.

The four orthotropic elastic constants were established from tensile tests performed on specimens cut in the 0^o, 90^o, and 45^o directions. The shear modulus was obtained from Tsai's relation (Reference 10):

$$\frac{4}{E_{45^o}} = \frac{1}{E_{11}} + \frac{1}{G_{12}} - \frac{2V_{12}}{E_{11}} + \frac{1}{E_{22}} \qquad (2)$$

where:

E_{11} is the 0^o modulus

E_{22} is the 90^o modulus

V_{12} is the major Poisson's ratio

G_{12} is the shear modulus in the 0^o or 90^o direction

E_{45} is the 45^o modulus

It is recognized that the shear modulus determined in this way can be in error because of boundary and coupling effects, however the computed values agree closely to predictions obtained using standard lamination theory and hence, are felt to be correct.

The accuracy of the NDT data was evaluated by performing mechanical tests on two graphite panels, 1117-61A and 1117-82A, which, as indicated earlier, represent high and low quality material. The mechanical tests (summarized in Appendix A) confirmed this; and in view of this correspondence, data from several abnormal test panels were eliminated.

The tensile strength deserves some discussion. Table 4 shows the tensile strength obtained at the various angles on the $\frac{1}{2}$ in. wide coupon specimens. It also lists a true ultimate tensile strength (UTS) in the 0° direction for each of the composites. The tensile strength of cross plied laminates increases as the specimen width increases until a limit is reached which is representative of the true strength of the material. With $\frac{1}{2}$ in. wide, 2 in. gage length tensile specimens the full strength of laminates such as those used in this program is not generally developed. Consequently, the control strengths used for all comparisons in the program were adjusted to reflect the true ultimate tensile strength of each material.

Using the Structural Design Guide for advanced composite applications (Reference 22) the following data was obtained: The boron/epoxy laminates have an average strength of 85 KSI, 114 KSI, and 68 KSI for the 0/45, the 0/45/90, and the 0/60 layups respectively. Unidirectional Thornel 50-S/epoxy has a strength of 134 KSI, hence the measured value of 71 KSI for the 0/45 graphite/epoxy laminate was felt to be realistic, based upon the percentage of 0° plys, in spite of the narrow width of the specimen. The 0/45/90 graphite/epoxy laminate should have 80% of the strength of the 0/45 laminate since the 90° plys are essentially ineffective in improving the longitudinal strength. This gives a predicted strength of 57 KSI. Similarly, the 0/60 layup receives very little benefit in the longitudinal strength from the 60° plys; therefore its strength is proportional to the percentage of 0° plys times the unidirectional strength which is 40% of 134 KSI or 53.6 KSI. The S glass/epoxy laminates have an average unidirectional tensile strength of 300 KSI. The 12 ply and 8 ply laminates have respectively, 33% and 50% of the plys in the 0° direction and hence have a true UTS of 100 KSI and 150 KSI, respectively. These values are summarized in Table 4 and are considered the true ultimate tensile strength of the laminates. Lastly, it should be pointed out that when the graphite/epoxy specimens failed, significant delamination was observed which is indicative of low shear strength. A typical failure is shown in Figure 5; for comparison the glass and boron composites are also shown.

3.2.2.3 Fracture Toughness Tests

In addition to the various elastic constants and strengths in several directions the fracture toughness of the composites was determined. The fracture toughness is defined as the upper limit of the stress intensity factor K. It can be shown (Reference 11) that at the tip of a crack the elastic stress field can be written as:

$$\sigma_{ij} = \frac{K}{(2\pi r)^{\frac{1}{2}}} F_{ij}(s, \theta)$$

TABLE 4

SUMMARY OF MATERIAL PROPERTIES

Material	Modulus ($\times 10^6$ psi) E11 0°	E22 90°	E45 45°	Strength (KSI) 0°	90°	45°	Poisson's Ratio ν_{12} 0°	ν_{21} 90°	ν_{45} 45°	Total Strain (%) 0°	90°	45°	Shear Modulus $\times 10^6$ psi, G_{12}	True UTS (KSI)
Graphite/Epoxy 0/60	14.0	7.0	10.0	41	11	18	0.30	0.20	0.24	0.25	0.13		4.4	53.6
Graphite/Epoxy 0/45/90	15.0	9.4	10.1	40	26	26	0.35	0.17	0.29	0.29	0.29		3.7	57.0
Graphite/Epoxy 0/45	18.5	3.9	10.2	71	12		0.81		0.05	0.39	0.31		4.1	71.0
Boron/Epoxy 0/60	11.8	11.6	11.3	52	42	38	0.36	0.34	0.30	0.64	0.45	0.51	4.3	68.0
Boron/Epoxy 0/45/90	18.0	8.8	8.7	102	19	30	0.41	0.14	0.32	0.64	0.27	0.45	3.0	114.0
Boron/Epoxy 0/60	11.4	4.3		63	16		0.68			0.60	0.42		5.0	85.0
Glass/Epoxy 12 Ply 0/45	5.4	3.9		94	18		0.86			3.29	1.76			100.0
Glass/Epoxy 8 Ply 0/45														150.0

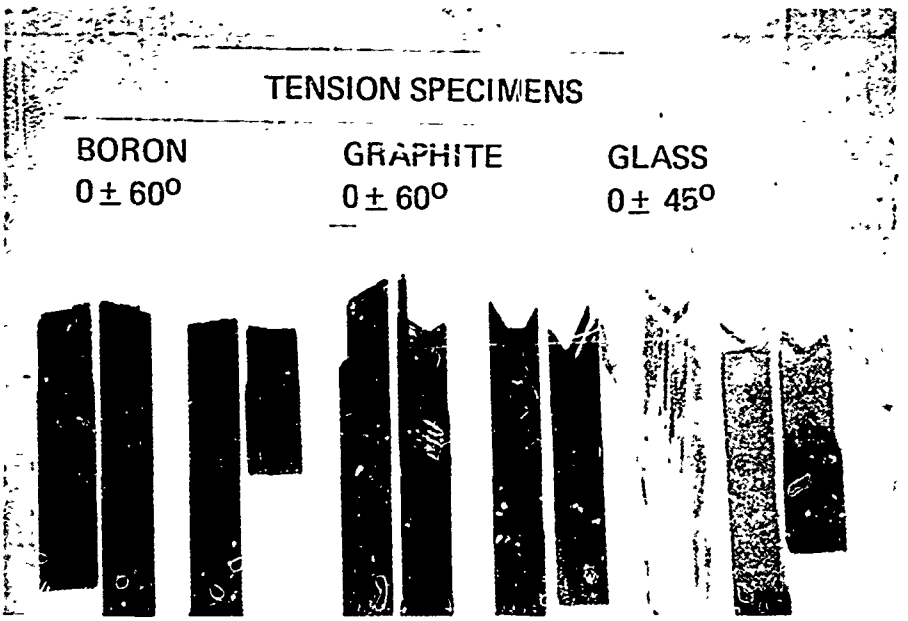

Figure 5 TENSILE SPECIMENS OF BORON, GRAPHITE AND GLASS EPOXY COMPOSITES

LEFT HAND SIDE OF EACH GROUP IS THE LONGITUDINAL TENSILE SPECIMEN (0°); RIGHT HAND SIDE IS THE TRANSVERSE TENSION SPECIMEN (90°). MASSIVE DELAMINATION OCCURRED WITH THE GRAPHITE/EPOXY INDICATIVE OF LOW INTERLAMINAR SHEAR STRENGTH. FIBROUS DELAMINATION OCCURRED WITH THE 0° GLASS SPECIMENS WHICH IS TYPICAL OF THIS COMPOSITE.

where:

K is the stress intensity factor

r, θ are polar coordinates

s is a parameter reflecting material properties

F is stress distribution function

σ is the local stress in the ij coordinates system

Fracture mechanics is based upon the premise that when K reaches its critical value the local stress field at the tip of the crack (or similarly the strain energy density) is sufficient to cause failure (crack extension). K can be written as:

$$K = Y \sigma_n (a)^{\frac{1}{2}} \qquad (4)$$

where:

Y is a boundary modification term

σ_n is the nominal stress

a is the crack length

At the present, the variation of the parameter Y is not known for the material constants, specimen geometry, and boundary conditions used. Olster, (Reference 12) using a plane stress finite element technique in conjunction with the so called compliance calibration method, generated the function Y for isotropic and orthotropic specimens having boundary conditions and geometries similar to those used here. From Olster's data it can be seen that Y is expected to be nearly constant and equal to 1.75 for all ratios of crack length to specimen width considered here. When σ_n is reached to the value where crack extension occurs K is equal to Kc, the fracture toughness of the material.

Fracture toughness tests were performed on only the composite materials. All specimens were loaded along their 0° axis by imposing uniform boundary displacements on single edge notch specimens (Figure 6). A typical test sequence is shown in Figure 7. Crack length was monitored using an optical measuring device manufactured by Physitech. From these tests a value for Kc was determined using equation 4 with a value of Y = 1.75. Detailed results are presented in Appendix B and the results are summarized in Table 5.

With the boron/epoxy specimens the fracture occurred uniformly over the entire thickness and progressed laterally across the specimen in a series of discrete steps. This behavior is indicative of a valid test. Figure 8a shows a typical fractured specimen. Excellent correlation was obtained between the predicted (using fracture mechanics) and experimentally measured values of residual strength for the ballistically impacted boron/epoxy panels. These correlations and supportive reasoning will be presented in a later section.

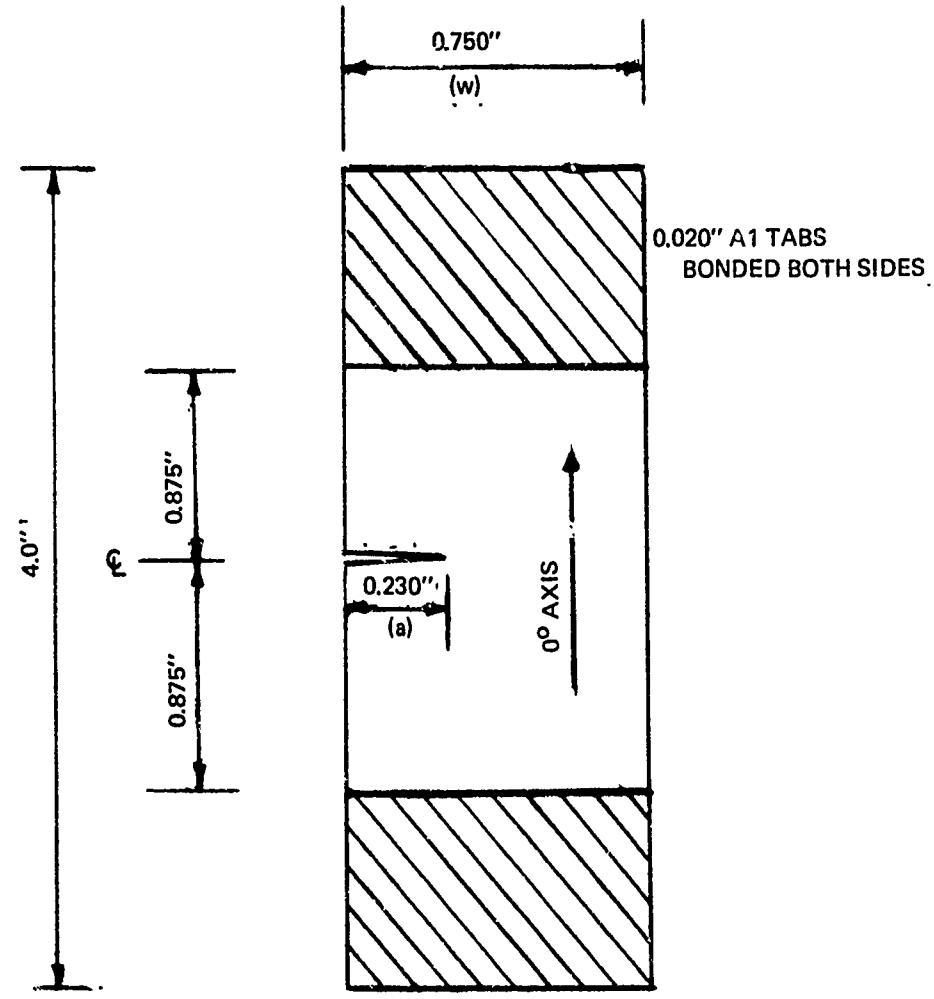

Figure 6 SINGLE EDGE NOTCH FRACTURE TOUGHNESS SPECIMEN

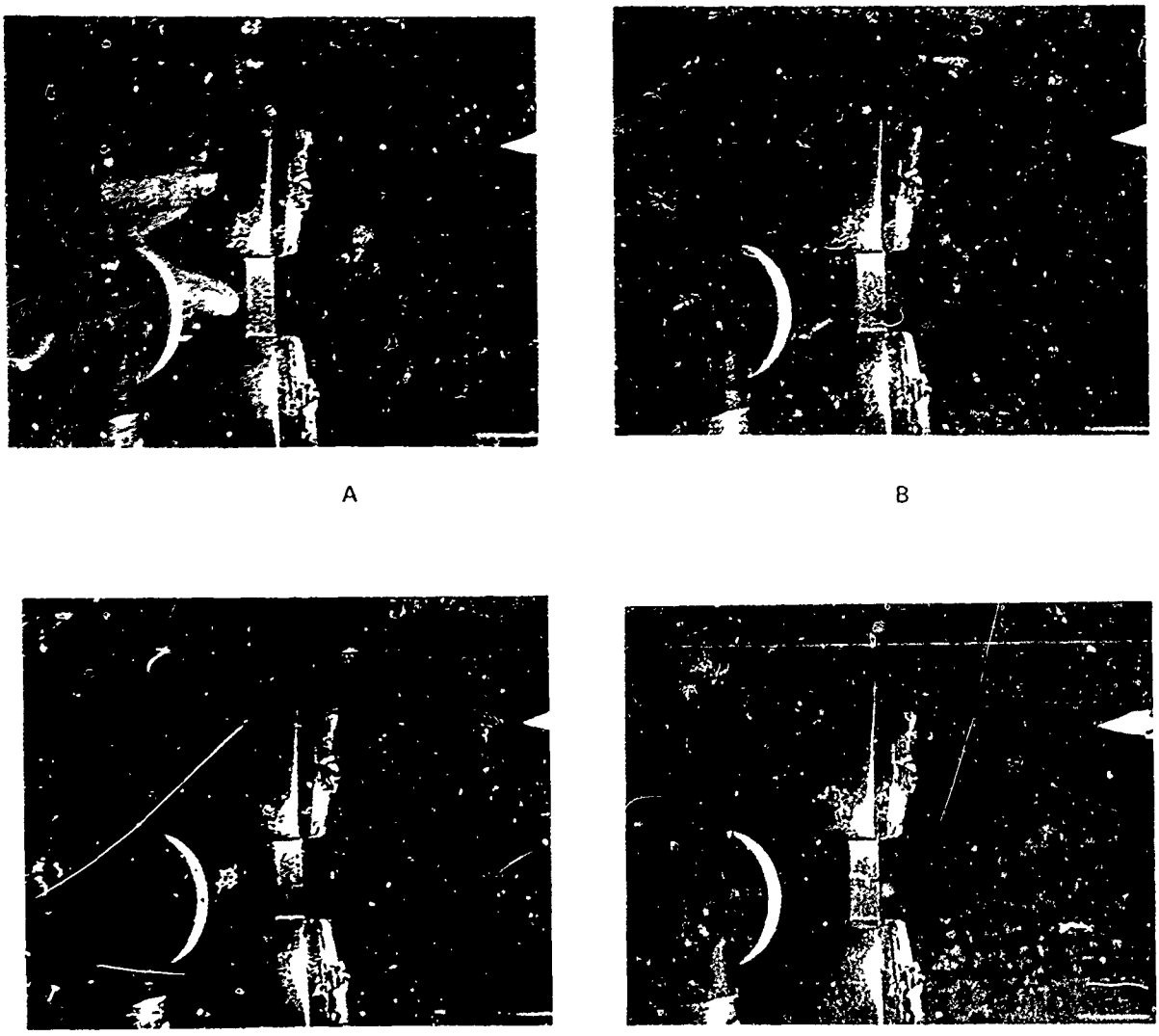

Figure 7 BORON EPOXY FRACTURE TOUGHNESS SPECIMEN, (A) PHOTO SHOWING TEST SPECIMEN PRIOR TO APPLICATION OF LOAD, (B) CRACK GROWTH BEGINNING, (C) FULLY DEVELOPED ZONE, (D) SPECIMEN AFTER CRACK RAPIDLY TRAVERSED THE SPECIMEN

TABLE 5

FRACTURE TOUGHNESS

Material	K' (At Onset of Fracture) KSI $\sqrt{in}$	K_c (Fracture Toughness) KSI $\sqrt{in}$
Boron/Epoxy		
B/E 0/45	15.2	21.1
B/E 0/45/90	25.8	32.6
B/E 0/60	14.8	18.2
Graphite Epoxy		
Gr/E 0/45	21.6	27.5*
Gr/E 0/45/90	13.5	20.8*
Gr/E 0/60	17.4	26.3*
Glass/Epoxy		
G/E 0/45 (12 Ply)	39	59.2*

*Values were computed but are not considered the true notch toughness. (See text for reasoning)

BORON SPECIMENS

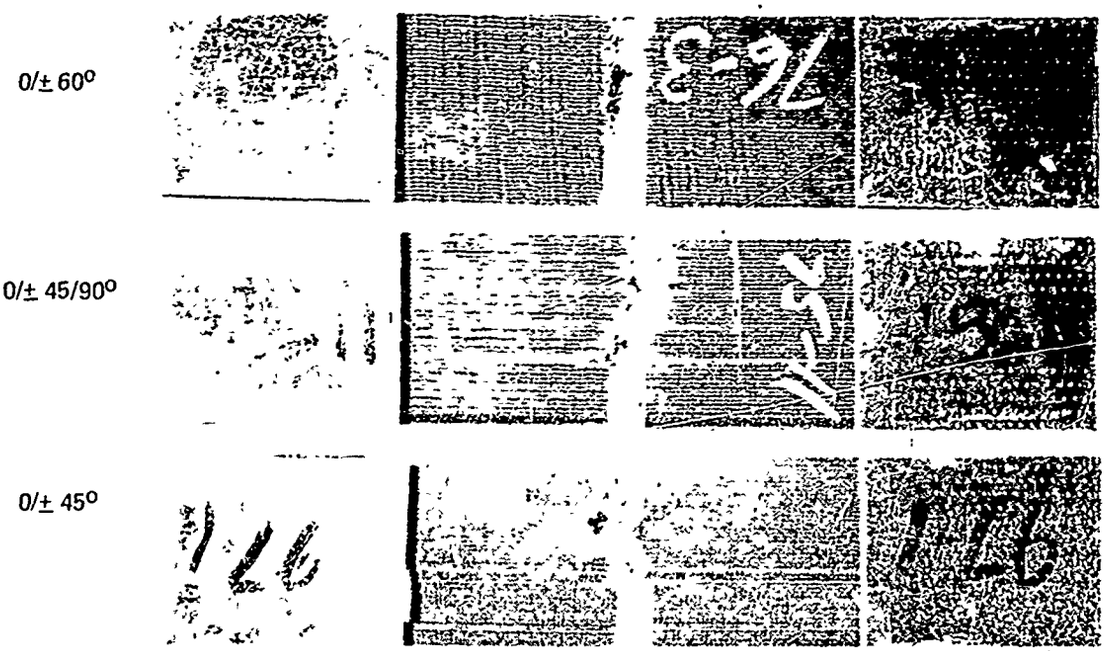

Figure 8a TYPICAL FRACTURE OF BORON EPOXY COMPOSITES SHOWING THE RELATIVELY FLAT FRACTURE SURFACE

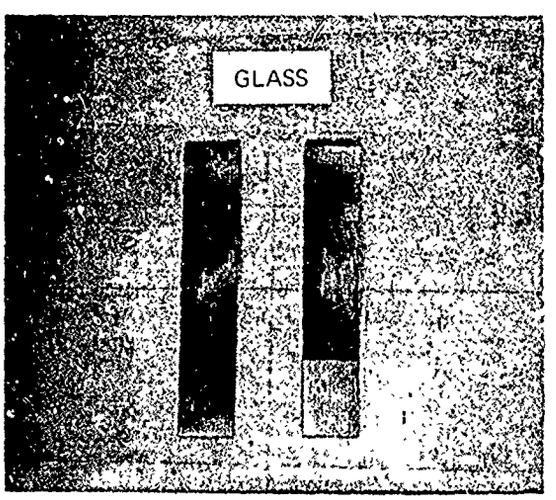

Figure 8b FRACTURE TOUGHNESS SPECIMENS OF GLASS/EPOXY

NOTE THE FIBROUS DELAMINATION SIMILAR TO THE BEHAVIOR OF THE LONGITUDINAL TENSION SPECIMENS (Figure 5).

No meaningful fracture toughness data could be obtained from the glass/epoxy composites. These specimens exhibited longitudinal cracking at the root of the notch as shown in Figure 8b. The specimens then failed as a tension specimen having a reduced cross section. The apparent toughness is greater than for any other composite tested which was also implied by data in the literature, (Reference 13).

All of the graphite/epoxy fracture toughness specimens failed by interply separation. This delamination was initiated at the crack tip and results in the behavior shown in Figure 9. The cause is felt to be low interlaminar shear strength which was not actually measured by implied by the behavior of the tensile specimens (See Figure 5). Consequently, the data is suspect. However, as will be shown, some correlation exists between the initial value of K and the residual strength of ballistically impacted panels. The data is presented in Appendix B and is summarized in Table 5.

3.2.2 Ballistic Characterization

3.2.3.1 Introduction

The objective of this phase of the program was to experimentally establish the "threshold strength" (the lowest prestress level at which the specimen will fail catastrophically when impacted by a bullet) and the residual strength (the strength after ballistic impact) of the advanced structural composites; specifically boron/epoxy and graphite/epoxy laminates.

In order to accomplish this the 8 in. wide and 22 in. long specimens were fitted with aluminum tabs (bonded using equal parts of Shell's Epon 812, Epon 828, General Electric's Versamid 115 and General Electric's Versamid 125) and preloaded in tension using a 50,000 pound capacity testing machine. The test setup is shown in Figure 10. The instrumentation used to monitor the test varied; in some cases strain gages were used to check the uniformity of load introduction and to determine modulus, other times strain gages were used in conjunction with a rapid sweep oscilloscope in an effort to study the plate dynamics, for other specimens high speed photography was used to capture the event in order to determine when cracking initiated and at what velocity the crack propagated.

The majority of the ballistic tests were performed using 30 caliber AP projectiles shot at either 2750 or 1250 fps. A limited number of tests were performed using 50 caliber AP projectiles traveling at 3000 fps. In all cases the projectile flight was stable and normal to the plane of the panels.

The preliminary tests were conducted on inexpensive materials, namely a 6061-T6 aluminum alloy and a 0/45 laminate made of glass reinforced epoxy, and served to check out the experimental techniques. The bulk of the testing, however, was performed on the high performance graphite and boron reinforced epoxy composites.

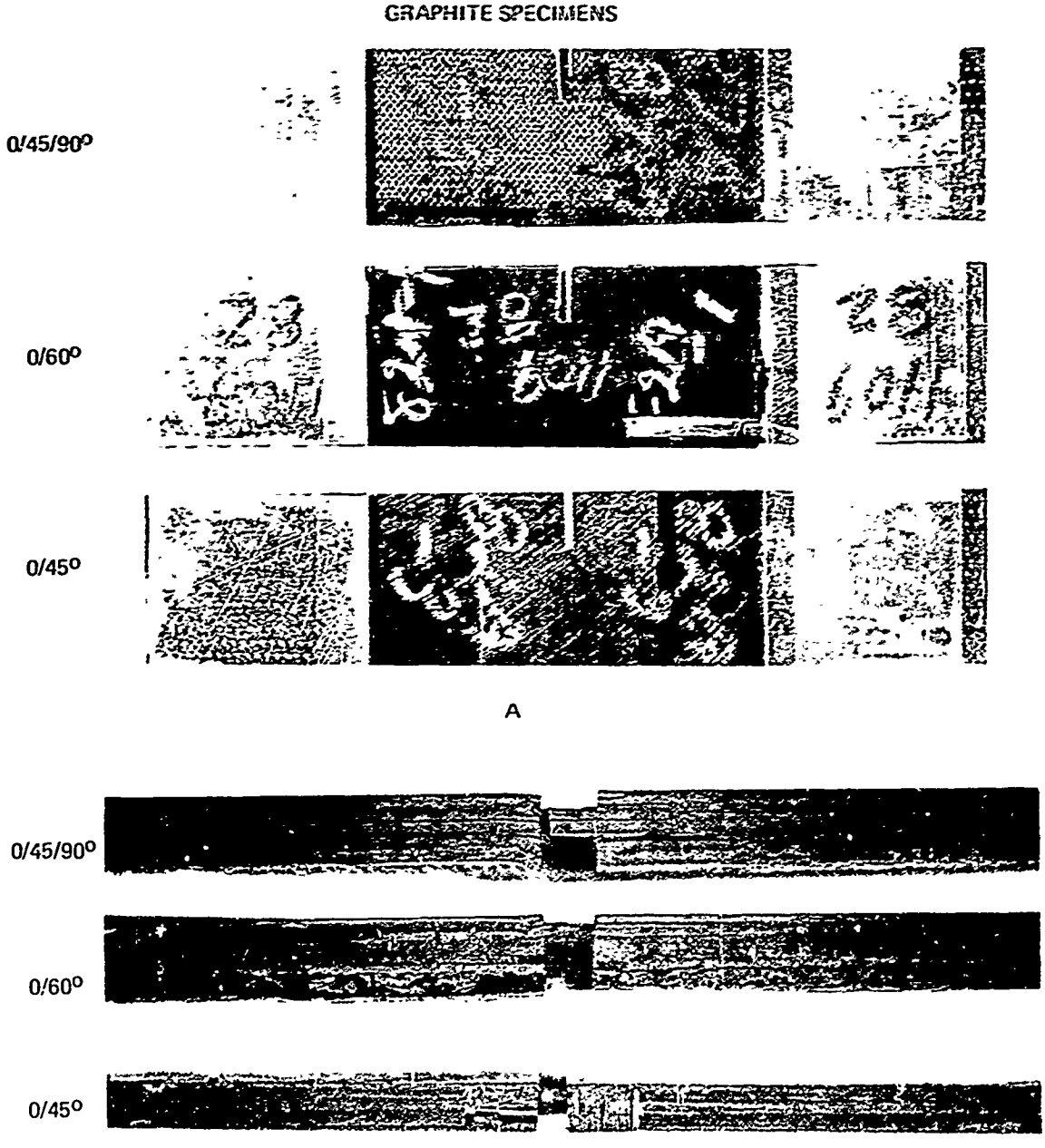

Figure 9 TYPICAL BEHAVIOR OF SINGLE EDGE NOTCH FRACTURE TOUGHNESS SPECIMEN OF GRAPHITE EPOXY

NOTE THE LACK OF A UNIFORM CRACK PATH (A) AND THE FORMATION OF INTERLAMINAR (CORE) FAILURE (B).

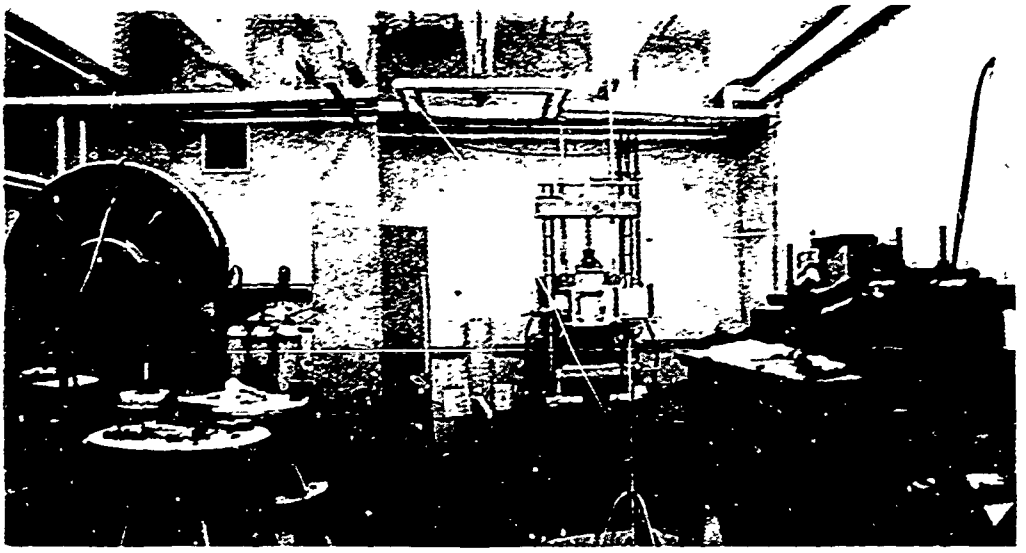

Figure 10 PHOTOGRAPH OF BALLISTIC TEST SETUP

AT THE LEFT IS THE BECKMAN WHITLEY CAMERA, IN THE CENTER IS A SPECIMEN LOADED BY THE BALDWIN TEST MACHINE, AND IN RIGHT (FOREGROUND) IS THE RIFLE.

3.2.3.2 Preliminary Studies

6061-T6 Aluminum Alloy

A total of 6 straight sided specimens 0.064 in. thick by 8 in. wide and oriented so that the rolling direction coincided with the load axis (See Figure 11) were tested. Two of the specimens had predrilled holes in the center of the gage section. These specimens were loaded monotonically to failure; the other four specimens were preloaded and shot with a 30 caliber AP projectile.

The first specimen (AL 1) had a 0.164 in. diameter drilled hole and had seven strain gages at locations indicated in Figure 12. As can be seen, the gages on the sides (numbers 1, 2, 3, and 4) experience nearly identical strains. Closer to the hole, gages 6 and 7 indicate identical strains which are slightly larger than the reading obtained at either side. Although the strains across the specimen are acceptably uniform as illustrated by gages 1, 2, 3, and 4, the slight eccentricity implied by this data was eliminated from all subsequent panels by the use of a modified fixture for aligning the tabs during the bonding operation. Table 6 indicates that specimen AL 1 failed at 20 kips or 39 KSI. Specimen AL 2 which had a slightly larger hole failed at 42 KSI. This material has a yield strength of 40 KSI and an ultimate of 45 KSI and the hole therefore has little effect as is expected.

Specimens AL 3 through AL 6 were preloaded and ballistically impacted. Each of these specimens was instrumented with at least two strain gages which were electronically tied to a Tektronic oscilloscope having a multiple channel plug-in. The scope was adjusted to read 300 μ in. strain per centimeter and set at a 2 micro second per centimeter sweep. The data was to have been used to provide some insight into the flexural and extensional behavior of the plate during the impact. Unfortunately none of the four experiments was successful; the electron beam intensity was not sufficient to get photographs and the trigger circuit did not operate properly. Specimens AL 6 and AL 4 were preloaded to 57% and 87% respectively of their yield strength prior to impact and as can be seen in Table 6 they did not fail upon impact; each could subsequently be loaded to the yield strength. Specimens AL 3 and AL 5 were loaded to the yield strength prior to impact. These specimens too sustained the impact and could carry a slight additional load prior to failure. High speed photography captured the event, but since it was not dramatic it has not been reproduced. Petaling was observed on the exit side but the damage was not severe and, as substantiated by the static tests after impact, the material was still capable of being loaded to its yield strength.

A typical final failure is shown in Figure 13. If the true residual strength of this material is desired, it would be necessary to determine it after cyclic loading. The endurance limit of 6061-T6 is only 14 KSI and after 10^5 cycles at 14 KSI if this material were to sustain a "hit" it is not likely that it would have any significant residual strength.

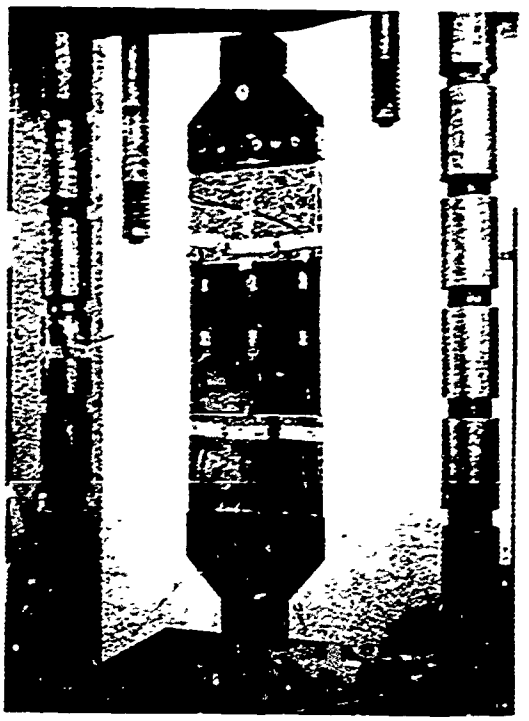

Figure 11 TYPICAL TEST SETUP FOR THE 6061-T6 ALUMINUM PANELS SHOWING THE INSTRUMENTATION

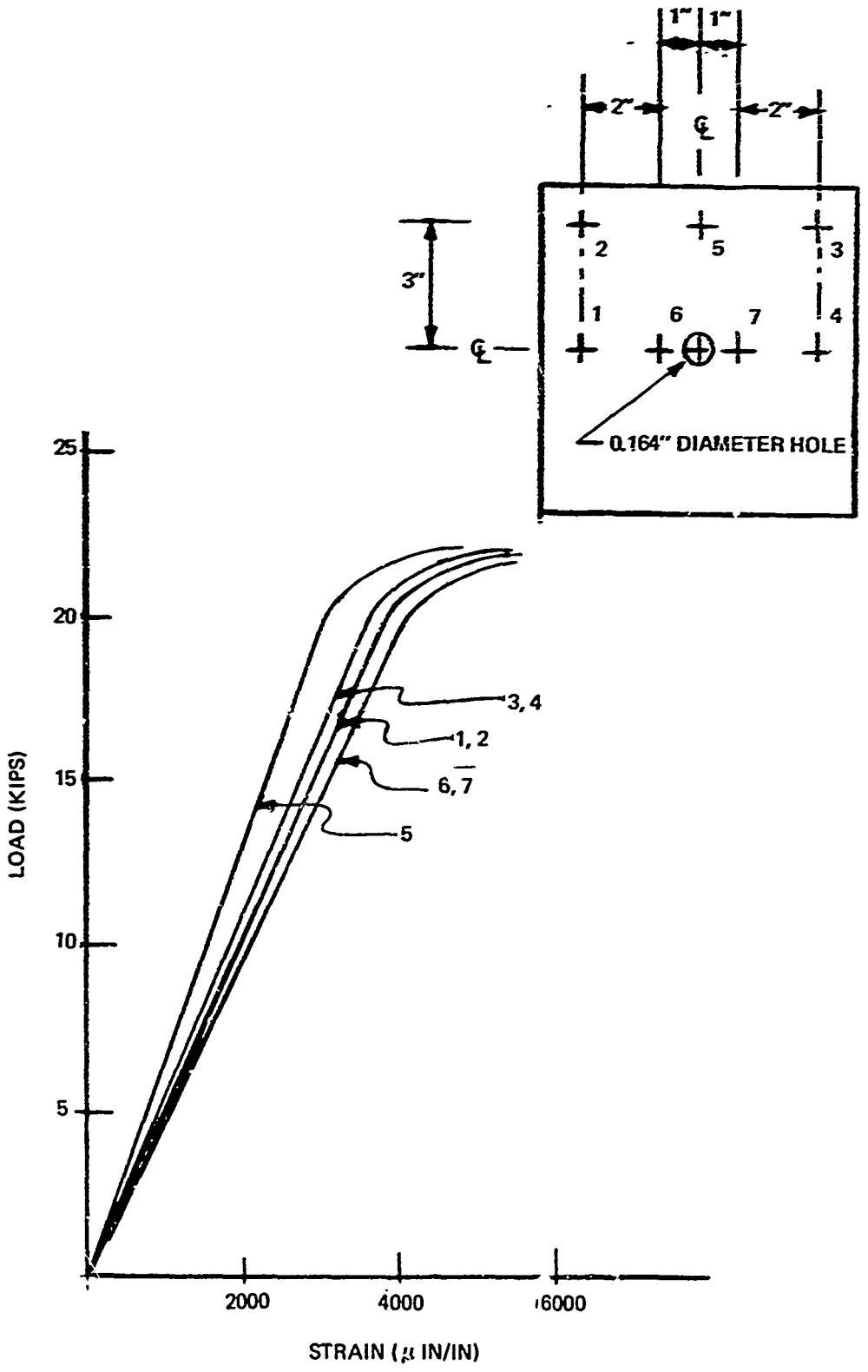

Figure 12 RESPONSE OF ALUMINUM PANEL A.. 1 CONTAINING A 0.164 IN. DIAMETER HOLE

TABLE 6

BEHAVIOR OF 6061-T6 ALUMINUM ALLOY

Panel (Specimen Designation)	Modulus ($\times 10^6$ psi)	Static Test (Strength) KSI	Ballistic Tests 30 Caliber - 2750 fps		Remarks
			Preload (KSI)	Residual Strength (KSI)	
AL1	10.7	39			0.164 in. drilled hole
AL2		42			0.250 in. drilled hole
AL3			40	41	
AL4			35	41	
AL5			40	41	
AL6			23	40	

Figure 13 TYPICAL FAILURE OF 6061-T6 ALUMINUM PANELS

THE RESIDUAL STRENGTH OF THIS MATERIAL IS EQUAL TO ITS YIELD STRENGTH.

Glass/Epoxy

Two types of laminates were manufactured from unidirectional S glass/Epoxy prepreg. These were 8 ply (0, +45, -45, 0) sym. and 12 ply (0, +45, -45, +45, -45, 0) sym. panels having a thickness of 0.045 and 0.059 in. respectively.

The eight ply specimens were the first to be tested. Of these the first three were straight sided and had predrilled holes. Specimen 1117-63B had a 0.300 in. diameter hole. The strain gage data is given in Figure 14 and as can be seen gages 1, 2, and 3 give nearly identical readings indicating uniform load introduction. Gage 4 is within one hole radius of the predrilled hole and therefore, as expected experiences increased strains. This specimen could not be loaded beyond 21,000 pounds because of tab failure. Specimen 1117-62A was identical and exhibited similar behavior up to 17,500 pounds at which point tab failure occurred. Specimen 1117-62B had a 0.104 in. diameter hole; deformation was as anticipated up to 9900 pounds where tab failure occurred. Panel 1117-63A was a preloaded to 16,000 pounds (46.5 KSI) and shot with a 30 caliber AP projectile (muzzle velocity). The specimen did not fail upon impact; however, as with the aluminum panels no scope trace was left on the film. Monotonic loading to determine the residual strength was aborted by tab failure of 20,000 pounds (58 KSI). In the four cases described, the tests were prematurely ended due to tab failure. In order to lessen the total tab load and hence the shear stress in the tab adhesive a contoured specimen (See Figure 15) was used. This specimen, 1117-64 failed first by shearing at the contour radii and then by tab failure at 15,800 pounds.

It was obvious that the load introduction scheme provided uniform strain throughout the gage section however it was impossible to load the specimens to their ultimate strength due to the combination of tab design and adhesive strength. The 12 ply panels were all contoured and several tab variations were investigated which are shown in Figure 16. (A more complete description is given in Appendix C). None of these substantially increased the total load which could be introduced into the specimen (23,000 pounds). More severe cross section reductions merely increased the propensity for longitudinal splitting as shown in Figure 17. It was therefore decided to perform the ballistic tests under preload, using the standard tab configuration with clamps (Figure 15), observe the ballistic damage, and continue to load until tab failure occurred. Of the seven remaining 12 ply glass/epoxy laminates prepared, four were used for 30 caliber, and three for the 50 caliber firings. The data is summarized in Table 7 where it can be seen that two of these specimens failed during the preloading, due to tab failure.

The panels which were ballistically tested were loaded to between 28 to 58% of their ultimate (limited by tab failure). None of these panels failed by parting in two during impact. Damage typical of a 30 caliber (and similar for 50 caliber) AP projectile is given in Figure 18. There is gross delamination on the exit side but this delamination is independent of preload level and increases only slightly with the larger projectile. Again, due to load introduction problems, the residual strength could not be determined; however loads up to 72% of ultimate did not cause failure.

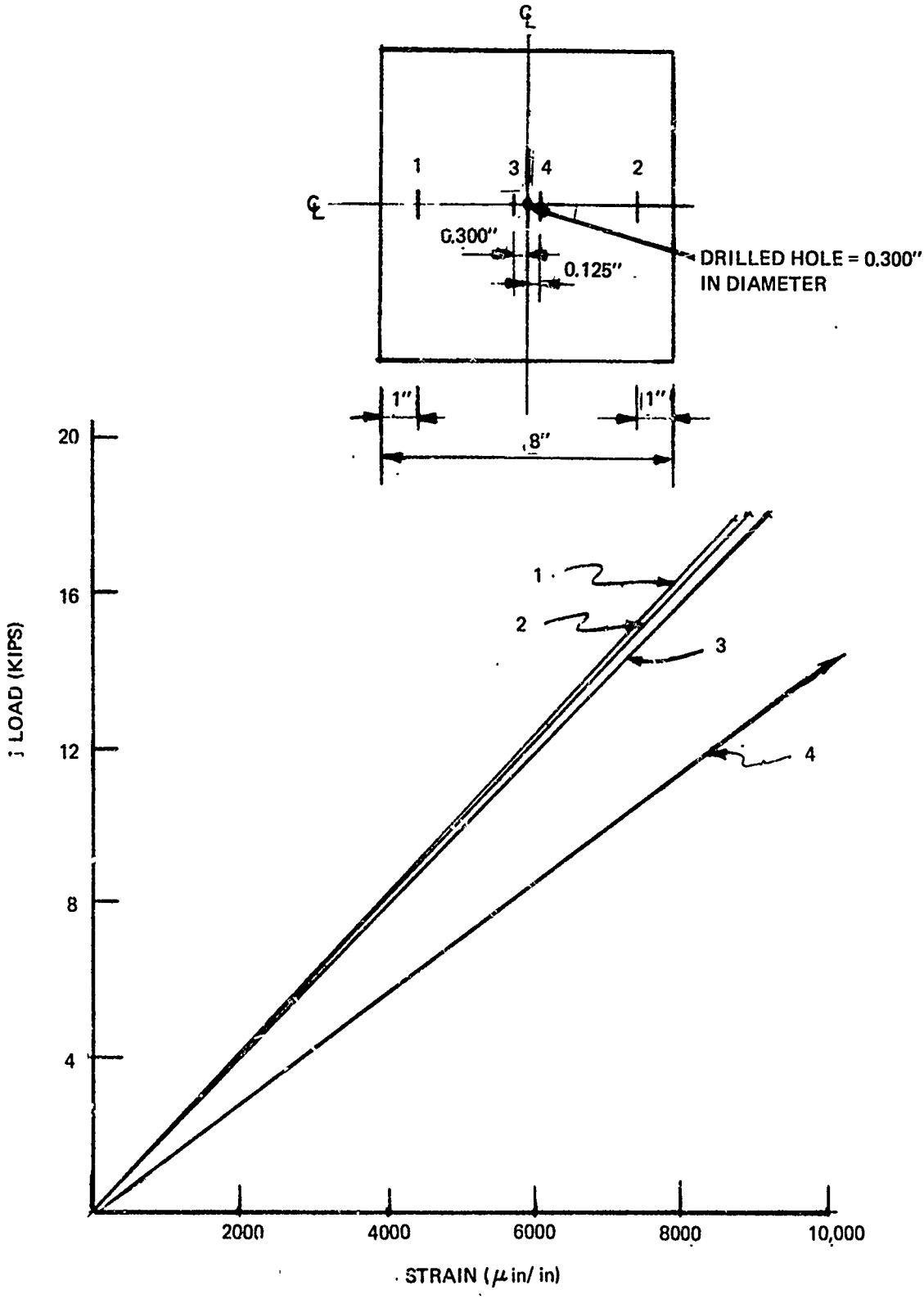

Figure 14 RESPONSE OF PANEL 1117–63B – AN 8 PLY, 0/45, GLASS/EPOXY LAMINATE WITH 0.3 IN. DIAMETER HOLE

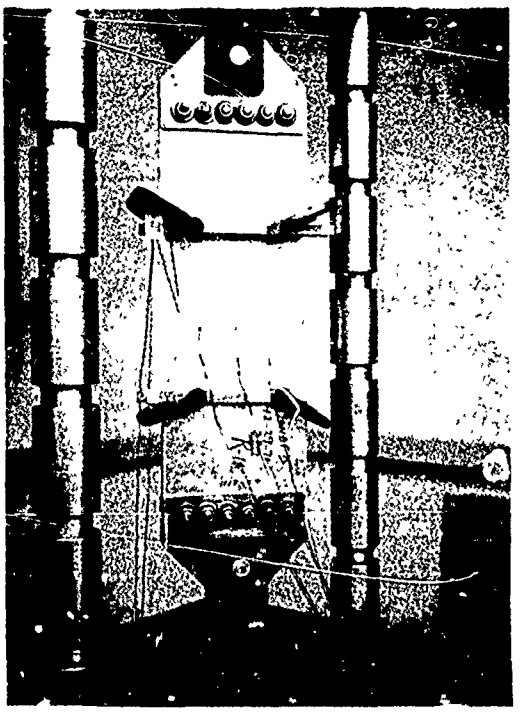

Figure 15 INSTRUMENTED 0/±45 GLASS LAMINATE WITH "C" CLAMPS ON TABS

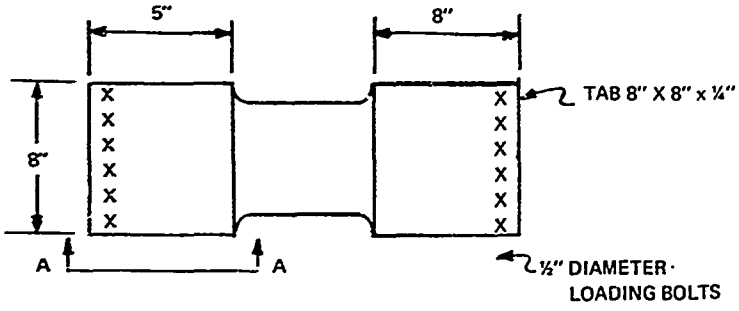

TOP VIEW OF SPECIMEN

BELOW ARE TAB CONFIGURATIONS – SECTION A–A

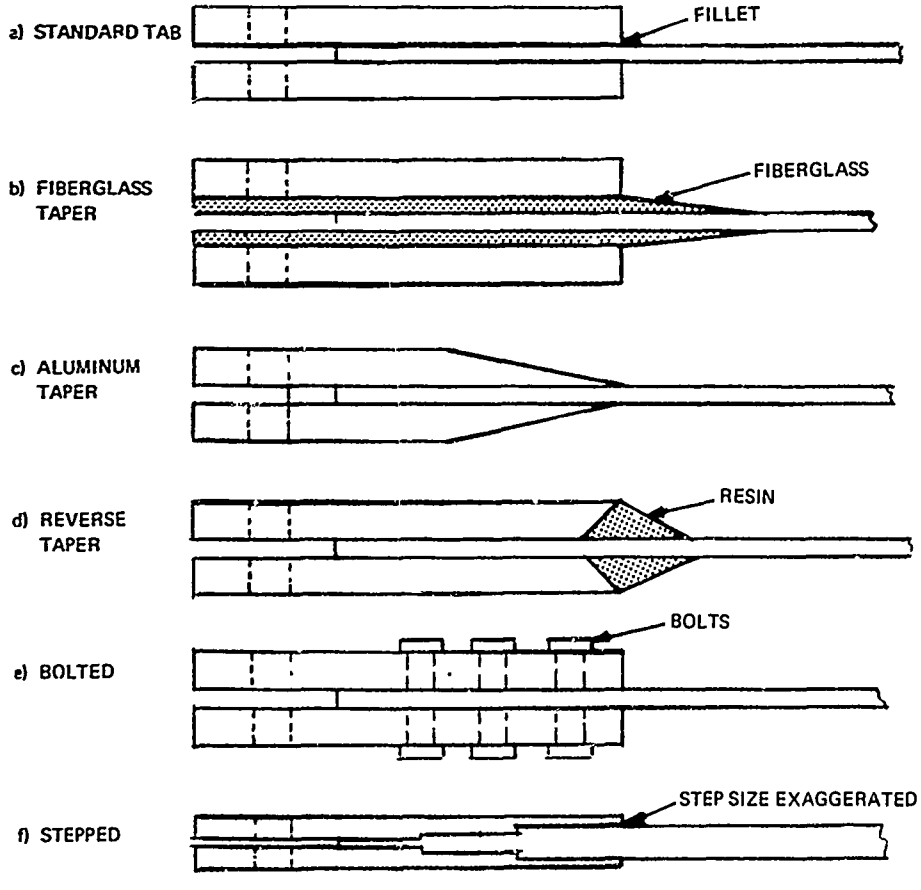

Figure 16 TAB CONFIGURATIONS FOR THE GLASS/EPOXY PANELS

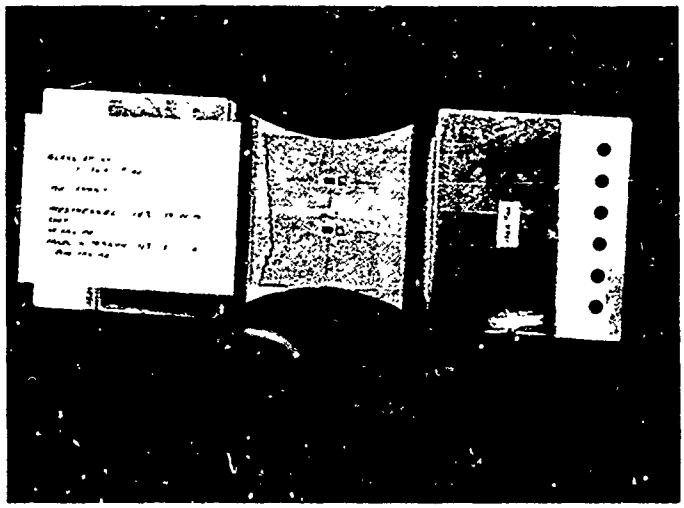

a. ENTRANCE SIDE

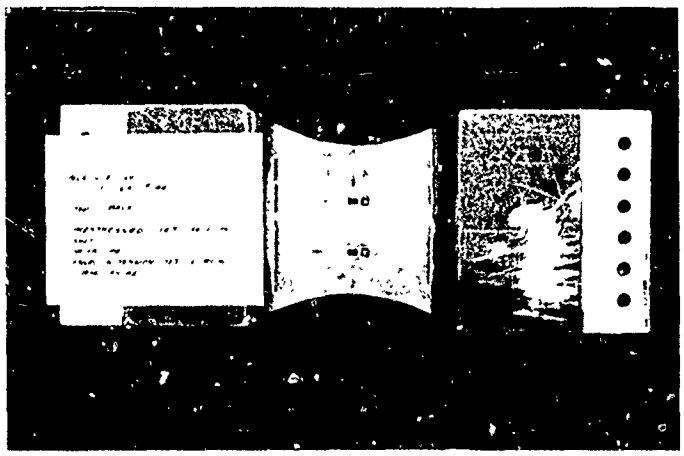

b. EXIT SIDE

Figure 17 ACCENTUATED CONTOUR SPECIMEN

SHEAR FAILURE (WHITE REGION) OCCURRED ALONG A LINE TANGENT TO THE CONTOUR AT THE MID SECTION. FINAL FAILURE OCCURRED AT THE TAB (LEFT SIDE OF TOP PHOTO).

TABLE 7

BEHAVIOR OF GLASS/EPOXY COMPOSITES

Specimen Designation	Type	Thickness (inches)	Modulus ($\times 10^6$ psi)	Static Tests* Load (kips)	Static Tests* Stress (KSI)	Ballistic Tests** Preload (kips)	Ballistic Tests** Preload (KSI)	Ballistic Tests** Residual Strength (kips)	Ballistic Tests** Residual Strength (KSI)	Remarks
0/45 - 8 Ply	UTS =	150 KSI								
1117-62A	A	0.048	4.3	17.5	45.6					drilled hole = 0.3 in. in diameter
62B	A	0.045	4.7	9.9	27.5					drilled hole = 0.14 in. in diameter
63A	A	0.043				16.0	46.5	20.0	58	30 cal - 2750 fps
63B	A	0.043	5.5	21.0	61.0					
64	B	0.040		15.8	65.8					drilled hole = 0.3 in. in diameter
0/45 - 12 Ply	UTS =	100 KSI								
1117-120A	A	0.055				21.5	48.9	ND***		50 cal - 3000 fps
120B	A	0.055				12.4	28.2	ND***		50 cal - 3000 fps
121A	B	0.057	5.8			17.0	49.7	ND***		30 cal - 2750 fps
121B	A	0.055				18.0	40.9	ND***		50 cal - 3000 fps
122A	B	0.056				19.0	56.5			failed during preload
122B	-	0.055								damaged during machining
123A	-	0.055								coupon tests
123B	B	0.059	5.0			16.0	45.2			failed during preload
136A	C	0.057				17.1	54.7	21.2	67.5	30 cal - 2750 fps

Type A = Straight Sided - 8 in. Width
B = Contoured - 6 in. Width
C = Contoured 5.5 in Width

*Not a true static strength - tab failure occurred in all cases.
**Not a true residual strength - tab failure occurred in all cases.
***ND means not determined - saved for visual inspection.

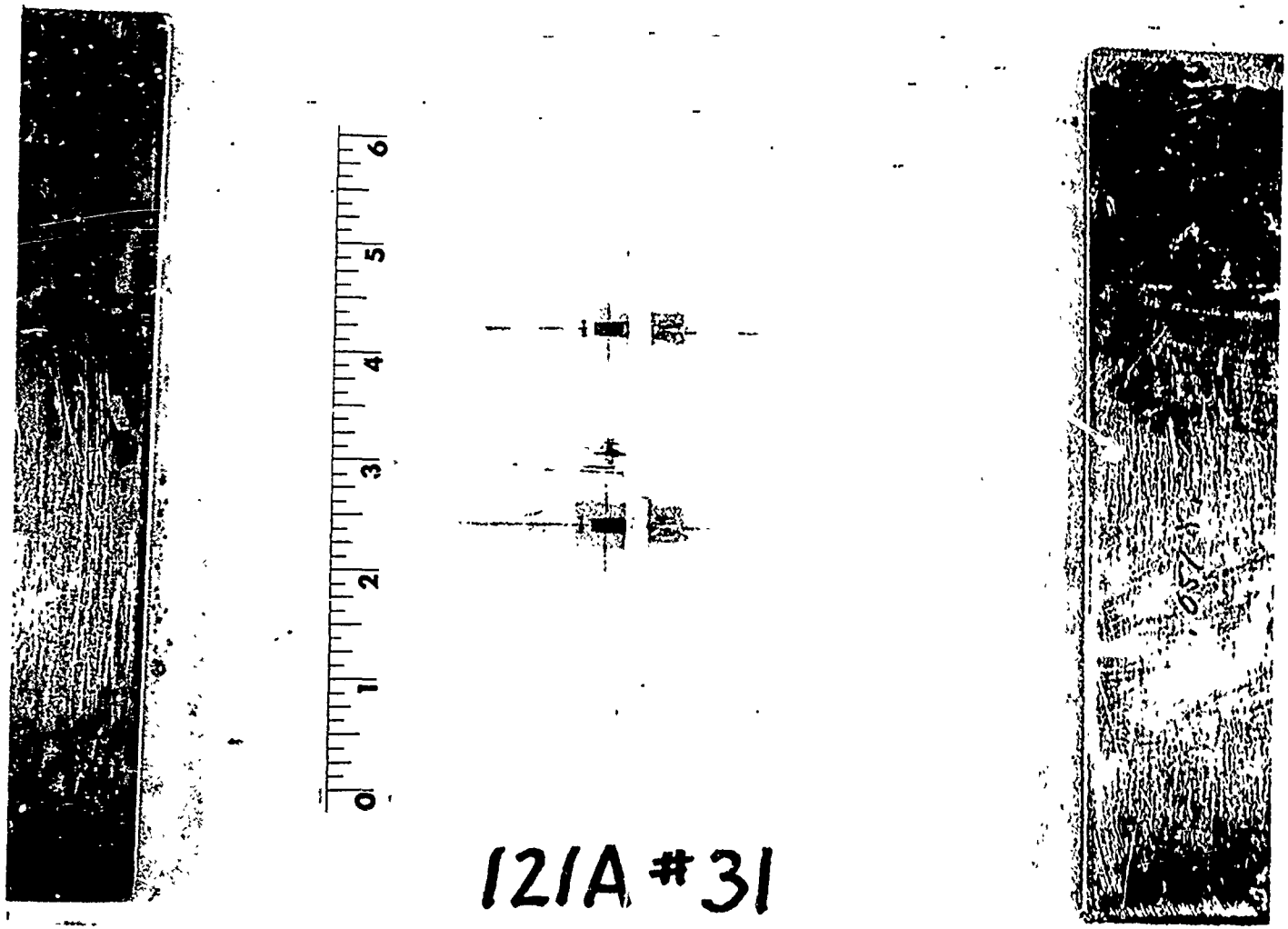

ENTRANCE – A

Figure 18a, TYPICAL DAMAGE OBSERVED WITH GLASS/EPOXY PANELS
LIGHT REGIONS INDICATE DELEMINATION.
a) DAMAGE AT ENTRANCE

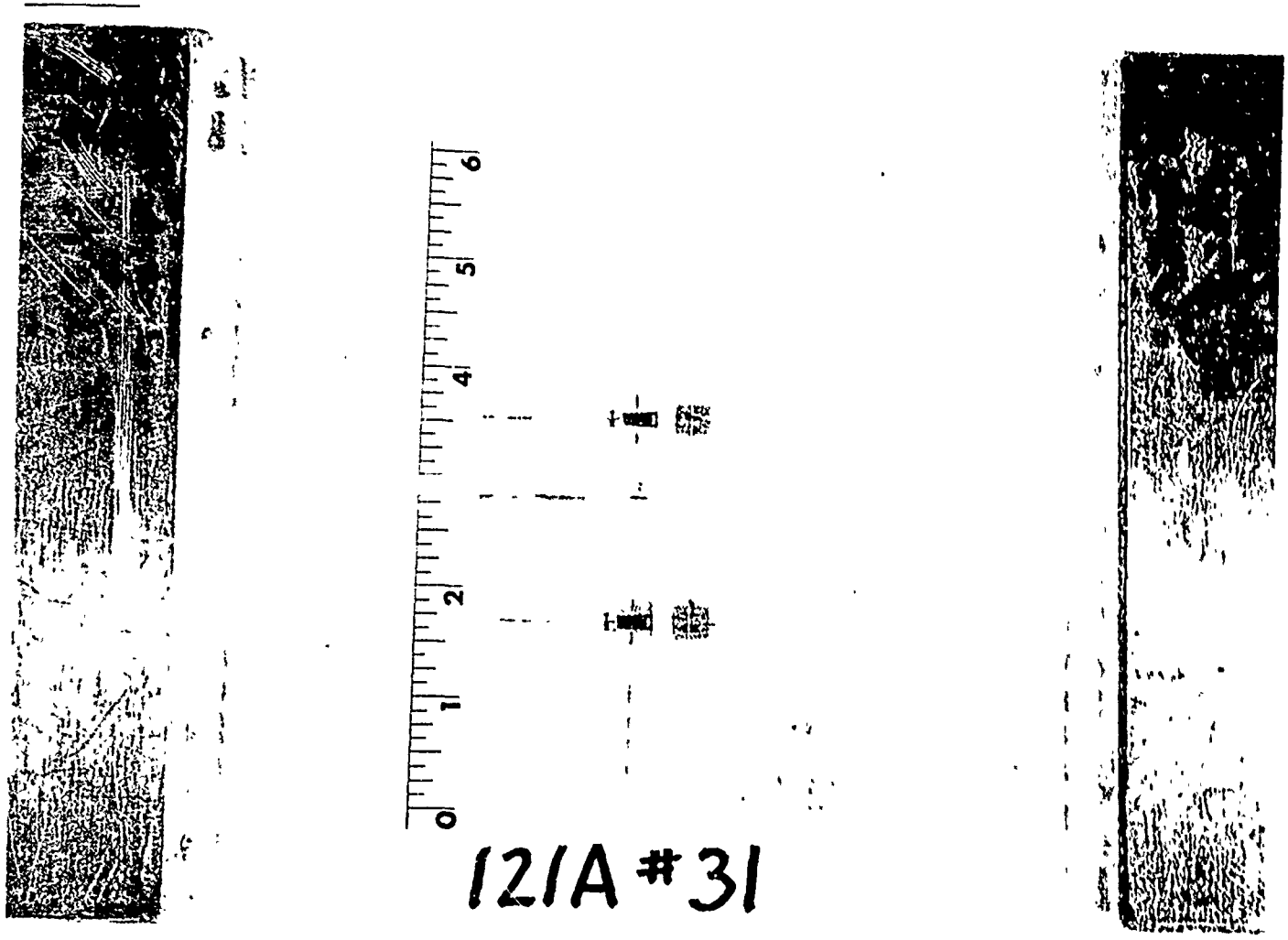

EXIT – B

Figure 18b. TYPICAL DAMAGE OBSERVED WITH GLASS/EPOXY PANELS

LIGHT REGIONS INDICATE DELAMINATION.
b) DAMAGE AT EXIT SIDE

For the type of tests performed, this glass/epoxy composite appears to have a high residual strength. However, glass/epoxy has a low endurance limit and hence cyclic loading would be required to establish a realistic residual strength level. Had the testing included compression, failure due to local buckling could have occurred at a low load level because of the massive delamination.

3.2.3.3 Behavior of Advanced Composites

Graphite/Epoxy

Four of the 36 graphite/epoxy panels manufactured were used for coupon tests; the remainder were used for ballistic studies. The panels, their stacking sequence, thickness and material properties are described in Tables 1 through 5. This section describes first, the physical response of the panels and second, the data in terms of threshold and residual strengths.

Upon final failure, irrespective of whether the panels failed upon impact or sustained the penetration and was subsequently loaded to failure, low to moderate delamination was observed as shown in Figures 19 and 20. This is indicative of the low interlaminar shear strength which was observed and discussed earlier. Several panels failed in the gage section prematurely during the preloading and exhibited the same magnitude of delamination suggesting that this phenomena was not introduced by the impact of the bullet.

Below the threshold level a rather clean hole was formed by the projectile. A typical example, where both the entrance and exit side of panel 1117-76B, is shown in Figure 21. This panel was prestressed to 63% of its UTS and shot with a high velocity AP projectile. The damage was limited to a small region around the periphery of the hole and several small longitudinal cracks in the surface plys. This is in great contrast to the massive delamination which occurs with the glass/epoxy composites. The damage shown in Figure 21 is typical regardless of the projectile velocity.

As a result of studying the high speed photographs it was found that when the panel failed upon impact the actual crack did not start to grow until the projectile reached its full diameter. This is perhaps due to the fact that the stress levels were not significantly higher than the threshold level. A typical example is shown in Figure 22 where panel 1117-75B can be seen being perforated by a low velocity (1250 fps) 30 caliber AP projectile. This behavior, however, was independent of projectile velocity. If the prestress were significantly higher than the threshold limit perhaps the crack would begin to grow prior to full tip penetration. From consecutive frames of the high speed photographs the crack velocity for this $0 \pm 45^{\circ}$ graphite panel was determined to be approximately 8500 fps. This is 55% of the acoustic wave velocity in the transverse (90°) direction as calculated from Renter's analysis (Reference 24); using the elastic properties given in Table 4 and the average density given in Table 3, Reuter's solution predicts the acoustic wave velocity to be 15,000 fps for this panel.

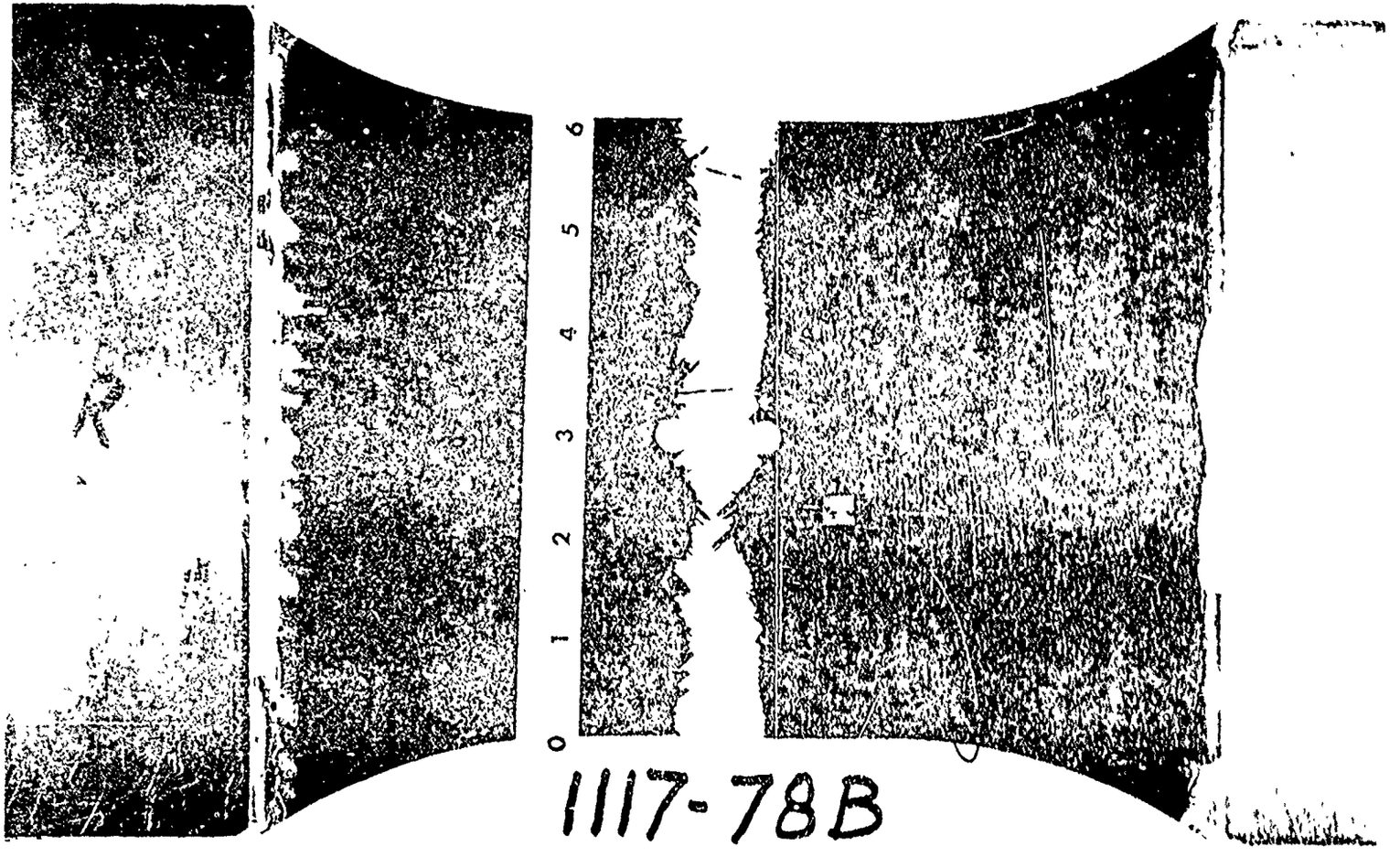

Figure 19 PHOTO SHOWING FRACTURE SURFACE AFTER RESIDUAL STRENGTH TEST OF SPECIMEN 1117-78B (GRAPHITE/EPOXY)

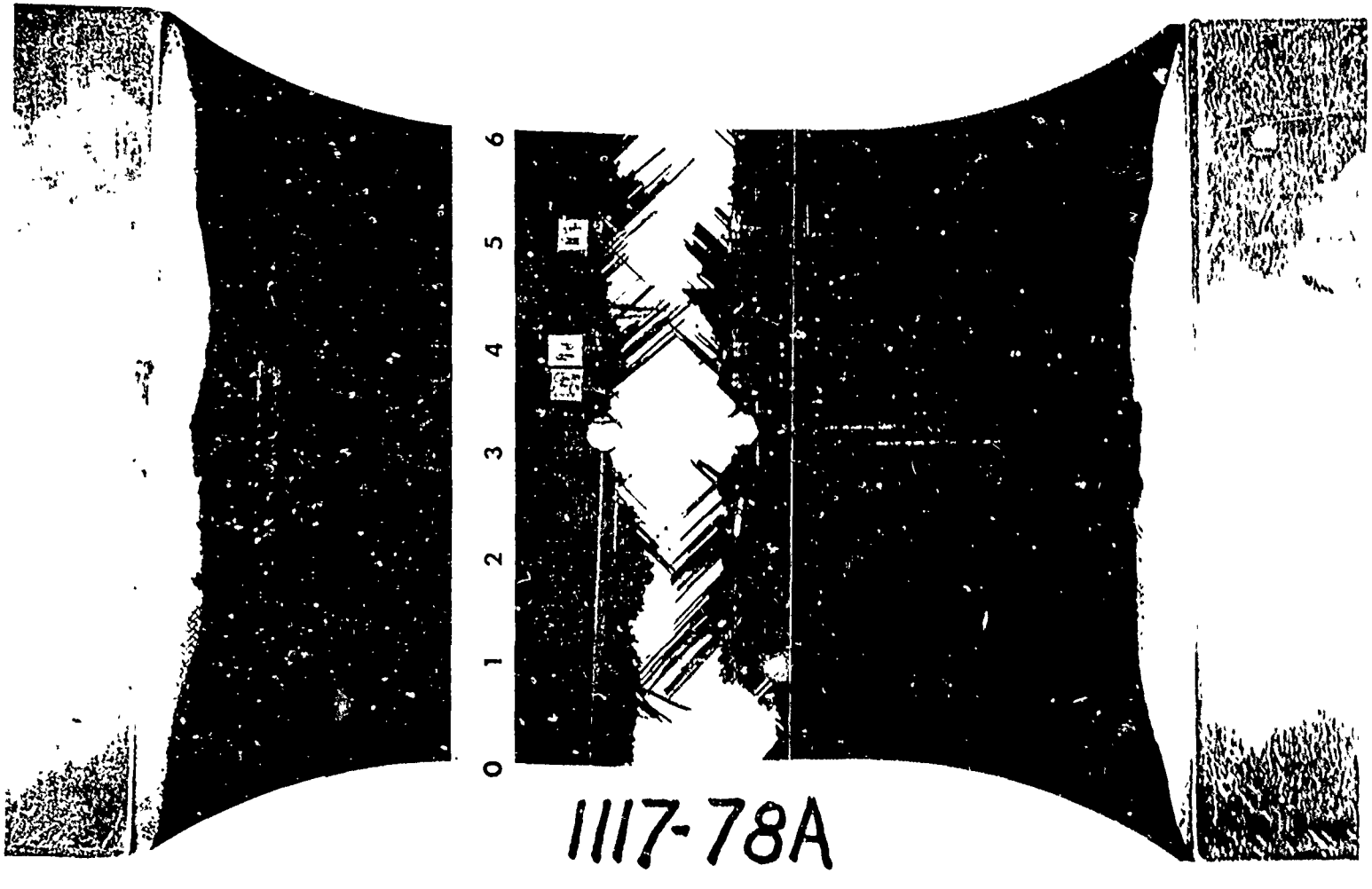

Figure 20 PHOTO OF PANEL WHICH FAILED UPON IMPACT
(1117-78A GRAPHITE/EPOXY)

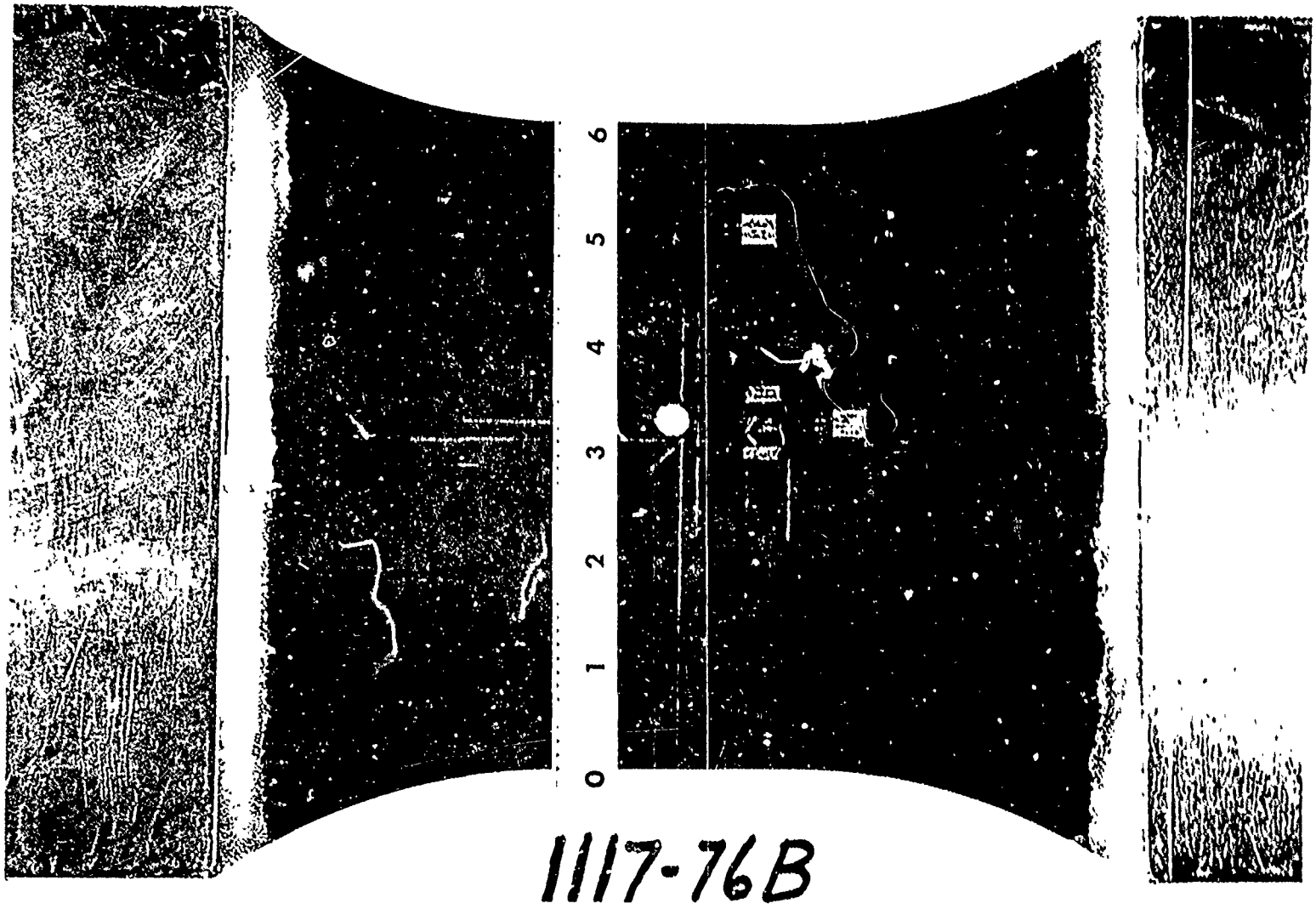

Figure 21 EFFECTS OF PROJECTILE ON GRAPHITE/EPOXY
PANEL 1117 76B WAS PRESTRESSED TO 63% OF ITS UTS AND SHOT WITH A 30 CALIBER AP PROJECTILE. NOTE THE RELATIVELY CLEAN HOLE AND ABSENCE OF DELAMINATION ON BOTH THE ENTRANCE SIDE (a) AND EXIT SIDE (b).

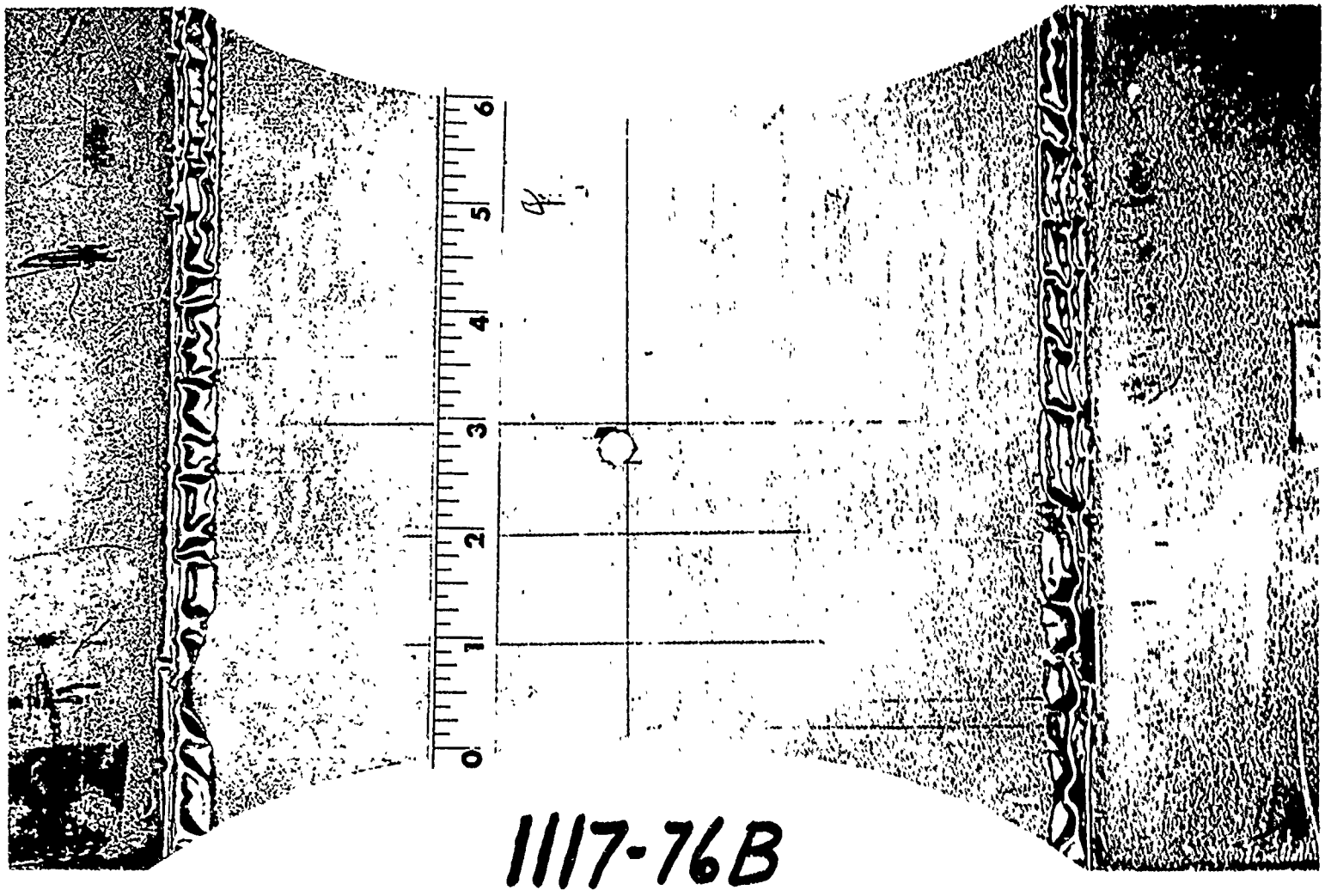

Figure 21 Continued EFFECTS OF PROJECTILE ON GRAPHITE/EPOXY
(b) EXIT SIDE

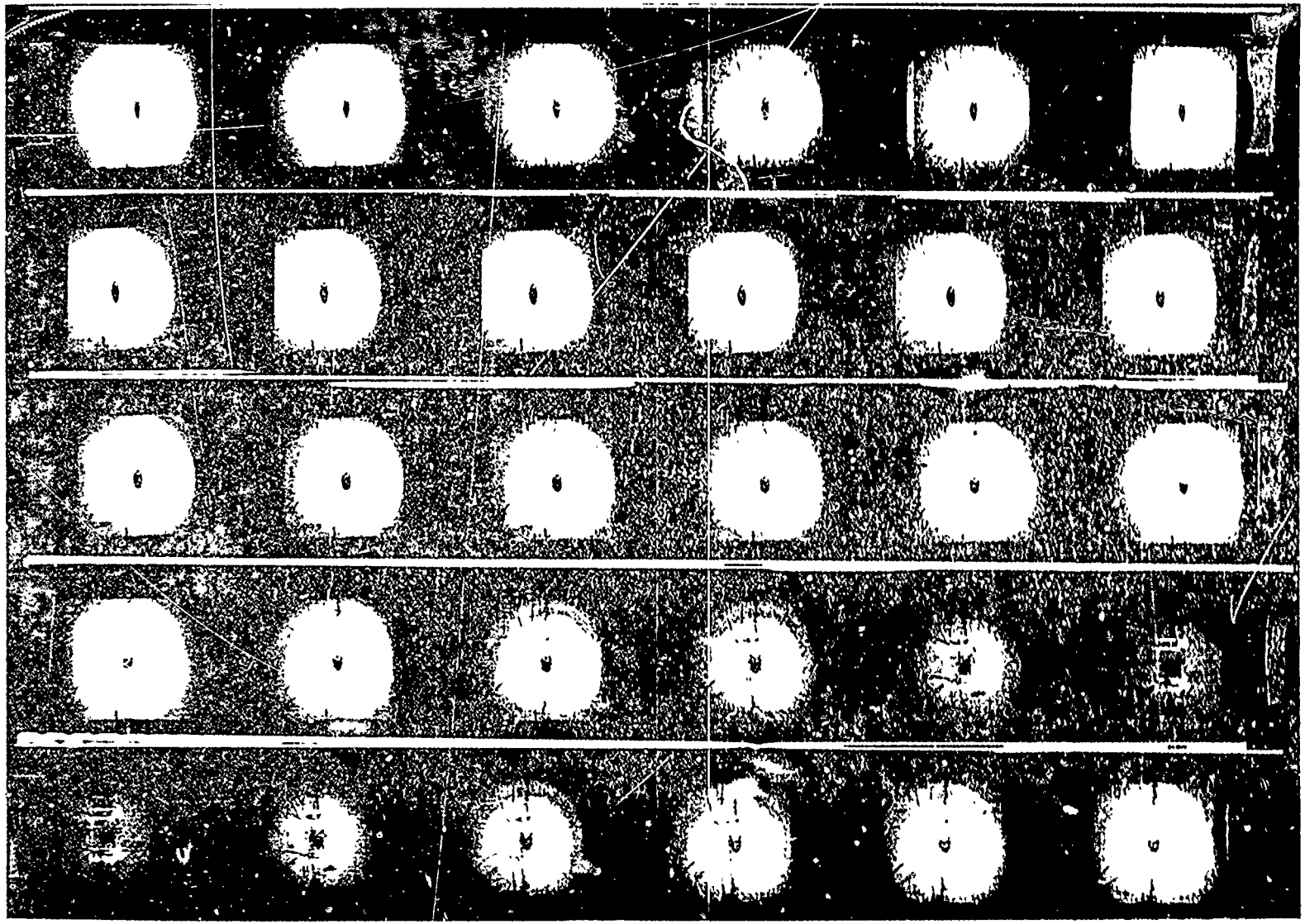

Figure 22 HIGH SPEED PHOTOGRAPHS OF IMPACT FAILURE OF SPECIMEN 1117 75B PROJECTILE VELOCITY WAS 1250 FPS AND TIME BETWEEN FRAMES IS 2.30×10^{-6} SECONDS. CRACK VELOCITY IS APPROXIMATELY 8500 FPS.

One 0/60 and one 0/45/90 panel was used for the 50 caliber tests. These panels were loaded to approximately 20 KSI and neither failed upon impact. Typical response is shown in Figure 23. The final failure of this specimen is shown in Figure 24 and although the delamination appears to be severe it is within the general range observed with this material. The residual strengths were not substantially lower than those found after perforation by the 30 caliber bullets.

The lighting for the photograph shown in Figure 23 permits the slight delamination of the surface ply on the exit side to be seen. The debris (Figure 23) is also clearly visable. It appears to develop into the form of a cone which moves rather slowly with respect to the projectile; it also grows in diameter, apparently with a diminishing average density.

The complete test results are presented in Table 8 and are summarized (for the 30 caliber data) in Table 9. No threshold strengths were obtained for the 0/45/90 and 0/60 layups due to the fact that a very limited number of panels of this type were fabricated of which several were lost during the preload stage at unusually low stresses. As can be computed from data in Table 9 the residual strengths vary from 61% to 73% of the true UTS depending upon the layup. The threshold strengths were slightly lower and range from a value of no less than 51% to 65%. On an absolute basis the residual strength and threshold strength of only the 0/45 laminate was better than the 6061-T6 aluminum alloy but on a specific basis (aluminum has a specific strength of 4×10^5 in.) all layups of graphite tested were superior to the aluminum.

Boron/Epoxy

Three of the 28 boron/epoxy panels were used for coupon testing; the remaining 25 were ballistically tests. The specific panels, their stacking sequence and material properties, are listed in Tables 1 through 5. In general, the behavior of the panels was similar to the graphite, however, the absolute values of the strengths were higher and the delamination was less pronounced.

The boron/epoxy panels, regardless of layup and regardless of whether final failure occurred during impact or as a result of additional loading of panels which had been shot, exhibited a relatively straight crack path with essentially no delamination as compared to the graphite composites. A slight amount of damage occurred at the exit surface as is shown in Figure 25. This damage is limited to the outer 0° ply. This overall behavior is identical regardless of projectile size, velocity, and preload.

At the "threshold strength" the panels failed upon impact. As can be seen in Figure 26 the crack began to grow then the projectile reached its full diameter. The behavior is similar when a 50 caliber AP projectile was used as can be seen in Figure 27.

Crack propagation velocities were determined from photographs of panels 1117-94A (a 0/45 laminate), 1109-69 and 1108-71 (0/45/90 laminates) and 1109-74A (a 0/60 laminate). The measured velocities were, in the order given above, 7200, 5600, 5800, and 4700 fps. Hence, the crack velocity in all cases was less than that observed in the graphite/epoxy laminate. Reuter's analysis (Reference 24) shows the acoustic wave velocities in the 90° direction (the direction corresponding to crack extension) to be 14,000 fps, 20,000 fps and 23,600 fps for the 0/45, the 0/45/90 and the 0/60 laminates respectively.

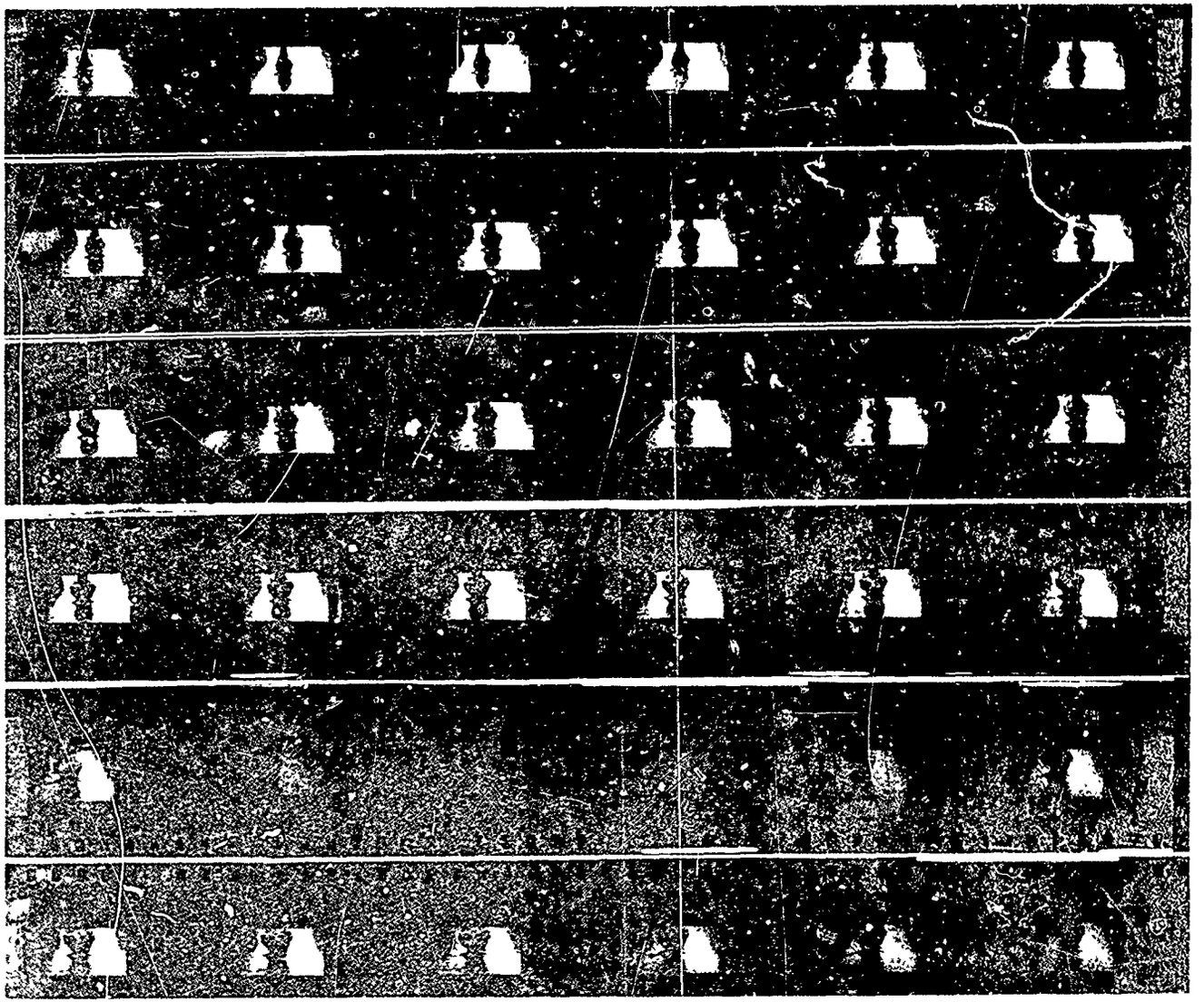

Figure 23 RESPONSE OF A 0/60 GRAPHITE/EPOXY PANEL (SPECIMEN 1109-78) TO A 50 CALIBER AP PROJECTILE
PROJECTILE VELOCITY IS 2980 FPS, TIME BETWEEN FRAMES IS 2.14×10^{-6} SECONDS

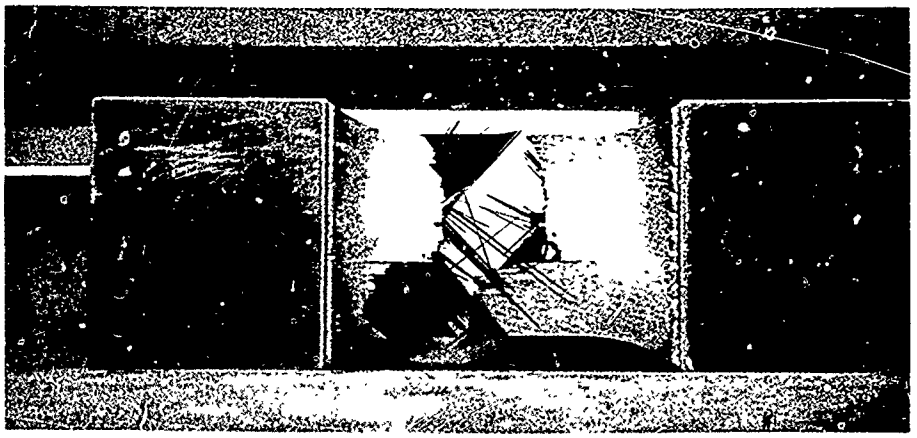

a

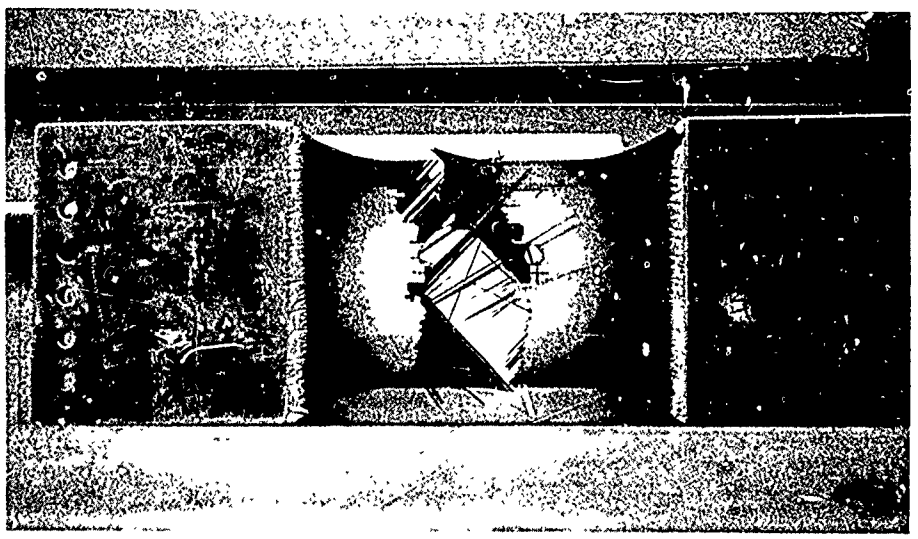

b

Figure 24 FINAL FAILURE OF SPECIMEN 1109-78 A 0/60 GRAPHITE/EPOXY PANEL IMPACTED WITH A 50 CALIBER PROJECTILE

a) ENTRANCE b) EXIT SIDE

TABLE 8

BEHAVIOR OF GRAPHITE/EPOXY

Specimen Designation	Type	Thickness (inches)	Modulus ($\times 10^6$ psi)	Preload (KSI)	Projectile (Caliber)	Failed on Impact	Residual Strength (KSI)	Remarks
0/45 - 8 Ply	UTS = 71 KSI							
1117-61A	- -							Coupon Tests
61B	B	0.051		40.8	30/HV	yes		Bad Panel
66A	B	0.051		29.4	- - -			Failed during preload
66B	B	0.051		31.9	- - -			Failed during preload
67A	B	0.051		44.8	30/HV	no	50.3	
67B	B	0.051		20.6	- - -			Failed during preload
72A	B	0.051		47.7	30/LV	yes		
72B	B	0.051		48.4	30/LV	yes		
73A	B	0.051		47.1	30/LV	no	57.2	
73B	B	0.051		47.4	30/HV	yes		
75A	B	0.052		44.9	30/LV	no	51.3	
75B	B	0.051		51.3	30/LV	yes		
76A	B	0.051		48.4	30/LV	no	52.6	
76B	B	0.051	18.2	44.9	30/HV	no		Saved for inspection
77A	B	0.052		49.8	30/LV	yes		
77B	B	0.048	20.7	46.2	30/LV	yes		
78A	B	0.051	18.5	48.3	30/HV	yes		
78B	B	0.052	21.0	41.0	30/HV	no	48.0	
82A								Coupon Tests
82B	A	0.050	18.5	37.5	- - -			Failed during preload
83A	B	0.052		38.5	- - -			Failed during preload
83B	B	0.052		46.5	30/LV	yes		

Type A = Straight Sides 8 in. Width
B = Contoured 6 in. Width
C = Contoured 5.5 in. Width

HV = High Velocity = 2750 fps
LV = Low Velocity = 1250 fps

TABLE 8 CONTINUED

Specimen Designation	Type	Thickness (inches)	Modulus ($\times 10^6$ psi)	Preload (KSI)	Projectile (Caliber)	Failed on Impact	Residual Strength (KSI)	Remarks
0/45/90 - 10 Ply	UTS = 57 KSI							
1117-78	B	0.072	18.9	23.1	50/HV	no	35.2	
85A	B	0.072		14.7	30/HV	no	19.6	Bad Panel
85B	B	0.072		15.0	30/HV	no	18.1	Bad Panel
86A	B	0.072		29.2	30/HV	no	35.9	
86B	B	0.072		19.7	30/HV	no	37.0	
87A	- -	0.072						Coupon Test
87B	B	0.072		13.1	- - -			Failed during preload
0/60 - 10 Ply	UTS = 53.6KSI							
1117-77	B	0.072	16.2	20.8	50/HV	no	29.4	
82A	- -	0.072						Coupon Test
82B	B	0.072	14.8	30.1	30/HV	no	37.5	
83A	B	0.072						Delaminated during machining
83B	B	0.072	14.5	21.0	- - -			Failed during preload
84A	B	0.072	14.9	16.2	- - -			Failed during preload
84B	B	0.072	15.0	27.8	30/HV	no	31.7	

TABLE 9

THRESHOLD AND RESIDUAL STRENGTH OF GRAPHITE/EPOXY - 30 CALIBER

Material	Coupon UTS (KSI)	True UTS (KSI)	Residual Strength (KSI)	Specific Residual Strength (inches)	Threshold Strength (KSI)	Specific Threshold Strength (inches)	Ratio $\left(\frac{\text{Residual}}{\text{UTS}}\right)$
Gr/E 0/45	71	71	51.9	9.3×10^5	46	8.4×10^5	73.0%
Gr/E 0/45/90	40	57	36.0	6.5×10^5	at least 29	at least 5.3×10^5	63.1%
Gr/E 0/60	41	53.6	32.9	5.9×10^5	at least 30	at least 5.4×10^5	61.4%

Note:

1. Residual strength is <u>average</u> of all valid tests. (Bad material excluded)
2. Threshold strength is <u>lowest</u> of all valid tests. (Bad material excluded)
3. True UTS is based upon percentage of plys in the 0° direction.

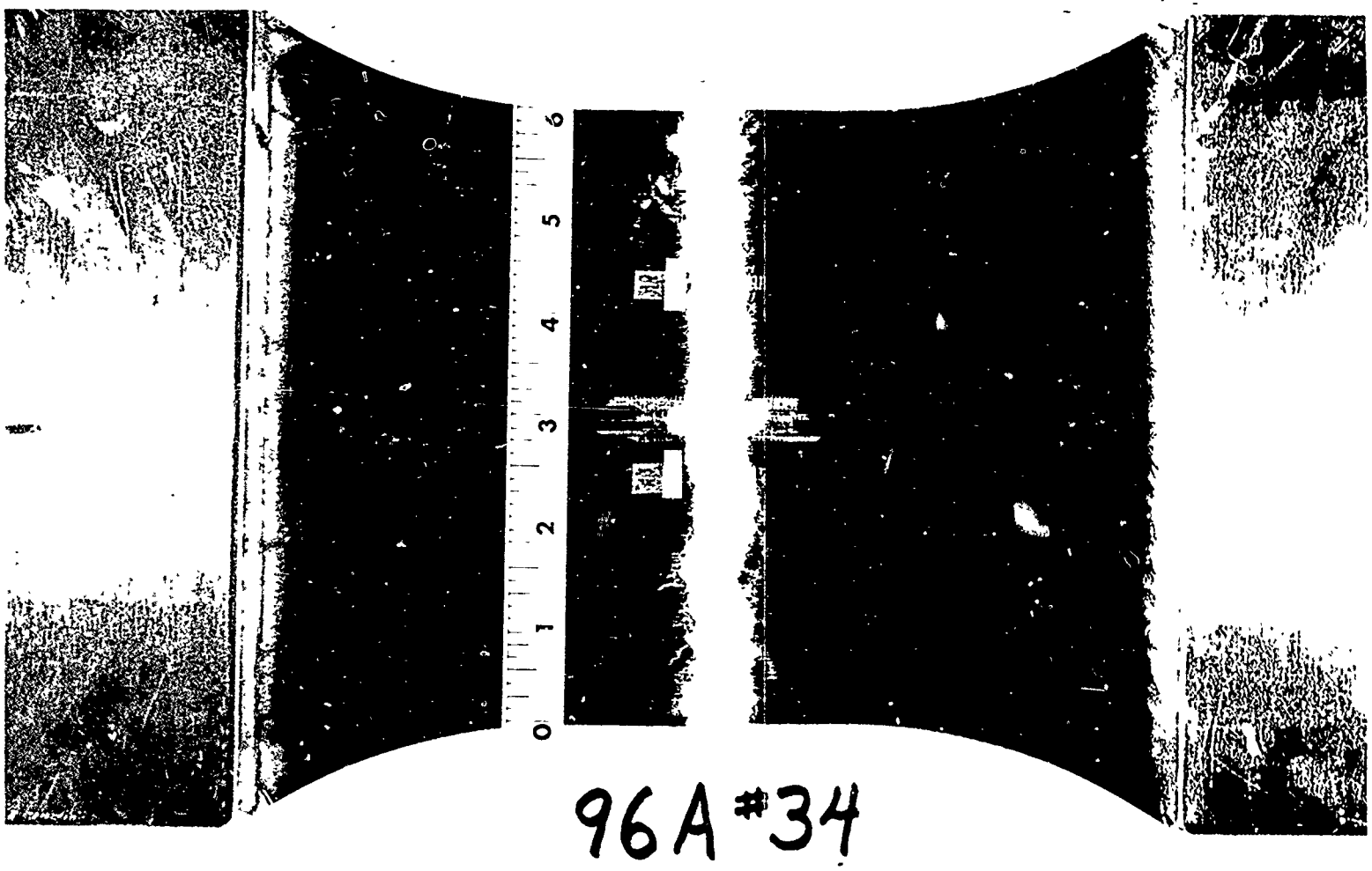

Figure 25 CLOSEUP SHOWING THE SLIGHT DAMAGE THAT OCCURS ON THE EXIT SIDE OF BORON/EPOXY SPECIMENS

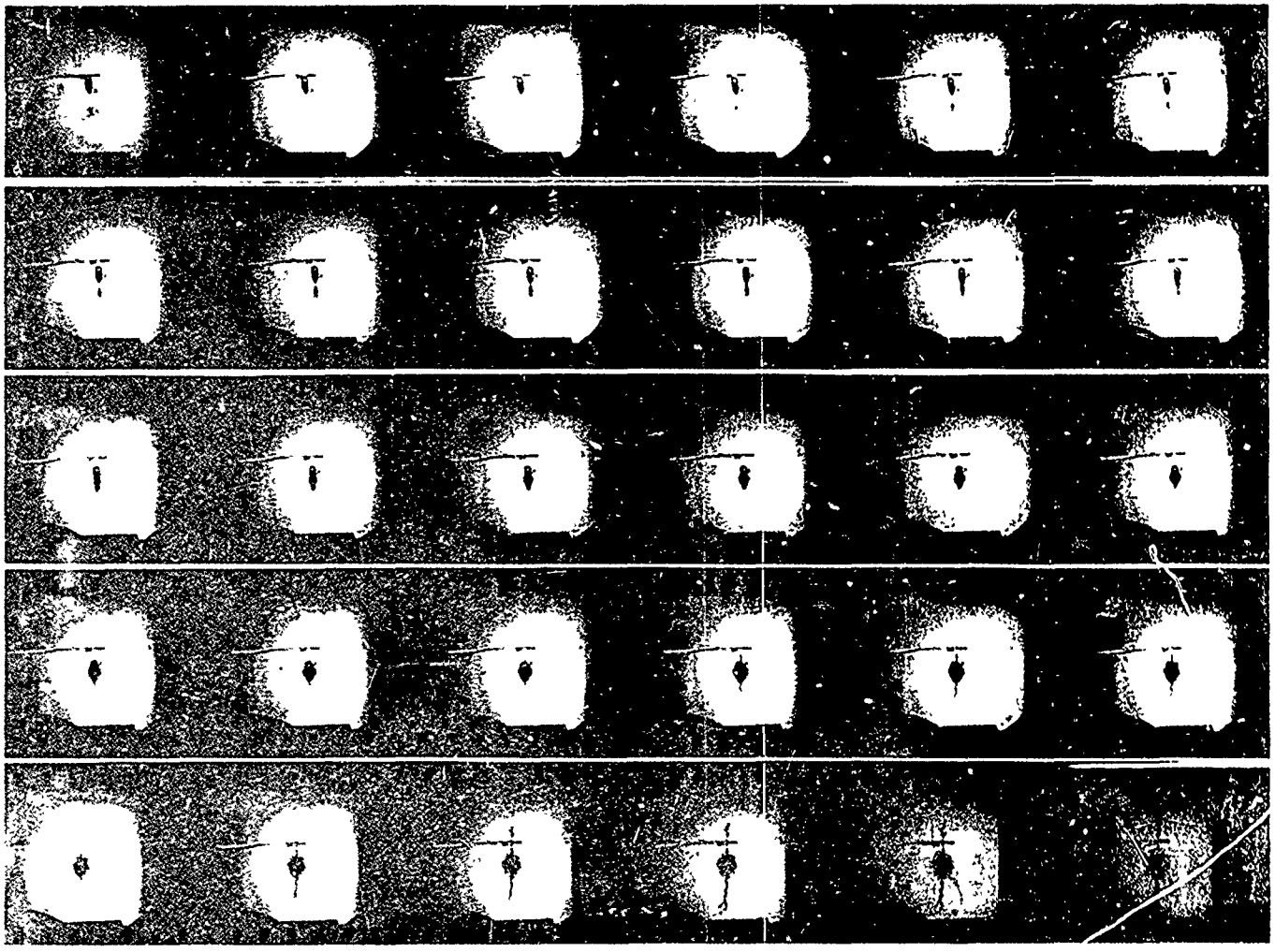

Figure 26 RESPONSE OF A BORON/EPOXY COMPOSITE TO BALLISTIC IMPACT (PANEL 1109-71 – 0/45/90 LAYUP)
HIGH SPEED PHOTO OF PENETRATION PROJECTILE – 30 CALIBER, 2750 FPS TIME BETWEEN FRAMES = 1.8 X 10^{-6} SECONDS. CRACK VELOCITY = 5900 FPS.

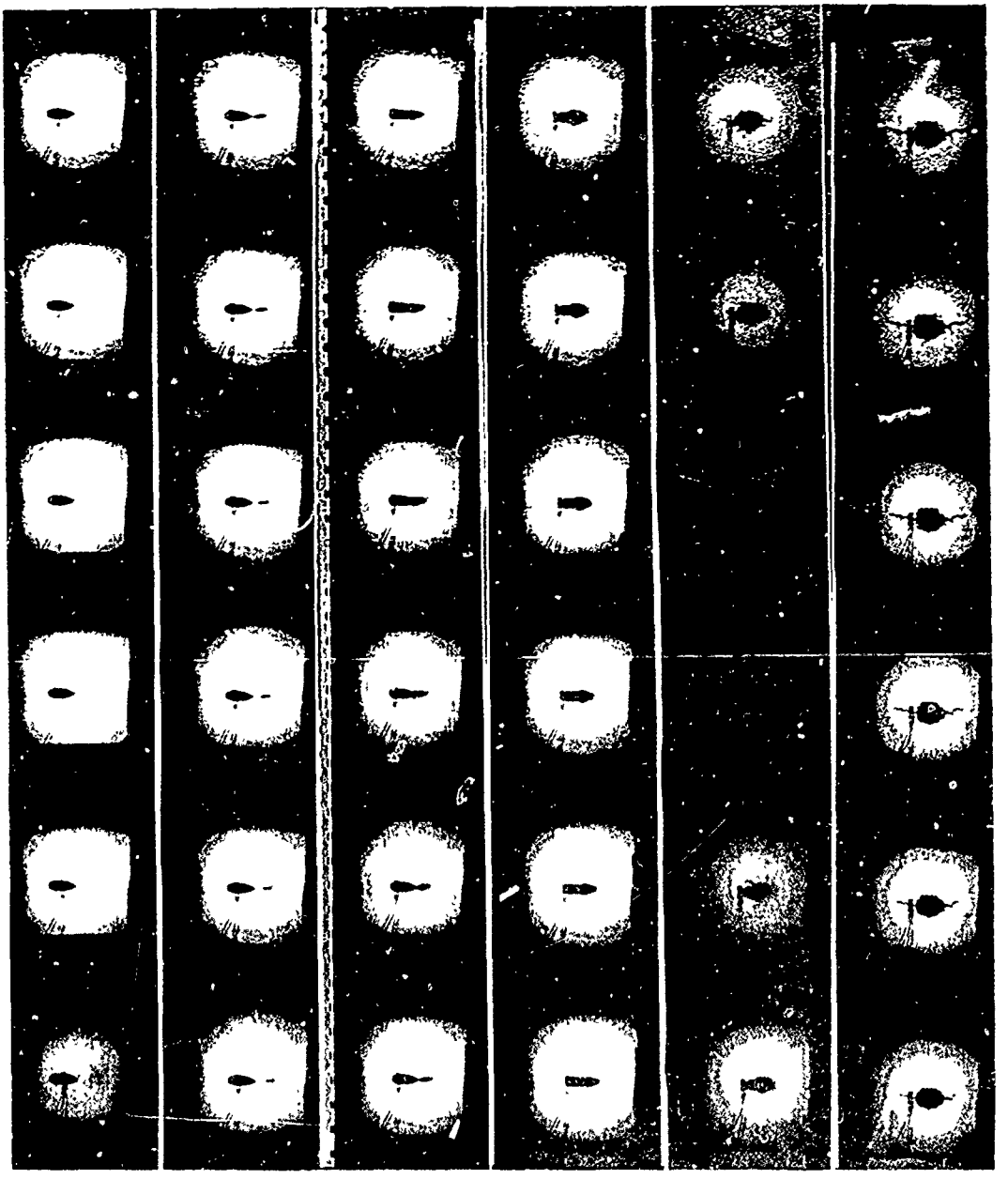

Figure 27a, RESPONSE OF BORON/EPOXY COMPOSITE TO BALLISTIC IMPACT
(PANEL 1109-70 – 0/45/90 LAYUP)
a) HIGH SPEED PHOTO OF PENETRATION
PROJECTILE 50 CALIBER, 2980 FPS
TIME BETWEEN FRAMES 2.07×10^{-6} SECONDS
CRACK VELOCITY 5600 FPS

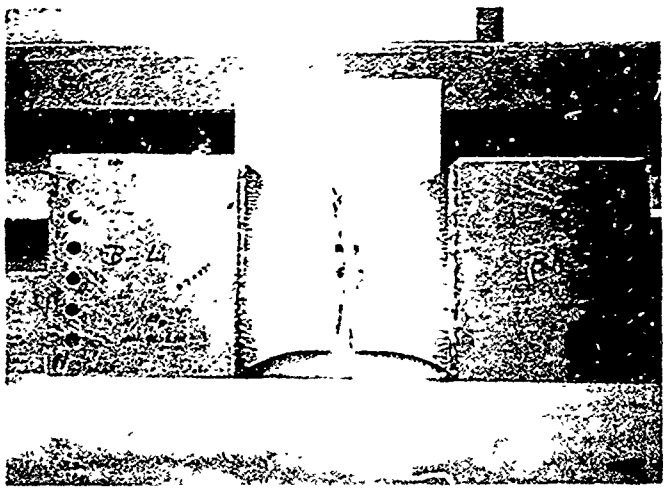

a) ENTRANCE

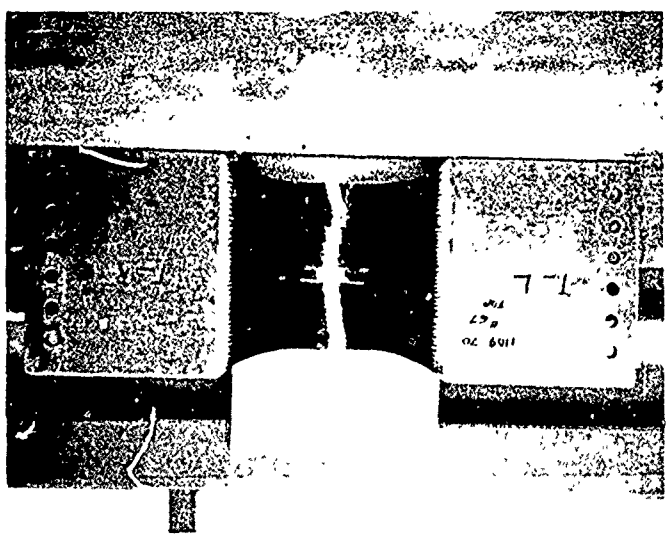

b) EXIT

Figure 27b, RESPONSE OF BORON/EPOXY COMPOSITE TO BALLISTIC IMPACT
(PANEL 1109-70 – 0/45/90 LAYUP)

b) FINAL FRACTURE APPEARANCE

The complete ballistic data including preload stress, projectile velocity, modulus and residual strength is given in Table 10. A summary of this data for the 30 caliber shots is given in Table 11 where it can be seen that the "residual strengths" were approximately 45, 75, and 41 KSI for the 0/45, 0/45/90, and 0/60 panels respectively. Similarly the "threshold strengths" based upon the lowest preload stress at which impact failure was observed, were approximately 41, 66, and 36 KSI respectively for the 0/45, 0/45/90, and 0/60 laminates.

As indicated by the data in Table 11 the "residual strength" varied from 52% to 65% of the UTS depending upon the layups; the threshold strength varied in the same manner and is approximately 92% of the residual strength. All three types of boron/epoxy laminates tested and higher absolute residual strengths than the 6061-T6 aluminum alloy. In fact the 0/45/90 panel had nearly twice the residual strength of the aluminum. On a specific strength basis the boron/epoxy was significantly better than aluminum and about equivalent to graphite/epoxy composites.

3.3 Analytical Investigation

It was desirable to develop the understanding and hence mathematical techniques which would permit accurate quantitative predictions of both the residual strength and the threshold strength of ballistically impacted composite materials. The determination of the "residual strength" is a static problem whereas the "threshold strength" is determined by the time dependent material response and the nature of the panel-projectile interaction. Because of these fundamental differences each problem was handled separately.

3.3.1 Residual Strength

The solution to the "residual strength" problem must reflect the behavior of the material and hence the starting point is a brief review of behavior of the panels. The aluminum behaved in a ductile manner and the residual strength of this alloy was nearly equal to its ultimate strength. Physically the glass/epoxy was found to delaminate severely but was tough enough so that it was impossible to measure its residual strength; premature failure occurred at the tabs in all cases. As pointed out earlier in the report, both the aluminum alloy and the glass/epoxy appear to be highly tolerant of ballistic damage; this deduction may, in fact, be misleading since the tests consisted only of monotomic loading and it is known that both of these materials are affected to a considerable degree by cyclic loadings. The boron and graphite fiber reinforced composites are of primary interest. These structural composites exhibited very localized damage when perforated by a 30 caliber AP projectile. The "residual strengths" are summarized in Table 12 and vary considerably depending upon the layup. This investigation was aimed at finding a consistent way of describing the retained properties of these materials.

If the holes were perfectly smooth and the material homogeneous, it would have been logical to approach this as a classical stress concentration problem in an orthotropic plate such as has been treated by in detail by Savin (Reference 3). However due to the heterogeneous nature of the material and the technique for introducing the hole, it more reasonable to assume that a good model is that of a hole with lateral cracks emanating from it as shown in Figure 28. In fact work by Waddoups (Reference 14) suggests that this type of model is appropriate even for carefully drilled holes in similar filament reinforced epoxy composites.

TABLE 10

BEHAVIOR OF BORON/EPOXY

Specimen Designation	Type	Thickness (inches)	Modulus ($\times 10^6$ psi)	Preload (KSI)	Projectile (Caliber)	Failed on Impact	Residual Strength (KSI)	Remarks
0/45 12 Ply	UTS = 85 KSI							
1117- 94A	B	0.063	12.3	41.4	30/HV	yes		
94B	|	0.063	12.7	38.2	30/LV	no		Save for inspection
95A	|	0.064	11.7	41.4	30/LV	no	45.8	
95B	|	0.064	11.6	43.3	30/LV	no		Save for inspection
96A	|	0.065	11.8	42.3	30/HV	yes		
96B	B	0.064		45.8	30/HV	yes		
97A	- -	0.065						Coupon Tests
97B	B	0.066		31.9	30/HV	no	43.9	
141A	|	0.076		36.2	30/LV	yes		Bad Panel
141B	|	0.075		31.9	50/HV	yes		Bad Panel
142A	|	0.072		39.0				Bad Panel - failed during preload
142B	|	0.072		37.3	30/LV	yes		Bad Panel
143A	|	0.065		44.6	30/LV	yes		
143B	|	0.065		43.3	30/LV	yes		
144A	B	0.064		45.9	30/LV	yes		
144B		0.065		44.6	30/LV	yes		
0/45/90 - 12 Ply	UTS = 114 KSI							
1117- 69A	B	0.061		61.2	30/HV	no	74.9	
69B	B	0.061		71.4	30/HV	yes		
70A	B	0.061	20.0	61.9	50/HV	yes		
70B	B	0.061		66.7	30/HV	yes		
71A	B	0.061		31.1	30/HV	no	74.9	
71B	B	0.061		69.4	30/HV	yes		
75	- -	0.061						Coupon Tests

HV = High Velocity = 2750 fps
LV = Low Velocity = 1250 fps

Type A = Straight Sided - 8 in. Width
B = Contoured - 6 in. Width
C = Contoured - 5.5 in. Width

TABLE 10 CONTINUED

Specimen Designation	Type	Thickness (inches)	Modulus ($\times 10^6$ psi)	Preload (KSI)	Projectile (Caliber)	Failed on Impact	Residual Strength (KSI)	Remarks
G/60 - 12 Ply	UTS = 68 KSI							
1117-72A	B	0.061	13.1	23.4	50/HV	no	38.3	
72B	B	0.061		36.3	30/HV	no	40.6	
73A	B	0.061		33.8	30/HV	no	44.9	
73B	B	0.061		36.4	30/HV	yes		
74A	B	0.061		37.6	30/HV	yes		
74B	B	0.061		39.0	30/HV	yes		
76	- -	0.061						Coupon Tests

TABLE 11

THRESHOLD AND RESIDUAL STRENGTH OF BORON/EPOXY

Material	Coupon UTS (KSI)	True UTS (KSI)	Residual Strength (KSI)	Specific Residual Strength (inches)	Threshold Strength (KSI)	Specific Threshold Strength (inches)	Ratio $\left(\frac{\text{Residual}}{\text{UTS}}\right)$
B/E 0/45	63	85	44.8	6.5×10^5	41.4	6.0×10^5	52.6%
B/E 0/45/90	102	114	74.9	10.9×10^5	66.7	9.7×10^5	64.5%
B/E 0/60	52	68	41.2	6.0×10^5	36.4	5.3×10^5	60.5%

Note:

1. Residual strength is <u>average</u> of all valid tests. (Bad material excluded)

2. Threshold strength is <u>lowest</u> of all valid tests. (Bad material excluded)

TABLE 12

SUMMARY OF PERFORMANCE FIBER REINFORCED EPOXY COMPOSITES

Material	Coupon UTS (KSI)	True UTS (KSI)	Residual		Threshold	
			(KSI)	(% of True UTS)	(KSI)	(% of True UTS)
Boron						
B/E 0/45	63.7	85	44.8	52.6	41.4	48.5
B/E 0/45/90	102	114	74.9	65.6	66.7	58.5
B/E 0/60	52	68	41.2	60.6	36.4	53.5
Graphite						
Gr/E 0/45	71	71	51.9	73.0	46	65
Gr/E 0/45/90	40	57	36.0	63.1	greater than 29	greater than 51
Gr/E 0/60	41	53.6	32.9	61.4	greater than 30	greater than 56
Glass/Epoxy	94	100	greater than 56.5	greater than 56.5	greater than 56.5	greater than 56.5

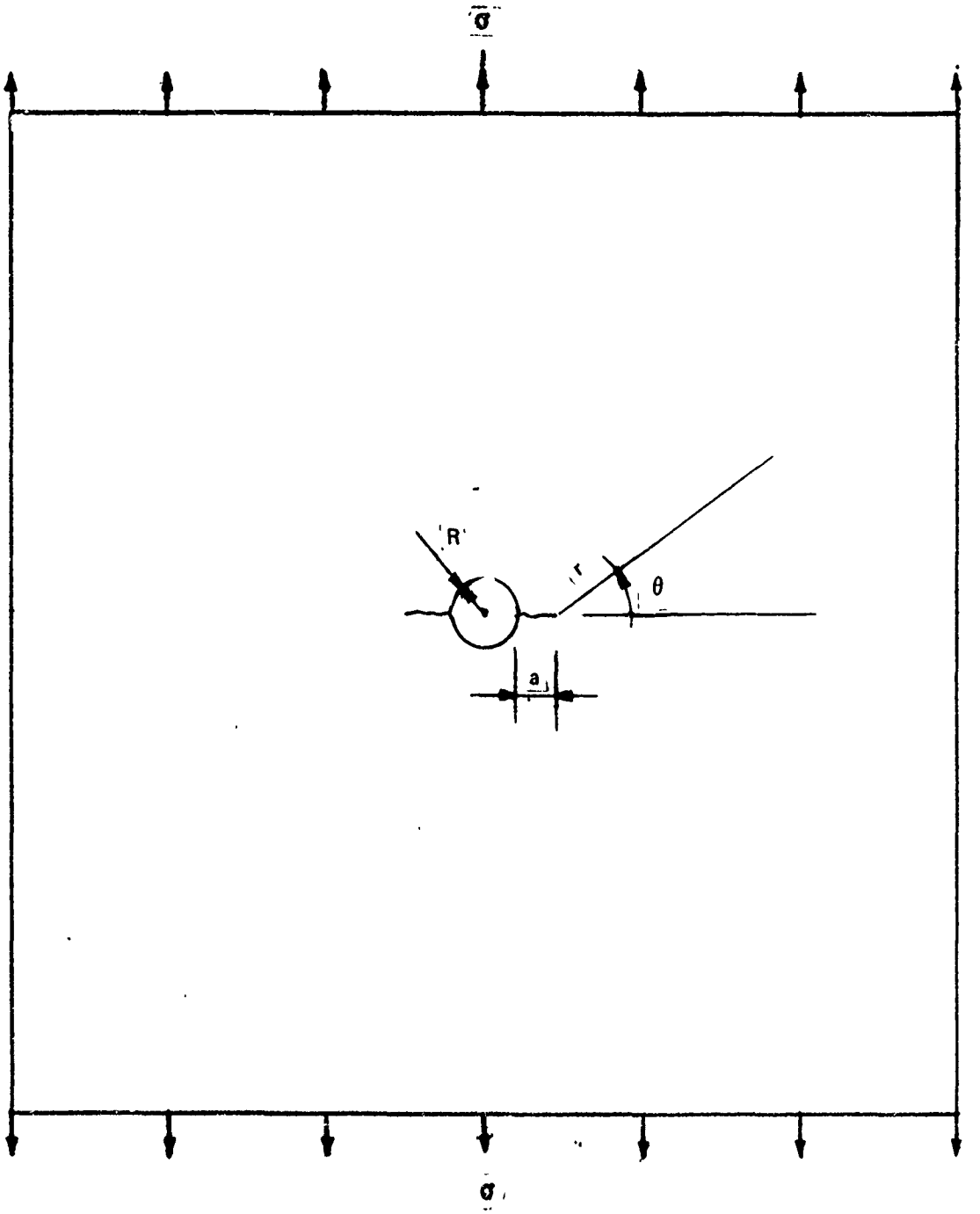

Figure 28 SCHEMATIC SHOWING A CRACK EMANATING FROM A HOLE

The stress field and hence stress intensity factor for cracks radiating from elliptical holes having an arbitrary orientation with respect to the principal planes in an orthotropic body have been determined by Bowie and Freese (Reference 15). The problem considered here is a specialized case where the hole is circular, the cracks are symmetric and located along a principal axis of the material, and loading is perpendicular to the crack and along the second principal axis of orthotropy.

The stress intensity factor, K, can be written as:

$$K = Y \sigma_n (a)^{\frac{1}{2}} \qquad (4)$$

where: Y is a boundary modification factor

σ_n is the nominal stress

a is the crack length defined in Figure 29

The factor Y is greatly influenced by the local stress field (Reference 4,15). Hence when "a" is short with respect to R, the radius of the hole, Y is large since it is affected by the stress concentration around the hole. When "a" is comparable to R then the effects of the hole are insignificant and hence, Y is equal to the same value obtained for a plate with a crack length equal to "a + R". Bowie and Freese (Reference 15) have computed the values of Y for the various composites studied in this program. These are given in Figure 29. Note that although the specific material properties affect the value of Y for small crack lengths the effect becomes negligible when the crack is greater than 0.040 in. which is about $\frac{1}{4}$ of the radius of the hole.

Our efforts in measuring the crack length of the ballistically impacted panels consisted of observations of the disturbed region. Based upon measurements which were necessarily crude it was concluded that the apparent crack length extended 0.04 in. beyond the hole. This is similar to apparent crack lengths observed by (1) Waddoups (Reference 14) who found crack lengths from 0.027 in. to 0.050 in. in a graphite/epoxy composite and (2) to observations made by Suarez (Reference 21) who concluded that in boron/epoxy composites the inherent crack length is 0.040 inches.

$$\text{Hence, } K = Y \sigma_n (a)^{\frac{1}{2}} = 2.24 \sigma_n (0.04)^{\frac{1}{2}} \qquad (5)$$

At fracture, the stress intensity, K, equals the fracture toughness, Kc, therefore, rewriting equation (5):

$$\sigma_n = \frac{Kc}{Y (a)^{\frac{1}{2}}} = \frac{Kc}{.45} \qquad (6)$$

The values of Kc was determined from single edge notch fracture toughness tests and hence could be used to obtain a predicted value of the residual strength (i.e., σ_n). The predicted values for the boron/epoxy panels are given in Table 13 and are compared to the experimentally measured values. As can be seen the correlation is excellent. It should be recalled that; (1) this material was extremely uniform as indicated by the coupon and fracture toughness tests, (2) that very little delamination occurred upon breaking, and (3) that the fracture toughness tests behaved as expected and hence the values were felt to be valid. All of these factors contributed to the accuracy of the prediction.

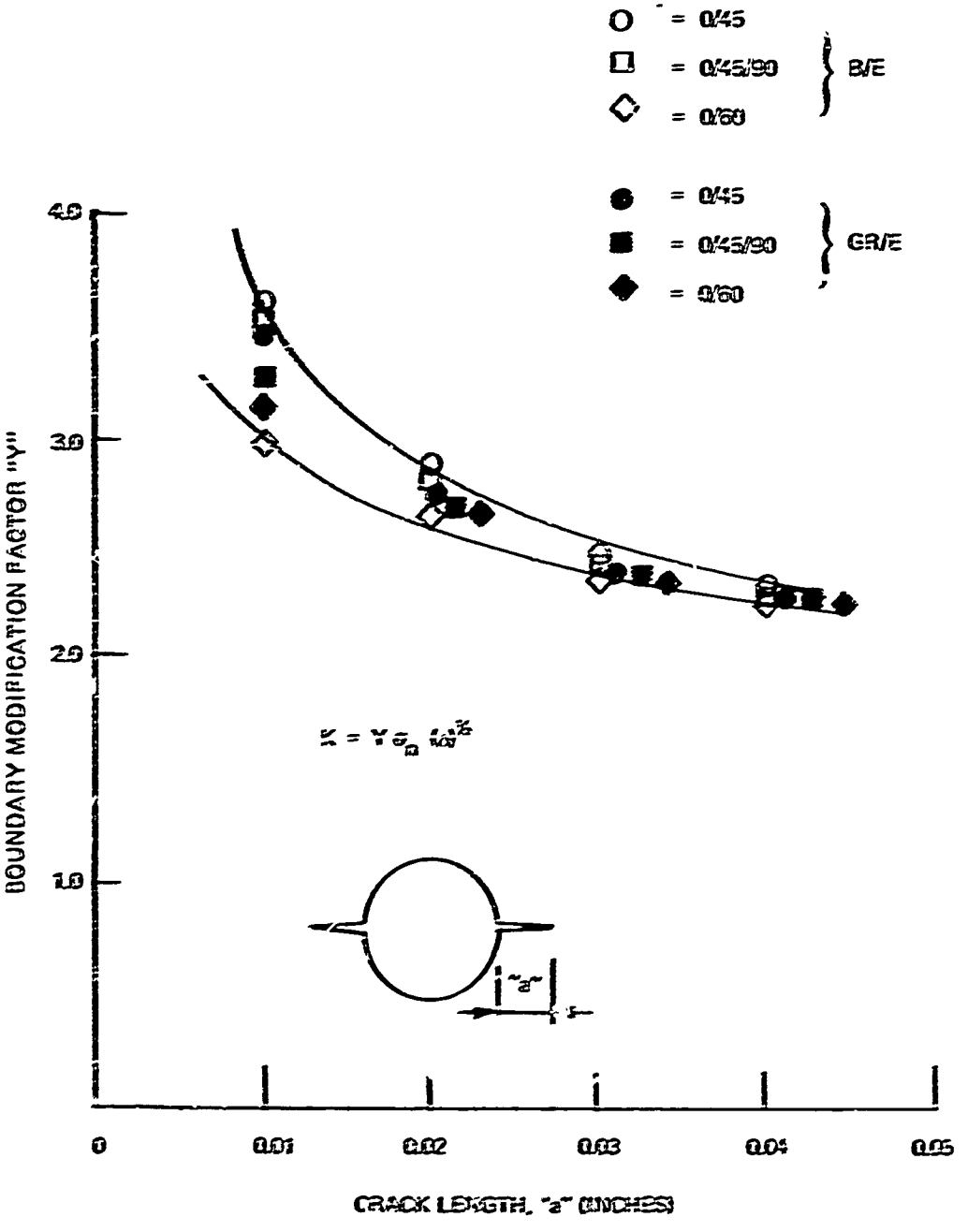

Figure 29 VARIATION IN "Y" WITH "a" – FOR A CRACK EMANATING FROM A CIRCULAR HOLE (REFERENCE 15)

TABLE 13

COMPARISON OF THE PREDICTED AND MEASURED RESIDUAL STRENGTH

Material	Fracture Toughness Kc (KSI $\sqrt{in}$)	Residual Predicted $\sigma_n = \frac{Kc}{Y(a)^{\frac{1}{2}}}$	Measured (KSI)
B/E 0/45/90	32.6	72.6	74.9
B/E 0/60	18.2	40.5	41.2
B/E 0/45	21.1	46.8	44.8

Becuase of the interlaminar unbonding observed at the crack tip with the graphite/epoxy specimens it was felt that the toughness data was not valid. The value of K when unbonding initiated was termed K' and since the same interlaminar failure was observed in the large panel tests there was the possibility of using K' in equation 6 as a measure of toughness. The data is given in Table 14 and although the predicted and measured values do not agree as well as was found with the boron/epoxy laminates, the correlations are quite reasonable.

3.3.2 Threshold Strength

The analytical determination of the "threshold strength" is complex and depends upon the interaction of several effects. These are the static effects caused by a hole in a stretched plate, the dynamic effects resulting from the sudden introduction of the hole, the flexural effects due to the impulse imparted during penetration, and the stress waves caused by the wedging action of the pointed projectile.

The dynamic effects were to have been studied experimentally using strain gages tied into an oscilloscope as well as with high speed photography. With the strain gages it was intended to study both the flexural and extensional response during penetration but, as described earlier, these experiments were unsuccessful. Using high speed photography it was found that the projectile velocity was not measurably decreased as a result of perforating the panels and that the plate deformation was negligible. Secondly it was possible to observe that for preloads equal to or slightly greater than the threshold strength the crack did not begin to grow until the projectile reached its full diameter. These observations, in conjunction with the fact that the threshold strength was approximately 90% of the residual strength suggested that the total dynamic effect was small.

The flexural response can be obtained in the following way. Consider a simplified model, namely, a simply supported square, isotropic plate loaded by a triangular pulse over the region cross hatched in Figure 30. The problem can be formulated using a modal analysis. The equations of motion can be obtained with the use of the Lagrangian relations. Once the equations of motion are known the displacements and hence stresses, which are related to the second derivative of the displacement coordinates, can be computed. The equations are given in Appendix D where it is shown that the displacement can be written as:

$$Y_{max} = A_{n\,st} \quad DLF$$

Where,

Y_{max} is the maximum deflection

$A_{n\,st}$ is the static deflection of the n^{th} mode

DLF is the dynamic load factor

TABLE 14

COMPARISON OF THE PREDICTED AND MEASURED RESIDUAL STRENGTH

Material	K' (at onset of failure) (KSI $\sqrt{in}$)	Residual Strength	
		Predicted $\sigma_n = \frac{Kc}{Y(a)^{\frac{1}{2}}}$ (KSI)	Measured (KSI)
G/E 0/45/90	13.5	30.0	36.0
G/E 0/60	17.4	38.6	32.9
G/E 0/45	21.6	48.0	51.9

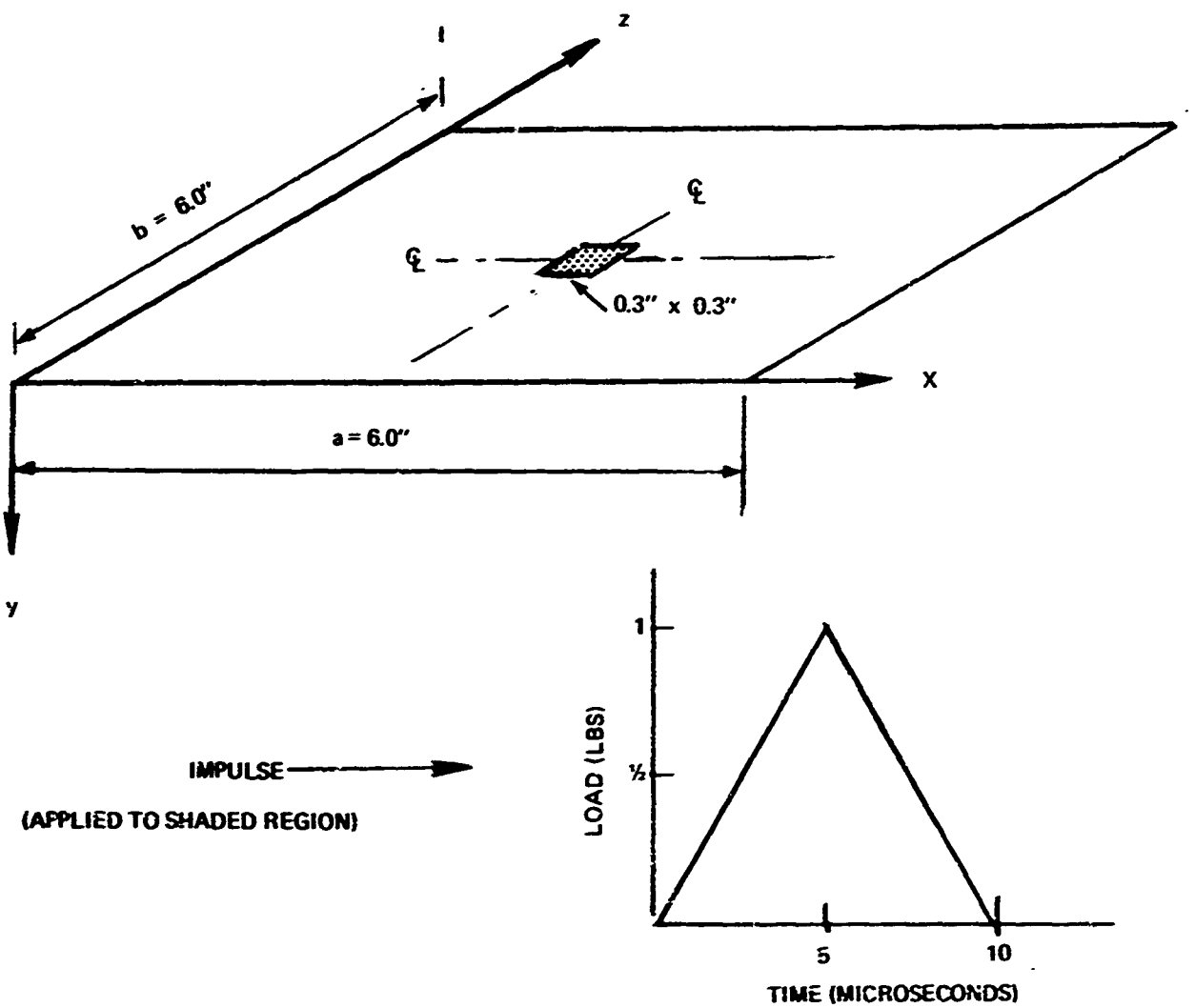

Figure 30 IMPULSIVELY LOADED PLATE

As shown in Figure 31 (Reference 16) the dynamic load factor (DLF) depends upon the ratio of the duration of the pulse, td to the natural period of vibration, T. The pulse duration is 10×10^{-6} seconds, or the time required for the projectile traveling at 3000 fps to reach its maximum diameter.

The period associated with the fundamental frequency is 4×10^{-3} seconds and hence td/T is 2.5×10^{-3}. The associated DLF is close to zero indicating that plate will not respond in this mode. At higher frequencies the ratio of td to T becomes large and thus the DLF will be of the order of one as shown in Figure 31. In Appendix D the calculations for mode 7 are given. The in-plane stresses are computed to be 0.14 psi for a peak pressure of 1.0 psi. Assuming the projectile velocity to decrease by 50 fps during perforation the peak load can be computed to be 7000 pounds. If this is uniformly distributed over the area removed by the projectile it corresponds to a pressure of approximately 100,000 psi. Hence the in-plane stresses would be (0.14 psi/psi) (100,000 psi) or 14,000 psi. This stress is developed at the centerline of the plate (which in actuality is removed by the projectile), and between the node points each of which are located on a grid 6/7 inch on a side.

At significantly higher natural frequencies the response again becomes negligible since the displacement decreases as the square of the natural frequency. Therefore a small band frequencies (modes 5, 7 and 9) control the response.

The peak stresses occur in between the node points. From the center of the plate these regions occur on a grid having sides 6/n inches long where n is the mode number. For modes 5 through 9 the points of inflection at which no flexural stresses are developed are located at the nodes, the first of which is at $\frac{1}{2}$ (6/n) inches from the center. The center of the plate is removed by the projectile. At the periphery of the hole which is formed the flexural stresses are substantially lower than the peak stress. At the tip of the 0.040 inch long crack which emanates from the hole the flexural stresses are even less since this distance is close to a node for the modes which respond to the impulse.

Orthotropic plates (Reference 17) can be analyzed in a similar manner and the effects of in-plane loads can be included. The results, however, are not substantially altered.

The flexural analysis indicated that at certain frequencies stresses of the order of 14 KSI could develop if damping did not surpress the response. These stresses however occurred at only several positions throughout the plate due to the fact that they resulted from the higher order modes. Other effects such as the wedging force and the dynamic effects of a suddenly formed hole are perhaps even more significant since these effects tend to be concentrated in the vicinity of the hole where the stresses are the greatest.

The total penetration occurs in the order of 10×10^{-6} seconds. During this time the compressional wave front travels away from the hole at the sonic velocity of the material (Refer to equation 1). Assuming an average extensional modulus of 12×10^{6} psi the wave front can travel 3 in. during the 10×10^{-6}

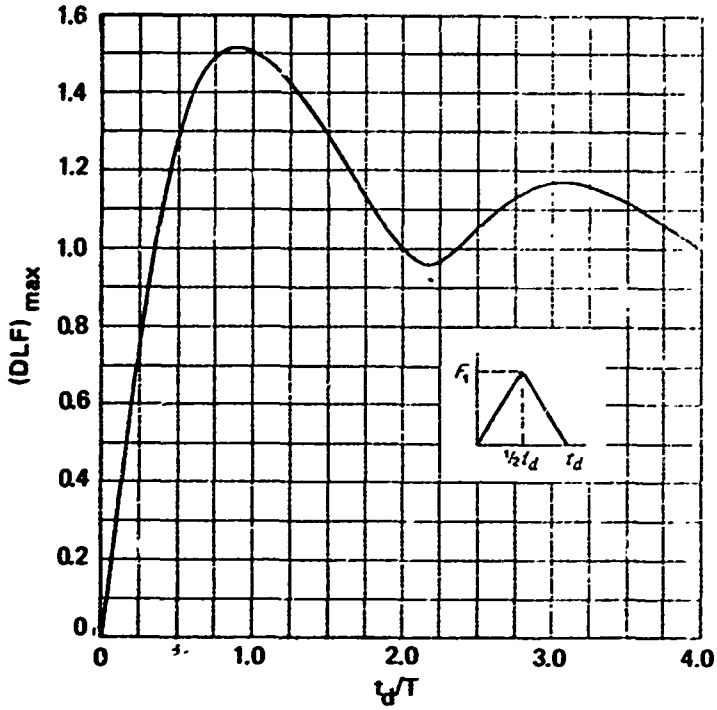

Figure 31 VARIATION IN THE MAXIMUM VALUE OF DLF AS A FUNCTION OF THE RATIO OF PULSE DURATION TIME, t_d, TO THE NATURAL PERIOD, T. (FROM BIGGS, REFERENCE 16)

seconds of penetration. This is a large distance with respect to the point of crack initiation which, from Figure 28, is R + a which equals 0.150 in. + 0.040 in. or 0.190 in. from the center of impact. Hence the bulk of the dynamic wave has traveled far beyond the crack tip and only the last portion of the stress wave is expected to have any effect. This portion is associated with the final wedging action (just as the projectile shape changes from an increasing to a constant diameter). The stress wave would be emanating from a hole approximately the full projectile diameter and would interact with the effects of the prestressing load at the crack tip which is 0.040 in. from the edge of the hole. The time required for the wave to travel this distance (0.040 in.) is 0.13×10^{-6} seconds. Events of this time duration would appear as instantaneous events on the high speed pictures since the time between frames was approximately 2×10^{-6} seconds. This is consistent with the photographic data since the crack appears to develop within one frame and after the projectile tip has fully penetrated the panel.

In discussions with Mr. I. E. Figge, Sr. and Mr. J. C. Newman, Jr. (Reference 18) they suggest that the problem can be approached as the static superposition of the effects of: (1) the in-plane loads and, (2) the wedging forces on a plate with cracks extending from a hole. This is shown schematically in Figure 32.

The wedging force can be approximated in the following manner. As the projectile enters a thin plate it is resisted by a shear V and a normal force P (See Figure 33). Perforation tests were performed using an Instron testing machine to drive a 30 caliber AP projectile through the remaining portions of panel 1109-74A. The load displacement curve is given in Figure 34. The maximum force reached was 180 pounds. After initial perforation the load dropped to approximately 140 pounds and remained relatively constant until the full projectile diameter was reached. The load then dropped to approximately 40 pounds. From this it was deduced that the additional 100 pounds was resisted by the in-plane forces.

Assume that the tangent to the projectile tip is 10° from the longitudinal axis as shown in Figure 35. The 100 pound force required to shove the projectile through the panel is resisted by the normal force F_T. The vertical component of F_T taken around the periphery of the bullet must equal 100 pounds. From geometry the horizontal force can be computed and equals 600 pounds per in. The thickness of this panel (1109-74A) is 0.061 in. and therefore the stress is 9850 psi. This is the magnitude of the internal pressure along the periphery of the hole. Sokolnikoff's (Reference 23) relation for the hoop tension in an infinite plate loaded by uniform pressure along a circular cutout is:

$$\sigma_{hoop} = P \frac{R^2}{\varepsilon^2} \qquad (16)$$

where: σ hoop is the hoop tensile stress

P is the pressure

R is the radius of the hole

ε is the distance from the center of the hole where hoop is to be computed

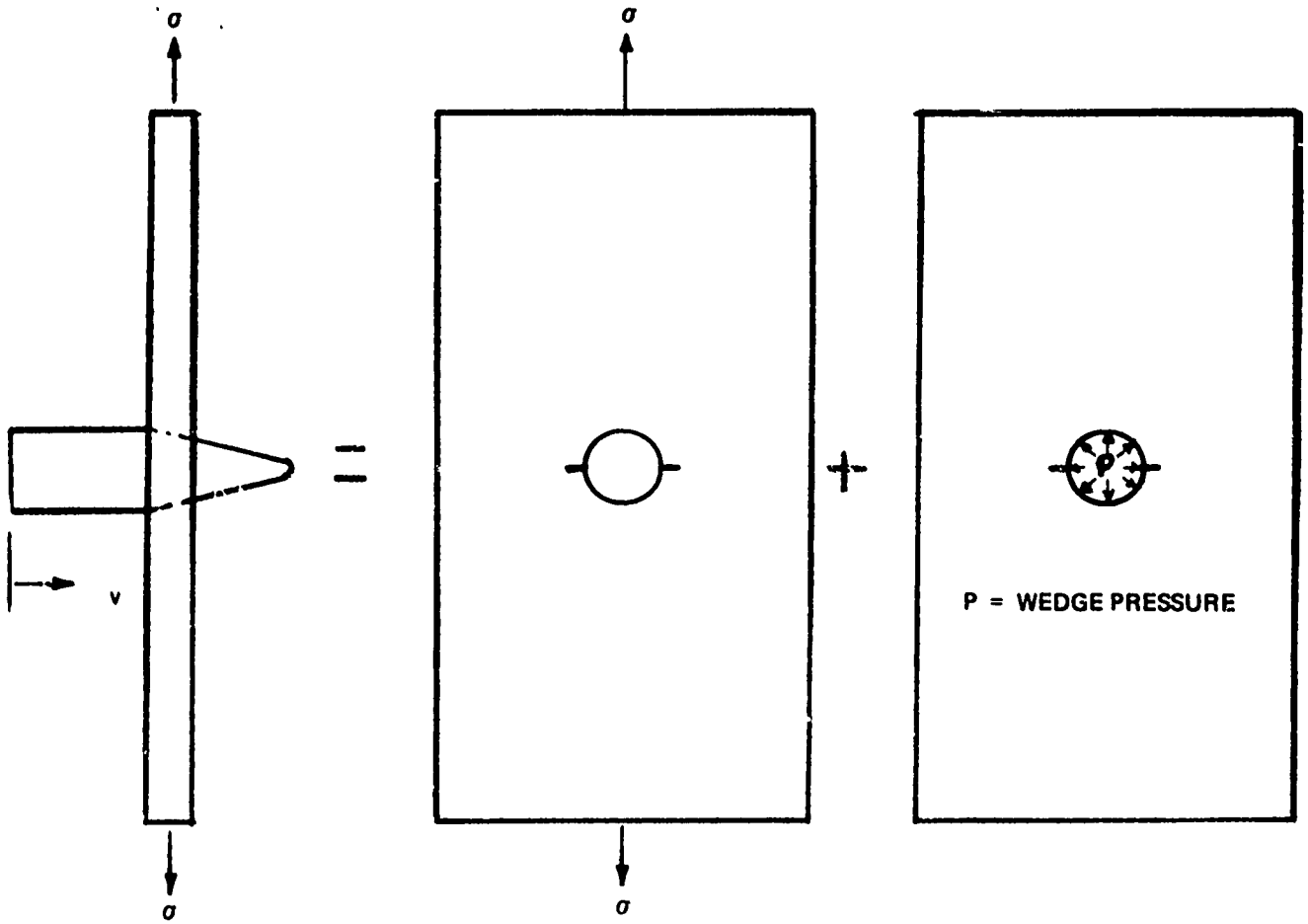

Figure 32 SUPERPOSITION TO MODEL EFFECT OF PROJECTILE AND PRELOAD

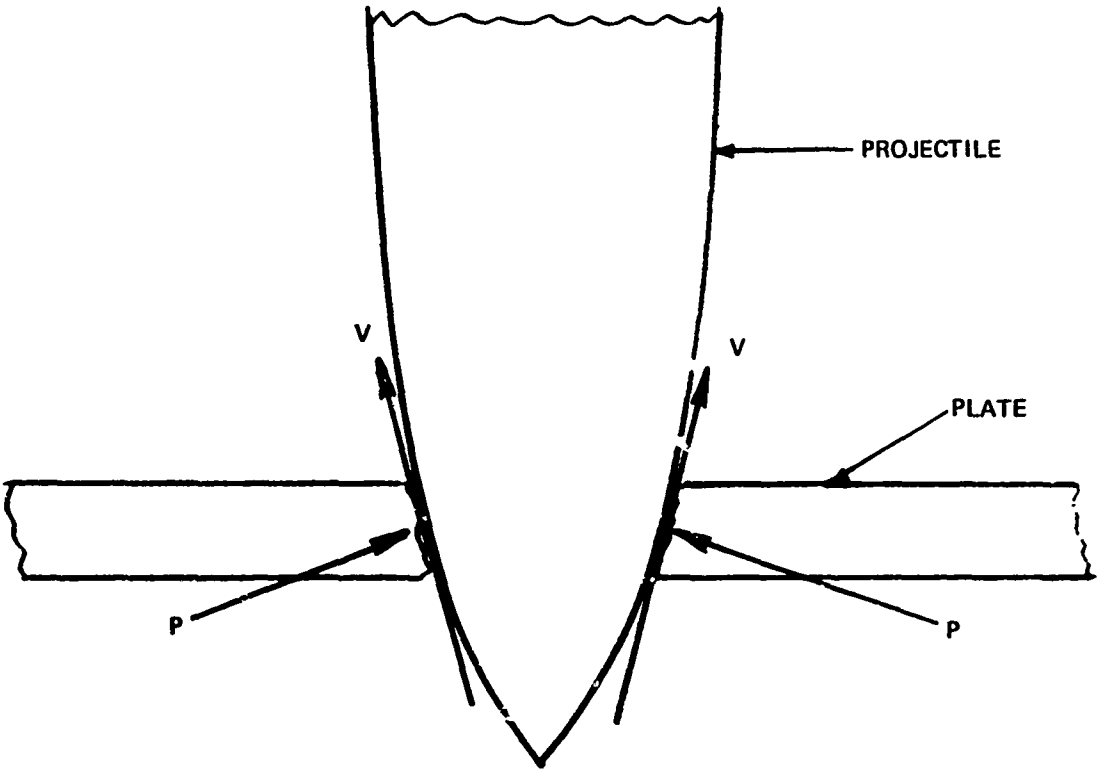

Figure 33 SCHEMATIC SHOWING THE GROSS FORCES DEVELOPED ON THE SURFACE OF THE PROJECTILE DURING PENETRATION

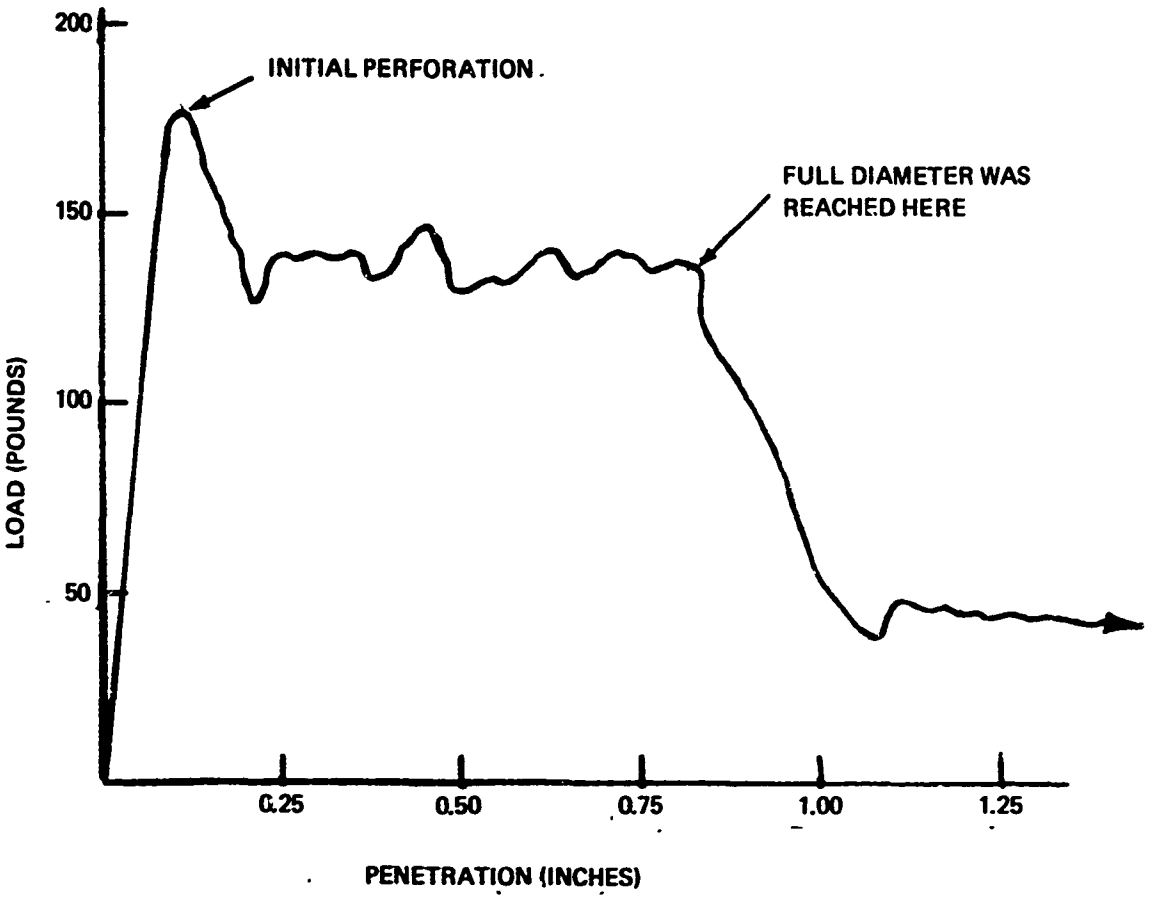

Figure 34 THE FORCE – DISPLACEMENT DIAGRAM FOR PENETRATION BY A 30 CALIBER AP PROJECTILE

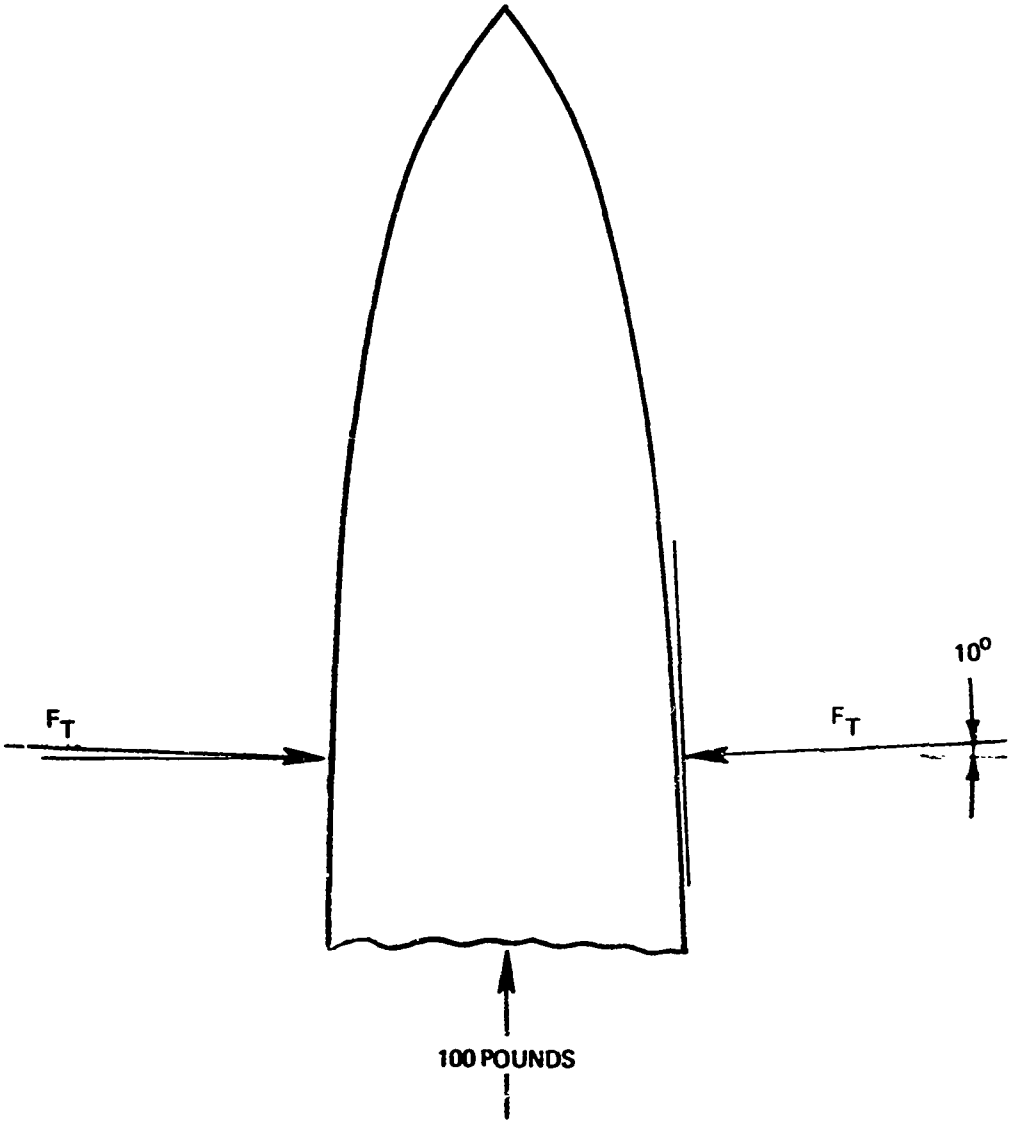

Figure 35 THE RESULTANT FORCES ON THE PROJECTILE DEVELOPED JUST PRIOR TO REACHING ITS FULL DIAMETER

For the example here P = 9850 psi, R = 0.15 in. and $g = R + a = 0.19$ in. With these values σ hoop equals 6300 psi. The actual value is subject to careful scrutiny because, (1) during ballistic perforation the force-time curve might differ from that found using an Instron test machine at a penetration velocity of $\frac{1}{2}$ in. per minute, and (2) the in-plane force was computed based upon a normal force acting 10° out of the plane of the laminate. Nevertheless the data is of the correct order of magnitude since as shown in Table 12 the threshold and residual strength for most laminates differ by approximately 6 KSI.

The last ballistic effect to be considered is the dynamic overshoot resulting from the sudden introduction of a hole. Forrestal (Reference 6) studied the dynamic stresses in a biaxially loaded isotropic plate. Along an imaginary circle in his analysis, Forrestal suddenly imposed a pressure equal in magnitude to the applied biaxial tensile stresses. This forced the stresses normal to the imaginary circle to go to zero thus modeling the conditions which exist if a hole were formed. The static superposition of this pressurized hole and the uniform tension field results in a hoop tension stress at the periphery of the hole equal to twice the applied tensile stress. Away from the hole the hoop stresses diminish rapidly while at the same time the radial stresses (which are equal to zero at the hole) increase until they reach the applied stress level. If the pressure on the circle is suddenly applied the hoop stresses rise over some finite time to a level slightly greater than the final static level (i.e. 1.3 times the static value) and then oscillate about the static stress level. It is important to realize that if the hole were enlarged the new hole would be that necessary to balance the radial stresses and depends upon time and distance from the former hole. The projectile tip can be considered to be composed of a series of short discrete steps rather than a continuous curve, each of which forms a slightly larger hole. The formation of the first hole requires the application of an internal pressure equal to the full magnitude of the applied stress. For all subsequent holes the internal pressure is much less since it need only balance the radial stresses which have developed prior to punching each subsequent hole and in this manner it is possible to ballistically form a hole in a preloaded panel without any significant dynamic effects.

An alternative approach is available. The threshold strengths were found to vary linearly with the notch toughness and, although the method lacks vigor, it is possible to use a modified crack length of approximately 0.060 in. in conjunction with equation 6 to obtain the threshold strength as will be discussed in the following section.

4.0 DISCUSSION

In cross ply laminates containing substantial amounts of reinforcement in the 0^{o} direction the longitudinal modulus, strength, and toughness are approximately proportional to the percentage of 0^{o} plys in the laminate. This is especially true if the off-axis plys are oriented at angles greater than 40^{o} as is the case here. These relations are plotted in Figures 36, 37, and 38 where it can be seen that the modulus curve is nearly identical for both the boron/epoxy and the graphite/epoxy laminates. This occurs because the two materials have approximately the same unidirectional modulus. This results because the graphite fibers have a modulus of 50 x 10^{6} psi and have a per ply volume fraction of 60% whereas the boron filaments have a modulus of 60 x 10^{6} psi and have a per ply volume fraction of 50%.

The UTS and toughness are directly related to the tensile behavior of the filaments and since the boron has a significantly greater strength than the graphite the trends are different for the two materials as shown in Figures 37 and 38. It should be noted that with composites the toughness and strength are linearly related whereas with conventional structural metals these parameters are inversely related.

The "residual strength" is linearly related to both the toughness and the UTS as shown in Figures 39 and 40. This occurs because of the unique relationship between strength and toughness coupled with the fact that the crack length and boundary modification factor were the same for all laminates tested.

The ballistically induced crack length was found to be 0.040 in. which complete agreement with published data (References 14 and 21). In fact ame damage zone was found for drilled holes and hence it is not surprising that the same strength reduction was found in Reference 1 for drilled and ballistically perforated panels.

The initial preload had no effect on the residual strength. This is felt to be due to the fact that the dynamic effects of a ballistically formed hole are negligible and that the flexural effects, in the vicinity of the crack tip, are small. The hoop tensile stresses associated with the wedging action of the projectile are felt to be the cause of the approximately 6 KSI decrease in the threshold strength as compared to the residual strength.

The residual strength was found to be independent of projectile velocity as was also found by Suarez (Reference 21). The 0/45/90 boron/epoxy layup had the highest residual strength. Although the magnitude of the residual strength depends upon the panel layup and on the basic reinforcing material as shown in Figure 40, the retained residual strength for nearly all the laminates tested was approximately 62% of the UTS. The exceptions to this were the $0/45^{o}$ laminates where the graphite/epoxy panels exhibited residual strengths of approximately 73% of the UTS, or the highest strength retention, whereas the boron/epoxy laminates resulted in the lowest value of strength retention with a residual strength of only 52% of its UTS. These differences carried over to the threshold strengths as shown in Figure 42. Comparing the strength to density ratios as shown in Figure 41 lessens the advantage of the boron/epoxy but nevertheless shows it to be superior to all other laminates tested.

The ratio of "residual strength" to UTS was significantly lower for the composites than for the 6061-T6 aluminum alloy which was tested. A more realistic comparison could have been obtained with a 7075-T6 aluminum alloy which has a residual strength of approximately 40 KSI which is 50% of its UTS. The residual

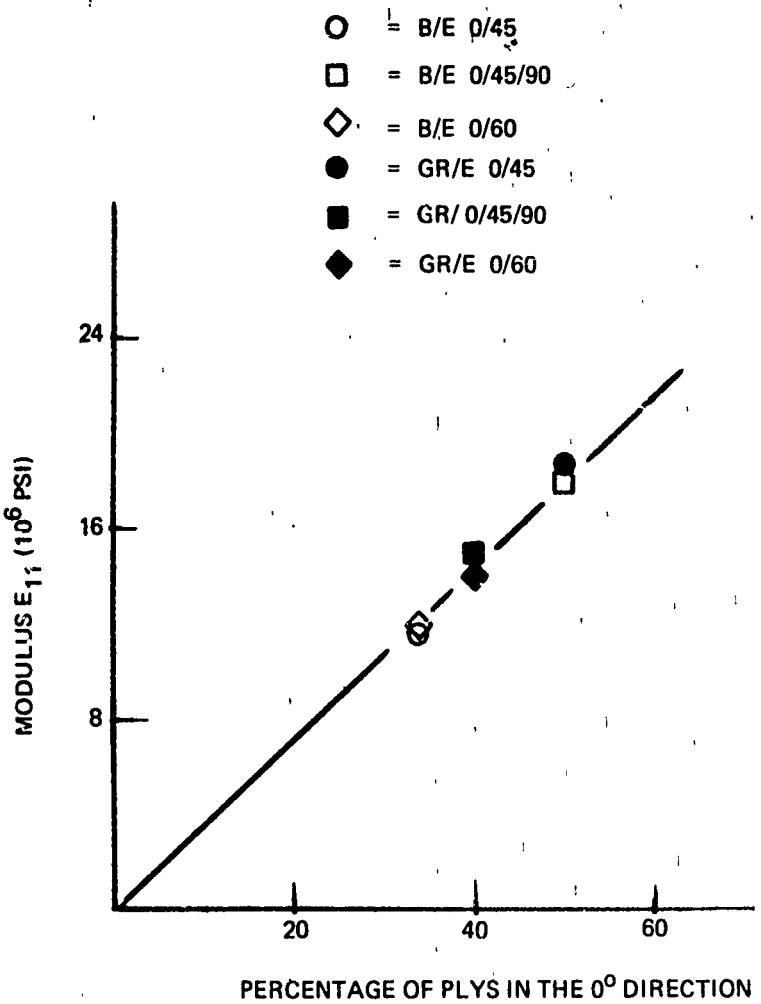

Figure 36 RELATION BETWEEN MODULUS AND PERCENTAGE OF 0^0 PLYS

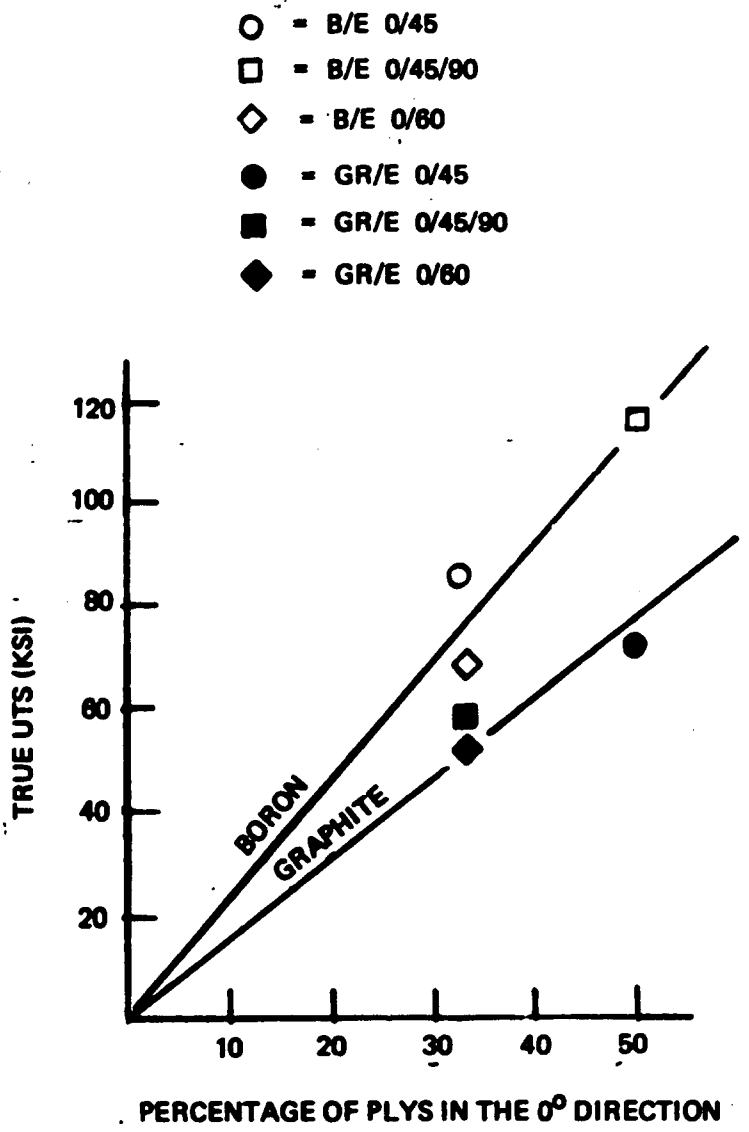

Figure 37 RELATION BETWEEN THE UTS AND THE PERCENTAGE OF 0° PLYS

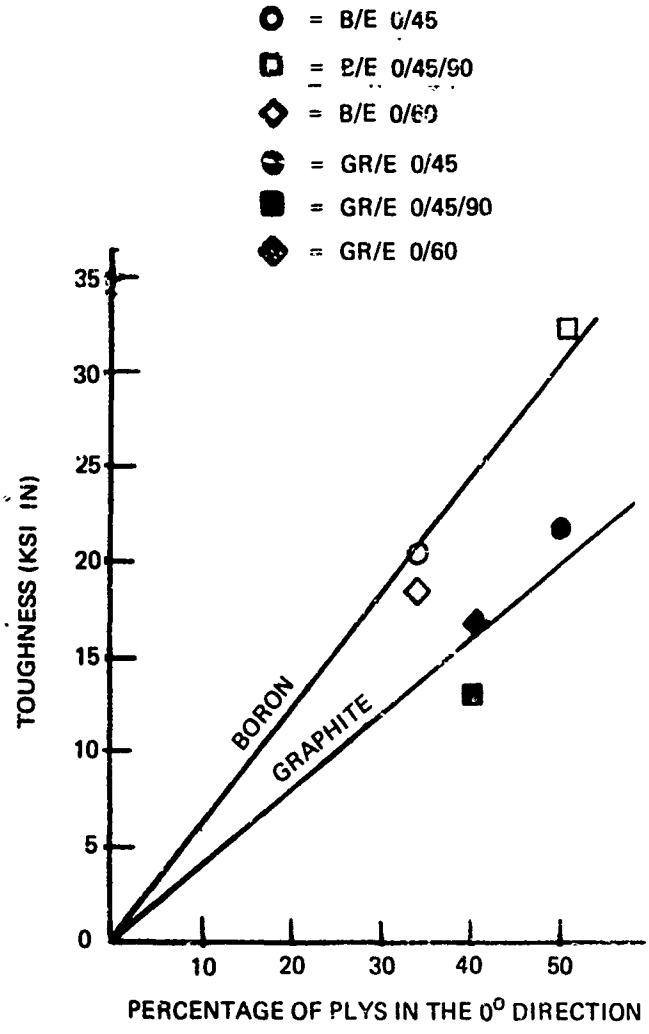

Figure 38 RELATION BETWEEN NOTCH TOUGHNESS AND THE PERCENTAGE OF 0° PLYS

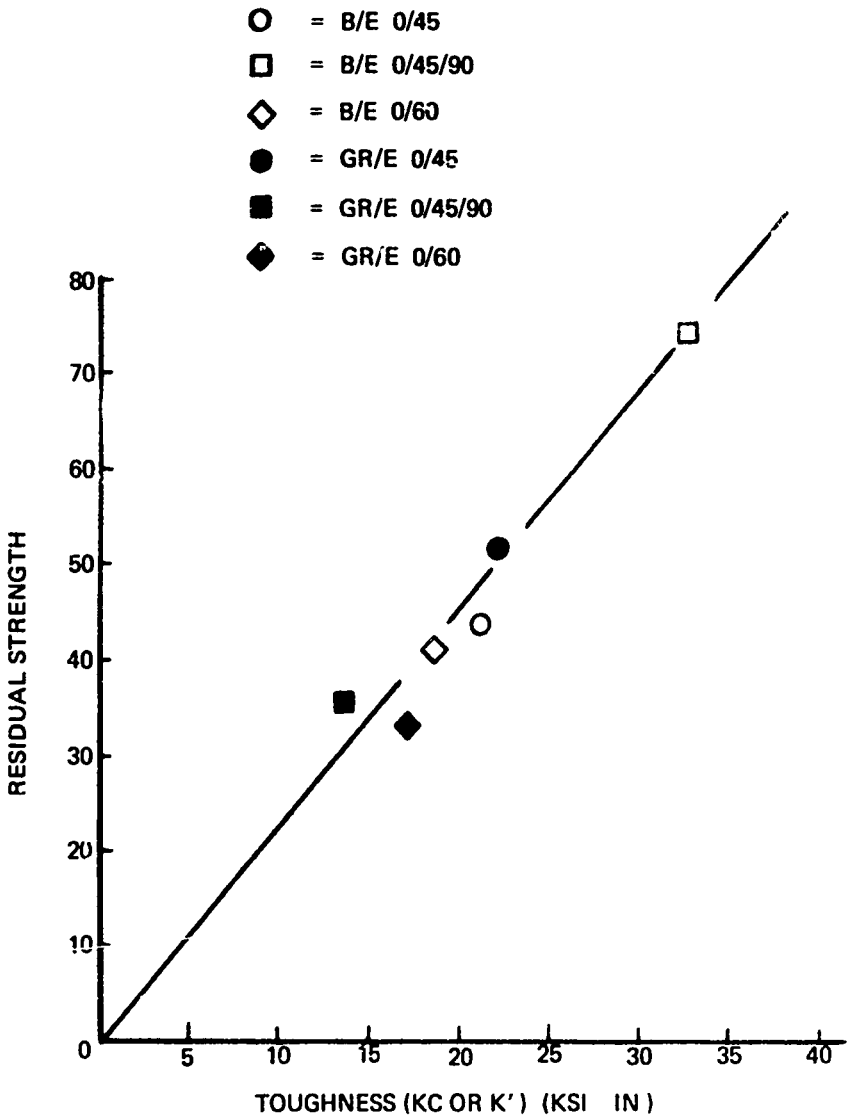

Figure 39 DEPENDENCE OF RESIDUAL STRENGTH ON THE FRACTURE TOUGHNESS OF ADVANCED COMPOSITES

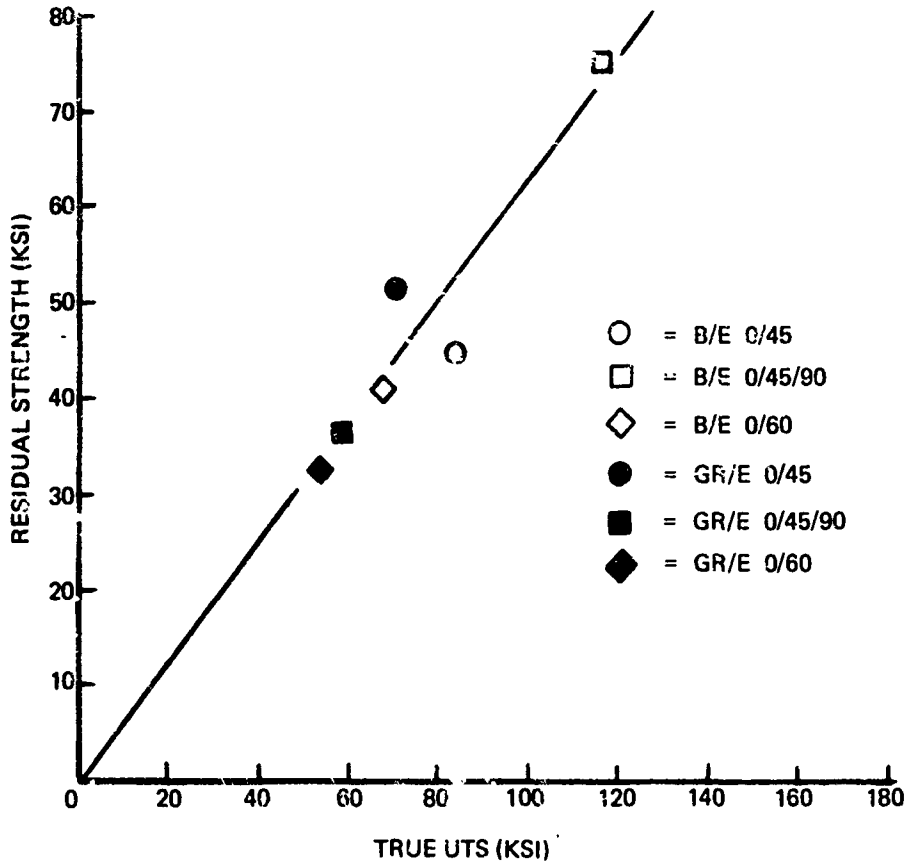

Figure 40 RELATION BETWEEN RESIDUAL STRENGTH AND UTS

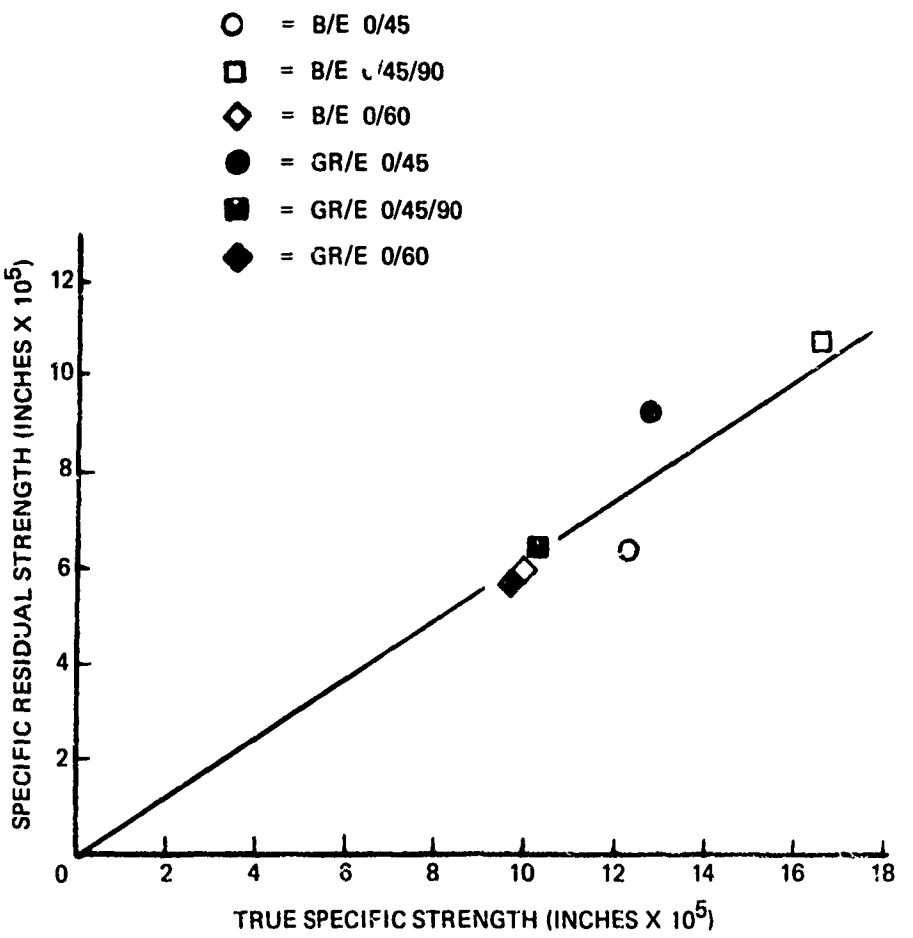

Figure 41 SPECIFIC RESIDUAL STRENGTH VERSUS SPECIFIC UTS

strength of either 7075 or the 6061 aluminum is 40 KSI whereas the boron/epoxy composites exhibited values from 41.2 KSI for the 0/60 layups to 74.9 KSI for the 0/45/90 layup. The only graphite/epoxy composite having retained properties greater than the aluminum was the 0/45 layup which had a residual strength of 51.9 KSI.

The "threshold strength" was only slightly lower than the "residual strength" implying that the dynamic effects were not severe. This was felt to be due to the fact that (1) the flexural effects, in the vicinity of the crack tip were small, (2) the formation of a hole by a shaped projectile can occur with negligible in-plane stress amplification and, (3) the stress waves travel away from the hole at such a great velocity that, at the time of crack initiation, the bulk of the energy is well beyond the zone where the crack initiates. As a result the final wedging action of the projectile was felt to be the primary factor contributing to the dynamic effects.

The threshold strength was found to vary linearly with the UTS as shown in Figure 42. Although variations were observed which were dependent on ply layup and on reinforcing material the data lies approximately on a line representing 55% of the UTS (Figure 42).

The threshold strength was also related to the fracture toughness (See Figure 43). By knowing the variation in the boundary modification factor, Y, as a function of crack length, it was possible to write equation 4 in terms of " σ n", "K", and "a". Letting σ n equal the threshold strength a modified crack length emerged which was equal to 0.06 in. for all the laminates tested. Hence the threshold strength can be predicted by either using a curve similar to Figure 42 of 43 or by using a modified crack length in the fracture equation. The most satisfying approach is that taken by Figge and Newman (Reference 18) in which fracture mechanics is applied and the wedge force is accounted for.

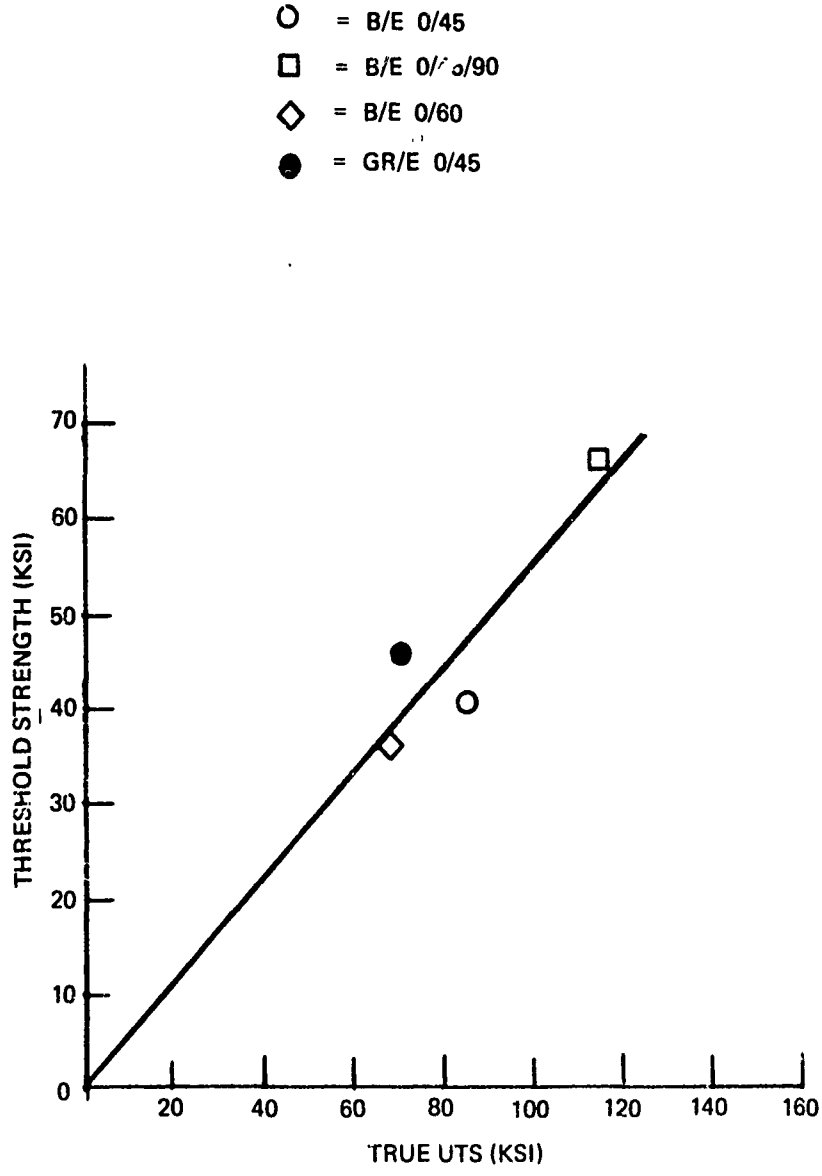

Figure 42 RELATION BETWEEN THRESHOLD STRENGTH AND UTS

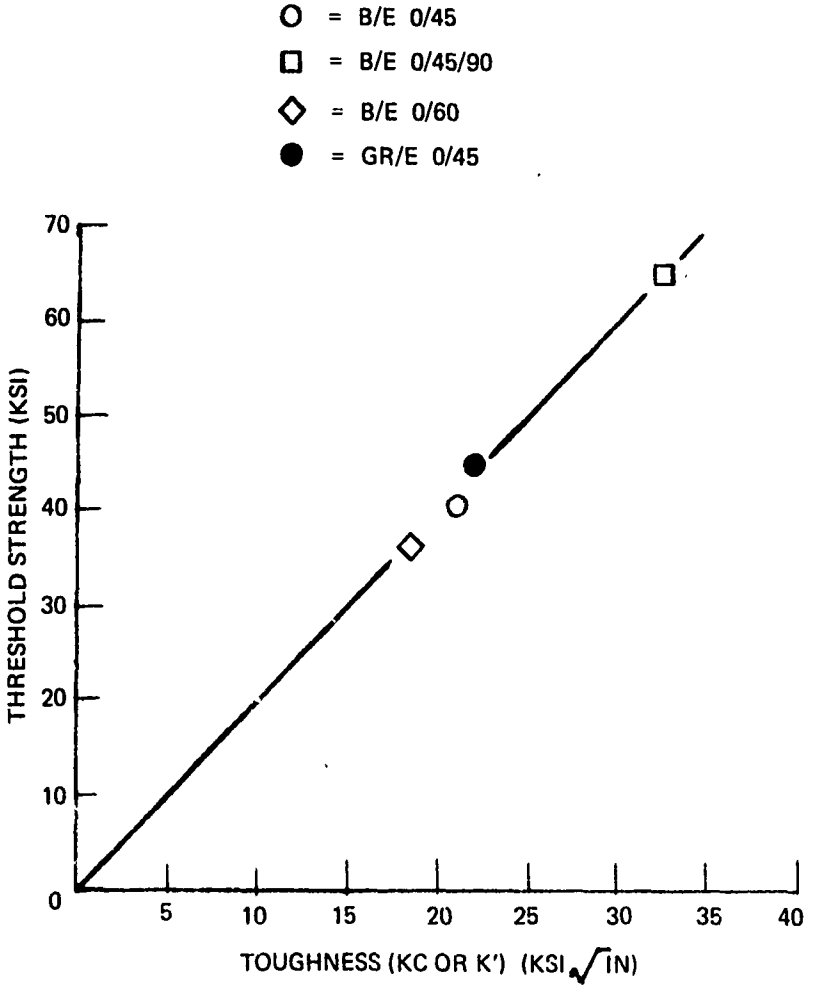

Figure 43 DEPENDENCE OF THRESHOLD STRENGTH ON THE FRACTURE TOUGHNESS OF ADVANCED COMPOSITES

5.0 CONCLUSIONS

1. For both the boron/epoxy and graphite/epoxy composites the "residual strengths" and "threshold strengths" were approximately 62% and 55% respectively of the ultimate tensile strength. Some variations from these averages were observed with different ply layups. The laminate exhibiting the greatest percent retained properties was the 0/45 graphite/epoxy composite which had a "residual and threshold strength" of 73% and 65% respectively of its ultimate tensile strength. The one having the lowest percent retained properties was the 0/45 boron/epoxy composite which had a "residual and threshold strength" of 52% and 48% respectively of its ultimate tensile strength. The other four laminates tested exhibited properties that were so similar that no differentiation could be made with respect to their tolerance to ballistic damage.

2. The absolute"residual and threshold strengths" of the 0/45/90 boron/epoxy composites were the highest measured in this program. The actual values were significantly higher than aluminum and sufficiently higher than the graphite/epoxy laminates to make this boron/epoxy the most attractive material even when compared on a strength to density basis.

3. The residual strength is independent of both the preload and the projectile velocity, for the two velocities considered.

4. The residual strength can be computed from the fracture toughness of each material. This is due to the fact that the damage was localized and can be modeled as a circular hole with symmetric cracks emanating from it.

5. The "threshold strength" is slightly lower than the "residual strength." The reduction was attributed to the additional hoop tension stresses resulting from the wedging force of the shaped projectile.

6. The "threshold strength" is linearly dependent on the toughness and can be predicted by modifying the crack length.

7. Based upon very limited results it appears that 50 caliber AP projectiles have only a slightly more detrimental effect than 30 caliber bullets.

8. Based on a limited number of measurements of crack velocity it was found that the 0/45 graphite/epoxy laminate exhibited the greatest velocity, 8,500 feet per second. The crack in this laminate traveled at 57% of the sonic velocity in the transverse direction of that composite which again was the highest percentage of the wave speed of any composites tested.

6.0 REFERENCES

1. Personal Communication with Gordon Griffith, Air Force Materials Laboratory.

2. Personal Communication with Gordon Griffith, Air Force Materials Laboratory.

3. Savin, G.N., "Stress Concentration Around Holes", Pergamon Press, 1961.

4. Bowie, O.L., "Analysis of an Infinite Plate Containing Radial Cracks Originating from the Boundary of an Internal Hole", Journal of Math and Physics, 35, pages 60-71, 1956.

5. Seely, F.B., and Smith, J.O., "Advanced Mechanics of Materials", 1965 John Wiley and Sons, New York.

6. Forrestal, M.J., "An Approximate Solution for the Circumferential Stresses in a Stretched Plate Caused by a Suddenly Punched Hole", Journal of Applied Mechanics December 1965, pages 949-950.

7. Suarez, J.A., "Vulnerability of Composite Aircraft Structures", Technical Report AFFDL-TR-72-8.

8. Clark, H.T., "Advanced Development on Vulnerability/Survivability of Advanced Composite Structures", AF Contract F33615-71-C-1414.

9. Hayes, R.D., et al, "Flightworthy Graphite Fiber Reinforced Composite Aircraft Primary Structural Assemblies", AFML Contract F33615-69-C-1490, (Project 6169CW).

10. Tsai, S.W., "Mechanics of Composite Materials", Part I, Technical Report AFML-TR-149, November, 1966.

11. Paris, P.C., and Sih, G.C., "Stress Analysis of Cracks", Fracture Toughness Testing and its Applications, ASTM, STP 381 American Society for Testing and Materials, 1965.

12. Olster, E.F., and Jones, R.C., "Toughening Mechanisms in Fiber Reinforced Metal Matrix Composites", Mass Institute of Technology, Research Report R70-75, Cambridge, Mass.

13. Outwater, J.O., and Murphy, M.C., "On the Fracture Energy of Unidirectional Laminates", 24th Annual SPI, 1969, Section 11-C, pages 1-8.

14. Waddoups, M.E., Eisenmann, J.R., and Kaminski, B.E., "Macroscopic Fracture Mechanics of Advanced Composite Materials", Journal of Composite Materials, Volume 5, October 1971.

15. Bowie, O.L., and Freese, C.E , U.S. Army Materials and Mechanics Research Center - Watertown, Mass., Personal Communications.

16. Biggs, J.M., "Introduction to Structural Dynamics", McGraw-Hill, 1964.

17. Goldsmith, W., "Impact", Edward Arnold, LFT Publications, 1960.

18. Figge, I.E., Sr., and Newman, J., of U.S. Army Aviation Material Laboratories, Fort Eustis, Vriginia and NASA Langley Research Center, Hampton, Virginia respectively, Personal Communication.

19. Lenoe, E.M., "Evaluation of Test Techniques for Advanced Composite Materials", August 1971, AFML-TR-68-166.

20. Roach, C.D., and Figge, I.E., Sr., "A Method for Preventing Catastrophic Failure in Aluminum Stressed Skin Panels", USA AVLABS, Technical Note 1, July 1969, U.S. Army Aviation Material Laboratories, Fort Eustis, Virginia.

21. Suarez, J.A., "Vulnerability of Composite Aircraft", Technical Report AFFDL-TR-72-8.

22. Design Guide - Structural Design Guide for Advanced Composite Applications by North American Rockwell Corporation - prepared under Contract F33615-69-C-1368.

23. Sokolnikoff, I.S., "Mathematical Theory of Elasticity", McGraw-Hill, 1965.

24. Reuter, R. C. Jr., "On the Plate Velocity of a Generally Orthotropic Plate," J. Composite Materials, Vol. 4, January 1970.

APPENDIX A

TENSILE DATA

Material	Test	Specimen	UTS (KSI)	Modulus (10^6 psi)	Strain (%)	Poisson's Ratio
Glass/Epoxy	Longitudinal	LT1	86.3	5.11	- -	0.86
12 Ply, 0/45	Tension	LT2	97.3	5.37	- -	
Panel 1117-1234		LT3	95.6	5.73	3.53	
		LT4	95.2	5.69	2.89	
		LT5	94.7	5.31	3.44	
		Ave	93.8	5.44	3.29	0.86
	Transverse	TT1	15.8	3.69	2.04	
	Tension	TT2	17.2	3.73	1.87	
		TT3	18.9	3.80	1.71	
		TT4	20.8	3.91	1.78	
		TT5	19.2	4.33	1.42	
		Ave	18.4	3.89	1.76	

Material	Test	Specimen	UTS (KSI)	Modulus (10^6 psi)	Strain (%)	Poisson's Ratio
Boron/Epoxy	Longitudinal	LT1	61.0	11.8	0.56	0.68
12 Ply 0/45		LT2	68.6	11.5	0.64	
Panel 1117-97A		LT3	65.8	11.2	0.64	
		LT4	59.7	10.9	0.57	
		LT5	63.3	11.4	0.60	
			———	———	———	———
		Ave	63.7	11.4	0.60	0.68
	Transverse Tension	TT1	16.0	4.51	0.39	
		TT2	17.5	4.25	0.45	
		TT3	14.6	4.02	0.39	
		TT4	16.1	4.42	0.41	
		TT5	16.8	4.47	0.44	
			———	———	———	
		Ave	16.2	4.30	0.42	

Material	Test	Specimen	UTS (KSI)	Modulus (10^6 psi)	Strain (%)	Poisson's Ratio
Boron/Epoxy 12 Ply, 0/60 Panel 1109-76	Longitudinal Tension	LT1	49	12	0.64	0.35
		LT2	46	13	0.58	0.38
		LT3	52	12	0.67	0.36
		LT4	49	12	0.57	
		LT5	50	12	0.57	
		LT6	55	11	0.67	
		LT7	55	11	0.69	
		LT8	53	11	0.70	
		LT9	54	11	0.67	
		LT10	54	12	0.61	
			———	———	———	———
		Ave	52	11.8	0.64	0.36
	Transverse Tension	TT1	38	11	0.47	0.32
		TT2	39	10	0.52	0.34
		TT3	38	11	0.47	0.35
		TT4	38	11	0.49	
		TT5	46	11	0.56	
		TT6	42	12	0.47	
		TT7	41	12	0.42	
		TT8	46	12	0.56	
		TT9	49	11	0.61	
			———	———	———	———
		Ave	42	11.6	0.45	0.34
	45° Tension	45T1	37.4	10.8	0.50	0.31
		45T2	39.5	11.8	0.52	0.29
			———	———	———	———
		Ave	38.4	11.3	0.51	0.30

Material	Test	Specimen	UTS (KSI)	Modulus (10^6 psi)	Strain (%)	Poisson's Ratio
Boron/Epoxy	Longitudinal	LT1	97	20	0.60	0.46
12 Ply, 0/45/90	Tension	LT2	99	19	0.62	0.37
Panel 1109-75		LT3	106	19	0.68	0.40
		LT4	98	18	0.64	
		LT5	- -	--	- -	
		LT6	111	17	0.70	
		LT7	105	17	0.66	
		LT8	101	17	0.63	
		LT9	98	18	0.59	
		LT10	105	17	Slippage	
			---	---	---	---
		Ave	102	18	0.64	0.41
	Transverse	TT1	17	8.1	0.25	0.14
	Tension	TT2	20	8.1	0.30	0.13
		TT3	18	8.9	0.24	0.14
		TT4	22	8.5	0.35	
		TT5	19	8.5	0.29	
		TT6	19	8.7	0.25	
		TT7	19	9.6	0.27	
		TT8	18	9.1	0.26	
		TT9	20	8.8	0.30	
		TT10	18	9.4	0.22	
			---	---	---	---
		Ave	19	8.8	0.27	0.14
	45° Tension	45T1	31.5	8.7	- -	0.31
		45T2	27.8	8.7	0.45	0.34
			---	---	---	---
		Ave	29.6	8.7	0.45	0.32

Material	Test	Specimen	UTS (KSI)	Modulus (10^6 psi)	Strain (%)	Poisson's Ratio
Graphite/Epoxy 8 Ply, 0/45 Panel 1117-82A	Longitudinal Tension	LT1	64.9	17.9	0.38	0.81
		LT2	77.5	19.2	0.41	
		LT3	58.3	19.4	0.31	
		LT4	77.5	18.4	0.42	
		LT5	78.0	17.6	0.45	
			———	———	———	———
		Ave	71.2	18.5	0.39	0.81
	Transverse Tension	TT1	10.2	3.5	0.31	
		TT2		3.9	0.30	
		TT3	13.0	4.1	0.32	
		TT4	11.1	4.0	0.29	
		TT5	13.1	4.1	0.35	
			———	———	———	
		Ave	12.0	3.9	0.31	

Material	Test	Specimen	UTS (KSI)	Modulus (10^6 psi)	Strain (%)	Poisson's Ratio
Graphite/Epoxy 8 Plys, 0/45 Panel 1117-61A	Longitudinal Tension	LT1	50.2	15.4	0.34	
		LT2	44.2	15.4	0.29	
		LT3	58.8	14.7	0.41	
		LT4	39.4	15.2	0.28	
		LT5	50.3	14.8	0.38	
			----	----	----	
		Ave	48.7	15.1	0.34	
	Transverse Tension	TT1	4.8	3.2	0.16	
		TT2	5.3	2.0	0.29	
		TT3	3.9	2.6	0.23	
		TT4	5.6	2.6	0.22	
		TT5	5.7	2.6	0.21	
			----	----	----	
		Ave	5.1	2.6	0.22	
	45° Tension	45T1	- -	9.1	- -	0.03
		45T2	- -	11.4	- -	0.07
			----	----	----	----
		Ave		10.2		0.05

Material	Test	Specimen	UTS (KSI)	Modulus (10^6 psi)	Strain (%)	Poisson's Ratio
Graphite/Epoxy	Longitudinal	LT1	48	13	0.38	0.26
10 Ply, 0/45/90	Tension	LT2	46	13	0.35	0.28
Panel 1109-82A		LT3	24*	14	0.17	0.36
		LT4	25*	14	0.17	
		LT5	28	14	0.20	
			—	—	——	——
		Ave	41	14	0.25	0.30
	Transverse	TT1	6.0**	6.3**	0.10**	0.20
	Tension	TT2	10	7.5	0.13	0.21
		TT3	11	7.8	0.15	0.19
		TT4	12	9.1	0.13	
		TT5	12	10.1	0.12	
			—	——	——	——
		Ave	11	7.0	0.13	0.20
	45° Tension	45T1	15.9	9.2	- -	- -
		45T2	20.0	10.8	- -	0.24
			——	——	——	——
		Ave	17.9	10.0		0.24

*Tab Failure
**Abnormal Data

Material	Test	Specimen	UTS (KSI)	Modulus (10^6 psi)	Strain (%)	Poisson's Ratio
Graphite/Epoxy	Longitudinal	LT1	34	14	0.26	.24
10 Ply, 0/45/90	Tension	LT2	43	15	0.30	
Panel 1109-87A		LT3	38	15	0.29	.39
		LT4	46	16	0.29	
		LT5	41	16	0.29	
		Ave	40	15	0.29	.35
	Transverse	TT1	25	8.6	0.26	0.16
	Tension	TT2	24	9.7	0.27	0.17
		TT3	28	10.0	0.30	0.18
		TT4	27	9.7	0.29	
		TT5	26	9	0.31	
		Ave	26	9.4	0.29	0.17
	45° Tension	45T1	26.2	10.3	- -	0.28
		45T2	25.3	9.9	- -	0.30
		Ave	25.7	10.1		0.29

APPENDIX B

FRACTURE TOUGHNESS DATA

	Specimen				Toughness	
Material	Number	Width (in.)	Thick. (in.)	Initial Crack Length (in.)	K' (KSI $\sqrt{in.}$)	K_c (KSI $\sqrt{in.}$)
Glass/Epoxy	1	0.750	0.061	0.225	51	61
12 Ply, 0/45	2	0.746	0.060	0.225	31	78
Panel 1117-123A	3	0.750	0.060	0.230	38	50
	4	0.750	0.062	0.225	44	58
	5	0.75	0.061	0.230	54	73
	6	0.749	0.060	0.230	45	48
	7	0.750	0.060	0.230	49	59
	8	0.750	0.062	0.225	22	52
	9	0.749	0.060	0.225	22	55

	Specimen				Toughness	
Material	Number	Width (in.)	Thick. (in.)	Initial Crack Length (in.)	K' (KSI $\sqrt{in.}$)	K_c (KSI $\sqrt{in.}$)
Boron/Epoxy 12 Ply, 0/45 Panel 1117-97A	1	0.749	0.066	0.240	13	20
	2	0.750	0.066	0.230	16	22
	3	0.750	0.066	0.240	16	21
	4	0.750	0.066	0.235	14	21
	5	0.749	0.066	0.230	11	18
	6	0.749	0.066	0.240	15	20
	7	0.750	0.066	0.240	16	19
	8	0.750	0.066	0.240	18	24
	9	0.751	0.066	0.240	18	25
Boron/Epoxy 12 Ply 0/60 Panel 1109-76	1	0.750	0.061	0.240	16	18
	2	0.753	0.061	0.240	15	20
	3	0.752	0.061	0.240	14	17
	4	0.752	0.061	0.235	16	18
	5	0.753	0.061	0.240	15	19
	6	0.753	0.061	0.230	13	17
Boron/Epoxy 12 Ply 0/45/90 Panel 1109-75	1	0.750	0.061	0.230	20	31
	2	0.750	0.060	0.235	25	33
	3	0.750	0.060	0.235	33	37
	4	0.749	0.061	0.225	25	31
	5	0.748	0.061	0.230	26	31

	Specimen				Toughness	
Material	Number	Width (in.)	Thick. (in.)	Initial Crack Length (in.)	K (KSI $\sqrt{\text{in.}}$)	K_c (KSI $\sqrt{\text{in.}}$)
Graphite/Epoxy 8 Ply, 0/45 Panel 1117-82A	1	0.750	0.052	0.235	23	26
	2	0.750	0.053	0.230	22	28
	3	0.751	0.053	0.240	21	24
	4	0.751	0.053	0.235	21	31
	5	0.751	0.053	0.230	23	26
	6	0.751	0.053	0.230	20	30
Graphite/Epoxy 10 Ply 0/60 Panel 1109-82A	1	0.751	0.074	0.235	14	27
	2	0.751	0.074	0.235	18	26
	3	0.751	0.072	0.230	20	26
Graphite/Epoxy 10 Ply 0/45/90 Panel 1109-87A	1	0.751	0.073	0.225	12	24
	2	0.751	0.073	0.230	12	19
	3	0.751	0.073	0.235	17	18
	4	0.751	0.073	0.230	13	22

APPENDIX C

TAB CONFIGURATION

Some problems were encountered in developing a satisfactory tab design; particularly for the glass/epoxy laminates. The very first tests were conducted using the straight sided, unclamped tabs shown in Figure 16a. This design proved unsatisfactory because of peeling which initiated at the fillet. Using a finite element analysis the shear and normal stresses developed in the adhesive were obtained and are presented in Figure 44 where because of the eccentricity, e, tensile stresses are developed in the vicinity of the fillet. With the aluminum, the boron/epoxy and the graphite/epoxy the application of an external compressive stress imposed by C-clamps eliminated the tendency for debonding and hence was used. The glass/epoxy laminates because of their unique combination of low modulus and high strength develop greater shear stresses in the adhesive than any of the other materials tested. This is due to the high loads required to break the specimens in conjunction with severe discontinuity in the overall stiffness near the fillet due to the tab. In an effort to eliminate tab failure the tab configurations shown in Figure 16 were tried.

The tapered tab, the reversed taper tab, and the tab with the fiberglass shim all tend to reduce the shear stresses at the fillet by gradually reducing the tab stiffness in the vicinity of the fillet. None of these however permitted sufficient load to be introduced to cause panel failure; in all cases the failure started at the fillet and propagated across the tab.

The step type tab was tried since it permitted load to be introduced to small groups of plys throughout the laminate. This too failed to achieve any significant increases in the maximum load that would be applied prior to tab failure. In a final effort the bolted tab was tried. Here in addition to the clamping action, which proved successful in the coupon tests, was the possibility of loading by bearing, as is done in metal structures. Once again the adhesive at the tab failed in shear and it proved impossible to properly load the glass panel with the bolts. Hence none of the tabs used could effectively load the glass/epoxy laminates to a stress level sufficient to cause true tensile failure. Failure in this material, as opposed to the other laminates, did not occur in the form of a well defined break. As discussed in the report, a brush effect shown in Figure 5 is created on both halves of the parted specimen. Even though this was desired in the large panel tests it may be well beyond other failure criteria. For example the large tensile specimens, when tested ballistically, exhibited a significant amount of delamination. Additional loading resulted in the propagation of these debonded portions. Had failure been based upon a compression strength or upon a retained stiffness the panels would have surely failed. In tension however it was impossible to load the panels sufficiently to part them as in the coupon tests, and as described in the text, the standard tab with clamps was used for the remaining panels.

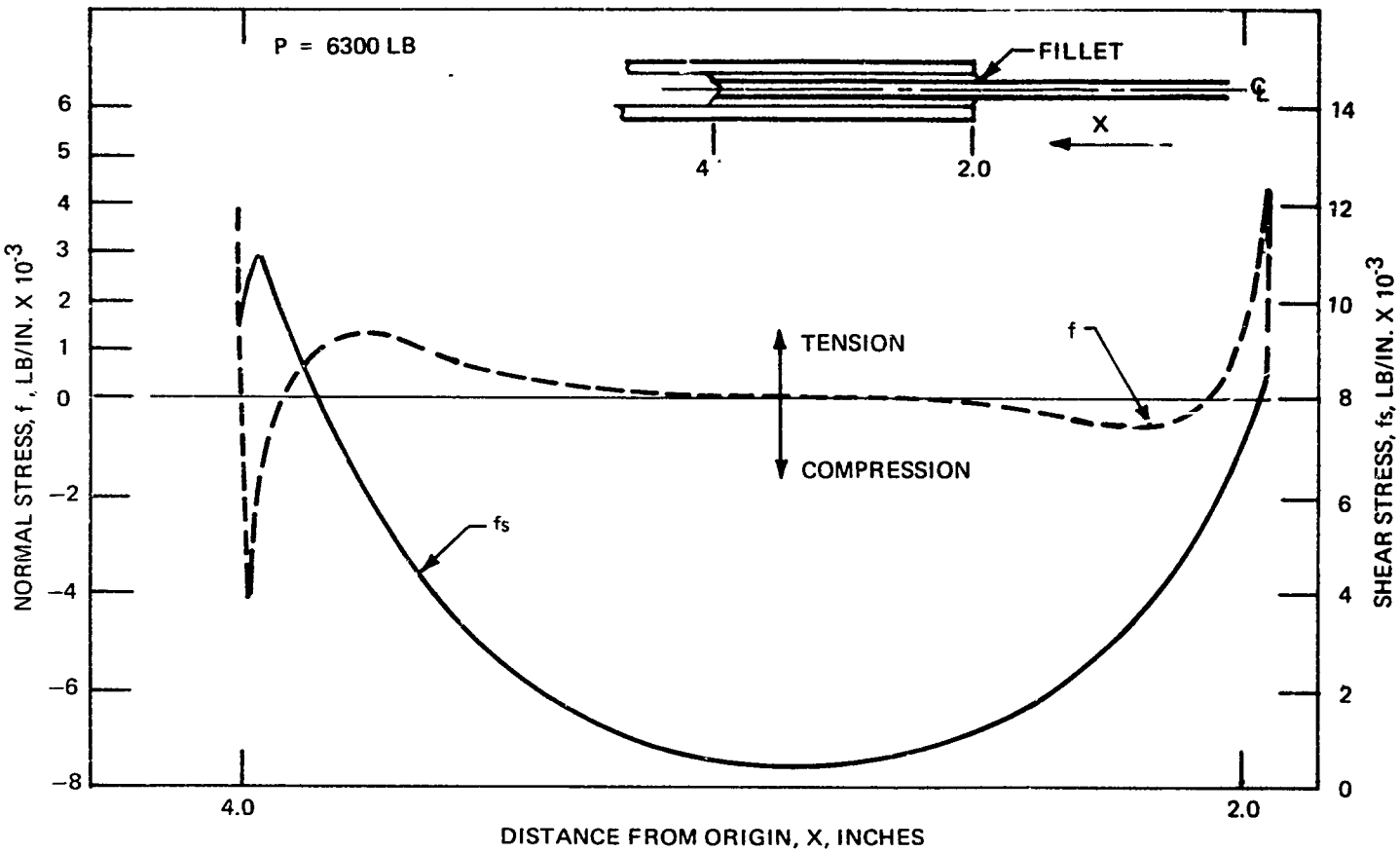

Figure 44 THE SHEAR AND NORMAL STRESSES IN A LAP–SHEAR JOINT

APPENDIX D

FLEXURAL RESPONSE

The flexural response of a simply supported, square, isotropic plate loaded by a triangular pulse distributed uniformly over the shaded region in Figure 30 can be obtained using a modal analysis. The equation of motion can be obtained from the Lagrangian relations. From the equationsof motion and the forcing function the displacements can be obtained. The stresses are related to the second derivative of the displacement function and can easily be computed.

The Lagrange equation can be written in the form:

$$\frac{d}{dt}\left(\frac{\partial K}{\partial \dot{A}_{ij}}\right) + \frac{\partial \mathcal{U}}{\partial A_{ij}} = \frac{\partial \mathcal{W}_e}{\partial A_{ij}}$$

where

t is time

$\dot{A}_{ij}$ is the time derivative of Aij

A_{ij} is a generalized modal displacement

K is the total kinetic energy

$\mathcal{U}$ is the total strain energy

$\mathcal{W}_e$ is the total external work

The vertical displacement, y, can be expressed as:

$$y = \sum_{i=1}^{\infty}\sum_{j=1}^{\infty} A_{ij} \sin\left(\frac{i\pi x}{a}\right) \sin\left(\frac{j\pi z}{b}\right)$$

where x, y, and z are coordinates shown in Figure 30 and a and b are the plate dimensions.

For simplicity consider only square modes where i = j = n. Also since the plate is square $a = b = \ell$. Therefore,

$$y = \sum_{n=1}^{\infty}\sum_{n=1}^{\infty} A_{nn} \sin\frac{n\pi x}{\ell} \sin\frac{n\pi z}{\ell}$$

The kinetic energy is obtained by considering a differential element.

$$dK = \frac{1}{2} m \dot{y}^2 \, dx \, dz$$ where m is the mass per unit area of the plate.

Hence $$K_{nn} = \frac{1}{2} m \int_0^{\ell} \int_0^{\ell} \left(\dot{A}_{nn} \sin \frac{n\pi x}{\ell} \sin \frac{n\pi z}{\ell} \right)^2 dx \, dz$$

Therefore $$\frac{d}{dt} \left(\frac{\partial K_{nn}}{\partial \dot{A}_{nn}} \right) = \frac{1}{4} m \ell^2 \ddot{A}_{nn}$$

The strain energy for plate flexure is:

$$U = \frac{Eh^3}{24(1-\nu^2)} \int_0^{\ell} \int_0^{\ell} \left[\left(\frac{\partial^2 y}{\partial x^2} \right)^2 + \left(\frac{\partial^2 y}{\partial x} \right)^2 + 2\nu \frac{\partial^2 y}{\partial x^2} \frac{\partial^2 y}{\partial z^2} + 2(1-\nu) \left(\frac{\partial^2 y}{\partial x \, \partial z} \right)^2 \right] dx \, dz$$

where E is the Young's modulus and ν is the Poisson's ratio

Hence

$$\frac{\partial U}{\partial A_{nn}} = \frac{\pi^4 Eh^3 n^4}{12(1-\nu^2)\ell^2} A_{nn}$$

The external work is:

$$W_e = y \, p(t) = \left[p(t) \right] \int_{\ell_1}^{\ell_2} \int_{\ell_1}^{\ell_2} A_{nn} \sin \frac{n\pi x}{\ell} \sin \frac{n\pi z}{\ell} \, dx \, dz$$

where ℓ_1 and ℓ_2 are coordinates which describe the shaded area in Figure 30 over which the load is applied.

$$W_e = p(t) \, A_{nn} \frac{\ell^2}{n^2 \pi^2} \left[\cos \frac{n\pi \ell_2}{\ell} - \cos \frac{n\pi \ell_1}{\ell} \right]^2$$

where ℓ_2 = 3.15 inches, ℓ_1 = 2.85 inches and ℓ = 6.00 inches

Hence

$$\ddot{w}_e = p(t)\, A_{nn}\, \frac{\ell^2}{n^2\pi^2} \left[\cos(1.66n) - \cos(1.50n)\right]^2$$

and

$$\frac{\partial \ddot{w}_e}{\partial A_{nn}} = p(t)\, \frac{\ell^2}{n^2\pi^2} \left[\cos(1.66n) - \cos(1.50n)\right]^2$$

Substituting values into the Lagrange equation.

$$\frac{1}{4}\, m\ell^2\, \ddot{A}_{nn} + \frac{\pi^4 E h^3 n^4}{12(1-\nu^2)\ell^2}\, A_{nn} = p(t)\, \frac{\ell^2}{n^2\pi^2} \left[\cos(1.66n) - \cos(1.50n)\right]^2$$

which reduces to

$$\ddot{A}_{nn} + \frac{\pi^4 E h^3 n^4}{3m\ell^4(1-\nu^2)}\, A_{nn} = p(t) \left(\frac{4}{mn^2\pi^2} \left[\cos(1.66n) - \cos(1.50n)\right]^2 \right)$$

This is of the form:

$$\ddot{A}_{nn} = \omega^2 A_{nn} = p(t)\, F$$

The static deflection, Annst, for each mode is $\frac{F}{\omega^2}$. The dynamic load factor (DLF) depends upon the ratio of td, the duration of the pulse, to T, the natural period. T is equal to $\frac{2\pi}{\omega}$ where ω is the natural frequency. The pulse duration td, was 10×10^{-6} seconds as shown in Figure 30. Using the following values:

$m = ph = 1.4 \times 10^{-5}$ pounds sec^2/in^3

$E = 12 \times 10^6$ psi

$\nu = 1/3$

$h = 0.1$ inches

The fundamental period is 4×10^{-3} seconds. Hence from Figure 31 the DLF is close to zero implying that the plate does not respond in this mode. The seventh mode, A_{77}, has a natural period of 2×10^{-5} seconds and so td/T is 1/2. The DLF for mode 7 is 1.2. The maximum deflection in mode 7 is $y_{max} = A_{77st}\, DLF_{max} = 1.4 \times 10^{-8} \times 1.2 = 1.7 \times 10^{-8}$ inches. Therefore, at its maximum responce the seventh mode will have the form:

$$y_{77} = 17 \times 10^{-8} \sin\left(\frac{7\pi x}{\ell}\right) \sin\left(\frac{7\pi z}{\ell}\right)$$

The flexural stresses are related to the second derivative of this shape function.

$$\sigma_{zz} = \frac{Eh}{2(1-\nu^2)}\left(\frac{\partial^2 y}{\partial z^2} + \nu \frac{\partial^2 y}{\partial x^2}\right)$$

Evaluating this expression at the most critical points it is found that σ_{zz} is approximately equal to 0.14 psi for a p(t) equal to 1 psi. If the projectile velocity decreases by 50 fps during the penetration the impulse requires 7000 pourds force. This force is equivalent to a 100,000 psi pressure over the area removed by the projectile. Hence the stresses are of the order of 14 KSI. An examination of the equation will show that much higher or lower frequencies will play only a minor part in the response to this load. It also must be noted that these stresses are very localized and occur midway between the nodes.